Synthesis of Fluorinated Benzophenones for Biological Activity Probing

A thesis submitted in a partial fulfilment of the requirement for the degree of

Master of Research

by

Bilqees Sameem

Department of Molecular Sciences

Macquarie University

April 2019

Table of Contents

Abstract

The benzophenone (BP) structure, with its unique biaryl twist, has been shown to be an important bioactive functionality and prevalent motif in natural products. In this work, the synthesis and characterization of new fluorinated BP synthons are reported. These new BP fragments may provide additional specificity in protein-ligand binding, due to new interactions that could come from the fluorine substituents in protein pockets. One monofluorinated BP fragment was accessed in 13 steps with an overall yield of 11% employing key reactions such as lithium halogen exchange, intramolecular anionic Fries rearrangement, and chemoselective oxidations. The second, difluorinated BP fragment was brought to the pre-oxidation stage. Current results demonstrate that the intramolecular Fries rearrangement is feasible for accessing mono- and difluorinated scaffolds. These fluorinated BP fragments will in future be incorporated into the natural product (-)-balanol framework for probing the isozyme selective inhibition within the AGC superfamily of kinases.

Declaration

I certify that this piece of work entitled “Synthesis of fluorinated benzophenones for biological activity probing” is original and has not be submitted for the fulfilment of any degree or course requirement at any other university/institution or Macquarie university. I also state that is an original piece of work written by me. Any assistance I received has been appropriately acknowledged. Finally, I certify that all literature and information sources mentioned are indicated in the thesis.

Bilqees Sameem

(SN: 45037566)

4/4/2019

Acknowledgments

First and foremost, I'm highly indebted to Dr Fei Liu for her enormous guidance, encouragement and support throughout this project.

Secondly, I would specially like to thank Alexander Moore for his helpful discussions regarding synthesis, encouragement and providing very patiently technical guidance. To all the present members of Liu group for their moral support and help regarding materials whenever needed, in particular Ivan Salazar Estrada for his help with LCMS data acquisition.

I'm highly grateful to the Morris group at UNSW for providing critical reagents.

I wish to thank Associate professor Bridget Mabbutt and Associate professor Louise Brown for their key administrative roles in the Mres program and CBMS groups including the Venkatesan, Jamie, Karuso, Piggot, Messerle groups for providing space and materials whenever needed.

I'd like to thank Dr Nicole Cordina for her assistance with NMR experiments and Dr Remi for his help with HPLC.

Last but not the least, my wholehearted thanks to my parents for their continuous support, guidance and love.

List of Abbreviations and Symbols

δ- chemical shift in ppm

μ- micro

Ac- Acetyl

ATP- Adenosine triphosphate

BOC- Terta-butylcarbonate

BP- Benzophenone

Bu- Butyl

cAMP- Cyclic Adenosine mono-phosphate

d- doublet

dd- doublet of doublet

DCM- Dichloromethane

DAST- Diethylaminosulfur trifluoride

DIBALH- Diisobutylalumminium Hydride

DMAP- 4- *N*,*N*-Dimethylaminopyridine

DMF- *N*,*N*-Dimethylformamide

DMSO- Dimethylsulfoxide

DVC- Divinyl carbinol

ESI- MS- electrospray ionization mass spectrometry.

IC_{50}- Half maximal inhibitory concentration

IPr- Isopropyl

IR- Infrared spectroscopy

K*d*- Dissociation constant

K*i*- Inhibitory constant

LRMS- Low resolution mass spectrometry

m- multiplet

n- Nano

n-BuLi- *n*-Butyllithium

Me- Methyl

MD- Molecular dynamics

NMO- *N*-Morpholine-*N*-Oxide

NMR- Nuclear Magnetic Resonance

OX- Oxidant

Ph- phenyl

PKA- Protein kinase A

PKC- Protein kinase C

ppm- parts per million

qt- quartet of doublets

SAR- Structure activity relationship

t- triplet

TBAF-*Tetra*-*n*-butylammonium fluoride

TBSCl- *tertra*-Butyldimethylsilyl chloride

td- triplet of doublets

THF- tetrahydrofuran

TLC- Thin-layered chromatography

TPAP- Tetrapropylammonium perruthenate

List of Figures

List of Schemes

List of Tables

1. Introduction

Benzophenone (BP), the simplest diaryl ketone with an intrinsic twist, enables the position and spatial orientation of polar substituents. The hindered rotation around a single bond of ortho substituents of the biaryl may result in atropisomeric isomerism. The size and number of the substituents highly influences the equilibrium of the atropisomers, decreasing the rate with increase in bulkiness of substituent. As such, BP is a ubiquitous motif in medicinal chemistry with a wide range of bioactive properties. The introduction is divided into four sections, starting with a brief overview of synthetic and naturally occurring bioactive BP containing molecules. The second section will focus on a highly substituted BP fragment from the natural product balanol and how such BP fragment, when derivatized appropriately, may confer unique interactions against the protein target in order to improve on isozyme inhibition specificity. The third section will examine the key synthetic strategies for making highly substituted BP fragments deriving from the balanol system. The last section will present the project aims for making new BP fragments for building new balanoids for biological testing.

1.1 Synthetic bioactive scaffolds containing benzophenone

Some of the recently reported, synthetic bioactive scaffolds with a BP motif are summarized in (Fig. 1). By substituting on the BP scaffold, a wide variety of biological activities are derived, ranging from antimicrobial to antiviral and anticancer agents. Romines *et al* reported BP containing scaffold **1.1** (Fig. 1) as a potent nucleoside reverse transcriptase inhibitor (NRTI) with IC_{50} values in the nanomolar range against wild and some mutant HIV strains. Optimization of the parent compound and SAR studies revealed that the BP carbonyl motif was important for activity[1, 2]. Husain *et al* modified Etomidate-an anesthetic agent into compound **1.2** by introducing a BP motif for probing binding site in ligand gated ion channel receptors[3]. Belluti and coworkers developed a series of potent, BP based anti-Alzheimer agents **1.3** as acetyl cholinesterase inhibitors that suppress AChE induced amyloid beta aggregation and β-secretase (BACE–1) activity.[4] Firestine and coworkers developed BP derivatives tethered to a tetraamide motif as anti-bacterial agents **1.4** for treating a wide range of drug resistant strains including methicillin-resistant Staphylococcus aureus (MRSA), vancomycin-intermediate

Staphylococcus aureus (VISA), vancomycin-resistant Staphylococcus aureus (VRSA) and vancomycin-resistant Enterococci[5]. Recently, Hayashi *et al* [6]modified the clinical anti-lung cancer candidate plinabulin into a potent antimicrotubule agent by substituting the phenyl ring of the parent compound with a benzophenone moiety. The resultant compound **1.5** displayed potent cytotoxicity (IC_{50} value = 7nM) against colon cancer cells by strongly binding to microtubule (K_d = 1.3 μM) and inducing microtubule depolarization. Drug efflux pump P-glycoproteins have been shown to promote multi drug resistances (MDR) in tumors and affect the pharmacokinetic properties of a drug. Jabeen *et al* reported BP derivative **1.6** as P-glycoprotein inhibitors with the BP fragment interacting with the protein pocket in a similar pattern as that of profenone. Moreover, the compounds displayed ligand efficiency and lipophilic efficiency as that of previously identified propafenone type inhibitors which entered phase III clinical trials[7].

-

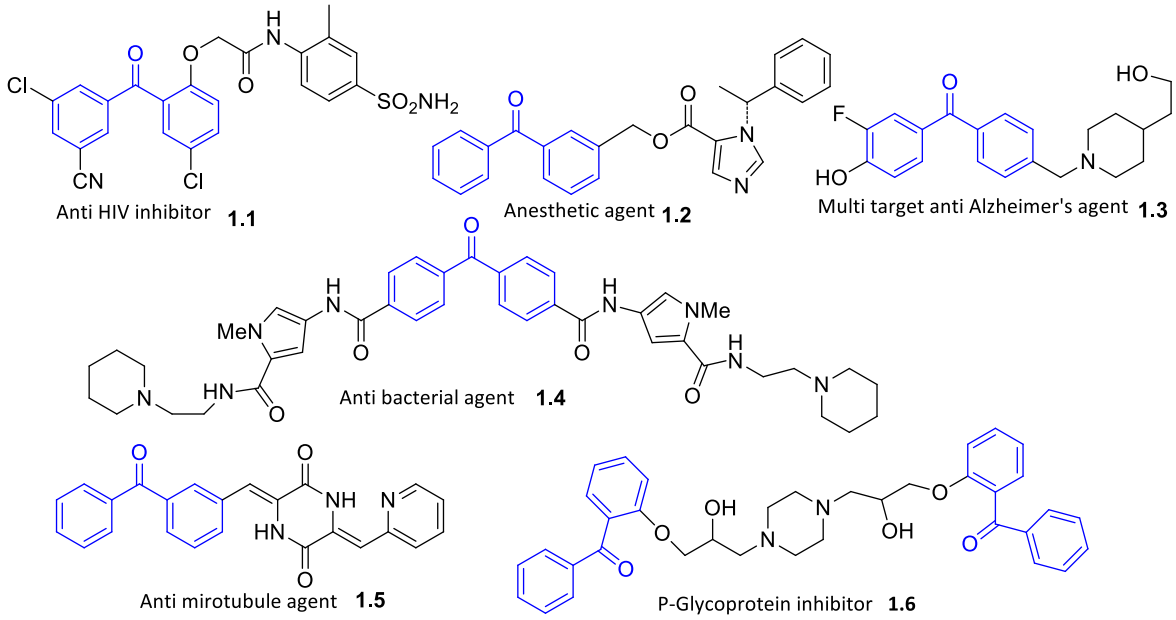

Fig. 1. Examples of synthetic benzophenone based bioactive compounds.

Much of the work reported on the synthesis of benzophenones in the literature is based on the derivatization of hydroxy groups on the BP scaffold, likely to mimic derivatization of the natural BP's with multiple phenolic moieties.

1.2 Bioactive natural products containing benzophenone

Natural benzophenones (BPs) are a class of compounds comprising of more than 300 members and exhibiting great structural diversity displayed around a common phenol-carbonyl-phenol skeleton. Natural BPs are mainly divided into two major classes: basic benzophenone skeleton (BPS) and polyprenylated benzophenone skeleton (PPBS) (Fig. 2).

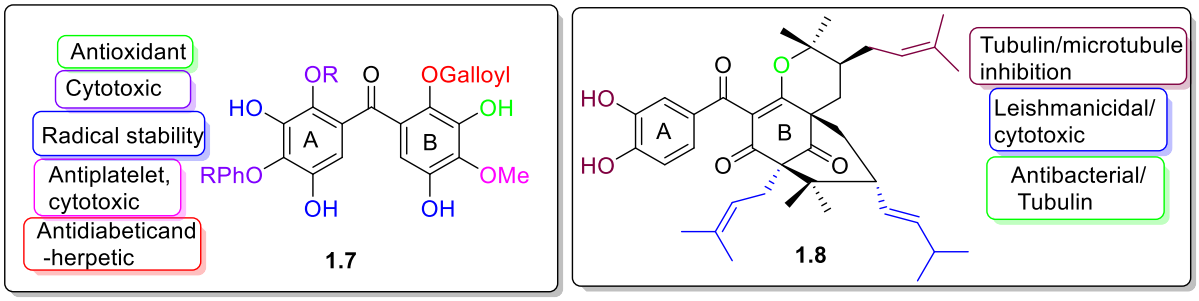

Fig. 2. SAR of the benzophenone motif in bioactive natural scaffolds; (**1.7**) Basic benzophenone skelton (BPS); (**1.8**) Polyprenylated benzophenone skelton (PPBS); the colored motifs correspond to their bioactivity displayed in the boxes.

The structure activity relationship (SAR) of the two main types of natural BPs is summarized in (Fig. 2). The A-ring of BP is a benzene ring, generally contains 0, 1 or 2 substituents. The B-ring is derived from acetate-malonate building blocks and undergoes prenylation or cyclization to produce various structurally unique compounds. The presence of phenolic, enolic and prenyl saturation are critical toward bioactivities in BPS and PPBS. Majority of the benzophenones have been isolated from higher plants with 77% from Clusiaceae (formerly Guttiferae) family only, with half of them polyprenylated. Many of the natural products containing BP fragment exhibit anti-tubulin[8], anti-bacterial, anti-fungal, anti-HIV, anti-oxidant activities, among others. BPs such as xanthochymol, isoxanthochymol, vismiaguianones-D exhibit their cytotoxic activities against Colo-320–DM and MCF–7 cells with IC_{50} values in the range of 0.47–0.48 μM[9]. Guttiferones A and D (bearing isoprenyl and hydroxy groups) have activity at 6.8 μg/mL against the human ovarian cancer cells. Vismiaguianones-D and E (bearing prenyl and hydroxy groups) exhibit cytotoxic activity against KB cells with an IC_{50} value of 3.36.8μg/mL[10]. Moronone, a PPBS (bearing geranyl and hydroxy groups), displays strong anti-proliferative activity against human breast cancer cells via glycolytic inhibition[11]. Mechanistically, this compound acts as a protonophore by dissipating mitochondria proton gradient given the

tumor cells may be hypersensitive to the protonophore due to their increased ATP consumption. Xanthochymol, guttiferones A and D elicit cytotoxic activity by activating the endoplasmic stress response and inhibiting the cell survival MTOR cascade. Emorosone, a polyprenylated BP exhibits its cytotoxic activity against HEG2 cells with an IC_{50} value of 1–4 µM by dissipating mitochondria membrane and depleting ATP depletion which could make it a good protonophoric mitochondrial uncoupler[12]. 7–epi-nemorosone (bearing isoprenyl and hydroxyl groups on ring A and B) has been reported to display anti-cytotoxic activity against both androgen dependent and independent prostate carcinoma LNCaP cells with an IC_{50} value between 4–7.5 µM. To summarize, natural BPs are highly substituted in order to achieve a wide range of bioactivities.

1.2 Balanol- a benzophenone containing natural product

1.2.1 Discovery and bioactivity profile

Balanol was isolated from *Verticillium balanoides* in 1993 and found to inhibit the protein kinase C (PKC) family (IC_{50} = 4–9 nM)[13] by targeting the catalytic active site as an ATP mimic. The PKC family consists of at least 10 serine/threonine protein kinase isozymes activated by diacylglycerol (DAG) and regulates gene expression, cellular metabolism, proliferation, growth and differentiation. Development of an isozyme specific inhibitor for the PKC family would unveil the unexplored and non-redundant role of these isozymes in various disorders[14]. To date, development of a single isozyme specific inhibitor or drug for the PKC family has remained elusive. Apart from inhibiting PKC isoforms, balanol also inhibits cyclic-AMP (CAMP) dependent protein kinase PKA (IC_{50} = 4–9 nM). Balanol, however, does not inhibit other members of the tyrosine protein kinases such as epidermal growth factor receptor tyrosine kinases.

Stereoelectronically, balanol resembles ATP and binds to an equivalent cleft in the catalytic domain of the kinase, as found by crystallographic studies of balanol bound to PKA[15] (Fig. 3). The azepane motif mimics the ATP ribose. The benzophenone and benzamide components align with the adenine and triphosphate groups of ATP, respectively[15]. The benzophenone (BP) moiety is the main contributor to balanol's overall potency, as it interacts with the flexible loops (e.g. activation and glycine rich loops) in the catalytic domain, mainly through hydrogen bonding, hydrophobic and π-π interactions.

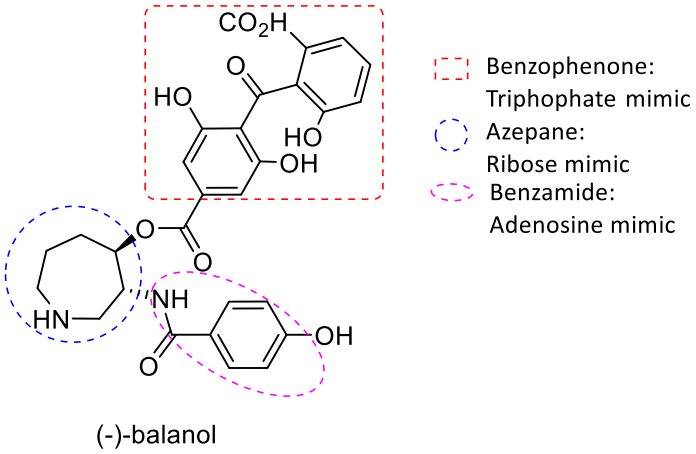

Fig. 3. Structure of (-)-balanol.

1.2.2 Modification of Balanol and Structure Activity Relationship (SAR)

Various attempts have been made toward the synthesis of balanol analogues, or balanoids, in order to improve the inhibition potency with isozyme specificity[16-18]. The key motifs modified in these studies are the biaryl ring, the azepane ring, the amide and ester linkage, and the benzamide ring, as summarized in (Fig. 4). Modification of the BP motif has exhibited more pronounced effects on the inhibitory activity against PKC isozymes in comparison to PKA. Prior studies found that the BP and hydroxybenzamide moieties of balanol are pivotal for activity, and modifications tend to cause deleterious effects on PKC inhibition[16]. The central azepane ring has been found to be more amenable for modification (Fig. 4).

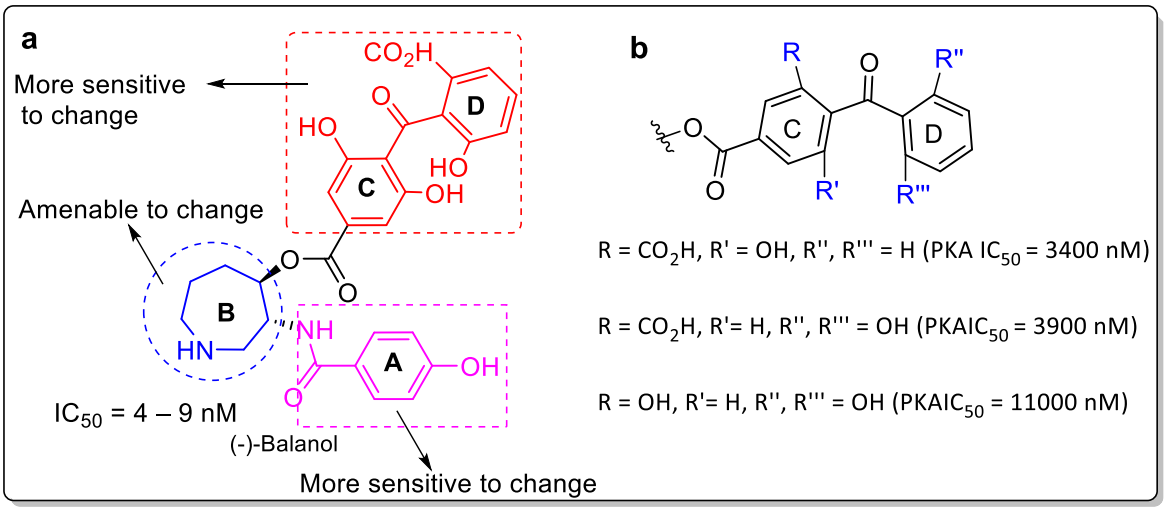

Fig. 4. Effects of the structural modifications of (-)-balanol on its activity; (a)Representation of effect on activity upon modification of balanol fragments; (b) Selectivity in inhibition for PKA over PKC isozymes on modification of the BP fragment.

Nicolaou *et al*[19, 20] accomplished a series of balanol analogues by modifying the BP motif (Fig. 4b). Withdrawal of both the hydroxy groups on the C ring resulted in enhanced activity against PKA and a severe decline against PKC. The study concluded that despite the high homology in the catalytic domains of PKA and PKC, they are adequately dissimilar to allow development of selective inhibitors.

Heerding *et al*[21] synthesized balanol analogues bearing carboxylic group replacements with tetrazoles, amides, sulfonamide. Introduction of sulfonamide retained PKCδ inhibitory activity comparing to balanol, while reducing the inhibition of all other isozymes. This study highlighted the importance of acidic proton on the BP motif, presumably required to mimic the triphosphate group. Lamp and associates[16] synthesized a series of benzophenone modified analogues against PKA and PKC. The results showed that minor modification in the benzophenone ring has substantial deleterious effects on activity. Alterations in internal C–ring with substituents resulted in PKA selective analogues.

Several modifications on azepane and benzamide fragments by perturbing ring sizes, heteroatoms, ester and amide linkages and nitrogen substitution have been investigated[22-26]. Replacement of the azepane ring with cyclopentane resulted in increased potency with enhanced isozyme selectivity against PKCδ and PKCη[23]. Substitution with an indane moiety increased PKC inhibitory activity along with selectivity over PKA[27]. Alteration of the amide linker (between ring A and B) by a methylene group with a cyclopentane motif in proximity increased PKC isozyme inhibition and selectivity over PKA[25, 28].

To sum up, extensive modification of balanol has shown that the benzophenone fragment and the *p*–hydroxybenzamide motifs are essential for the PKC inhibitory activity and are sensitive to perturbation. However, the central azepane ring is amenable to diversification. The flexibility of the seven-membered azepane ring contributes to multiple low energy and puckered ring conformations. This conformational flexibility allows the functional groups on the azepane ring to form dynamic interactions with the target protein. To date, few balanol

analogues have exhibited PKA selectivity[19]. The development of new analogues is also important to address the issue of PKC isozyme selectivity.

1.2.3 The role of fluorine in medicinal and natural products chemistry

Fluorine is a unique conformation tuning motif in drug design. The small size of fluorine and its high electronegativity produce pronounced pharmacological effects on small sized organic molecules, when installed at key position(s)[29]. The vital role fluorine plays in modulating properties of pharmaceutically important compounds is reflected by its presence in drugs approved over the past two decades. Currently the top 1/3rd selling drugs on the market contain at least one fluorine atom[30,31]. Carbon-fluorine bonds are found in over 200 fluorinated compounds used as anesthetic, anti-bacterial, anti-malarial, anti-cancer, anti- inflammatory and psychotic agents[32]. Fluorine–18 has also provided a unique tool for positron emission tomography (PET) in non-invasive imagining and diagnosis in CNS disease like Alzheimer and cancer[33].

Fluorinated analoges of natural products are emerging as important sccaffolds in drug discovery[34-38]. This trend is reinforced by the pronounced effect of fluroine on conformation and the pharmacological profile[34, 39-41]. Vinflunine is a fluoinated member of second gerneration *Vinca* dimer alkaloids with higer potency than its parent drug vinorelbine, and is currenctly under phase III clinical trails as a tubulin inhibitor[39]. Fluorination on Doxorubicin, an anthracyclin based broad spectrum anti-cancer agent with limited clinical use due its side effects (cardiac toxicty and drug resistance), led to the development of *Valrubicine*, a marked drug against bladder carcinoma. Fluorinatated stereoisomers[41] of neurotransmitter, ϒ-aminobutyric acid, displayed selective pharmacological effect on the $GABA_C$ receptor, with (2S,3S)-4-ammonio-2,3 difluorobutanoate as an agonist (IC_{50} = 155 µM) and (2R,3R)-4-ammonio-2,3 difluorobutanoate as an antagonist (IC_{50} =128 µM). In our group's prior work, we showed that stereospecific fluorination on the azepane ring of balanol increased PKC isozyme selectivtity[40].

1.2.4 Fluorinated balanoids for improved potency and PKC isozyme specificity

Fluorine significantly alters the binding interactions in protein-ligand complexes, through direct interaction of fluorine with the protein or indirect effects via modulating the conformation of the ligand[32, 40]. Apart from these effects, fluorine is bioisosteric with

hydrogen capable of forming halogen bonding[42, 43] (sigma hole donations), hydrogen bonding and polar interactions[44] (C–F…C=O) while improving protein-ligand binding affinities and hence pharmacokinetic properties. Inspired by approaches of natural product fragment based drug design and recent recognition on the role of conformational entropy in protein ligand interactions[45], our group has utilized stereospecific fluorination of natural products for conformational tuning, in order to enable conformationally coupled diversity-orientated (CDOS) synthesis of azepane-fluorinated analogues of (-)-balanol[40, 46-48].

We have first investigated stereoselective deoxyfluorination (Scheme 1) on the azepane ring of balanol for accessing fluorinated balanoids in order to improve on isozyme specificity in homologous ATP-pockets of PKC isozymes and PKA[40, 46, 49]. Deoxyfluorination of azepanols by either DAST or Deoxofluor® afforded fluorinated azepanes **1.34** in high yields[40, 48]. Computational (DFT studies) and spectroscopic data (qualitative *J*-coupling analysis) of monofluorinated azepanes[46] displayed that conformational bias can be imposed by a single fluorine due to benzyloxy azido diequitorial preference, azido gauche, and fluorine gauche effects. Furthermore, the conformational analysis of mono-, di-, and trifluoroazepanes indicated that synergistic conformational effects are highly dependent on position of the fluorine and multiple fluorinations do not necessarily exhibit additive effects in conformational control[49]. Fluorinated azepane fragments were coupled with the remaining two fragments to furnish fluorinated balanoids **1.40** – **1.43** for testing binding affinities against PKA and PKC isozymes (Table 1)[47]. C5-S fluorobalanoid **1.43** showed 1.8–fold increase in potency and selectivity of toward PKCε[47].

Table 1. SAR studies of mono- and difluorinated balanoids against PKA and PKC isozymes[47].

		K_d (nM)		
PKA/PKC isozymes	**(-)-balanol**	**1.43**	**1.40**	**1.42**
PKA	5.9	6.4	10	9.2
PKCδ	4.5	4.9	15	19
PKCε	0.73	0.4	24	110
PKCθ	25	24	140	580

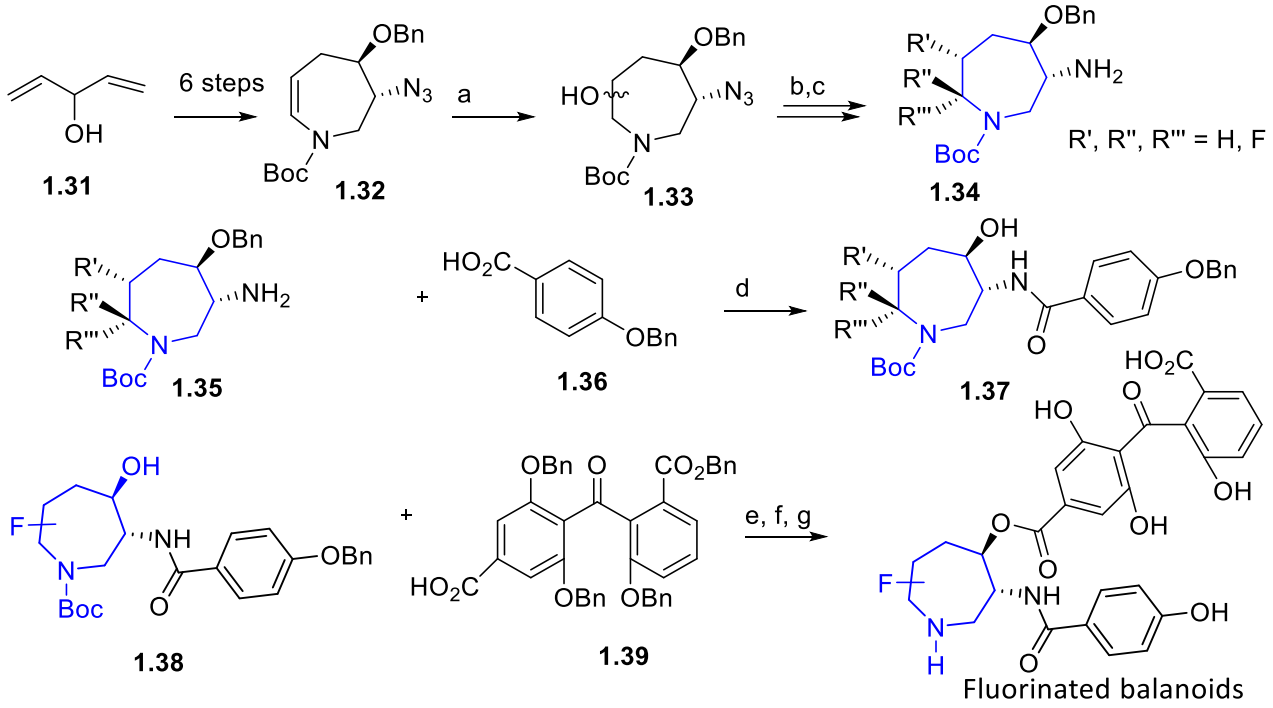

Scheme 1. Synthesis of fluorinated balanoids; reagents and conditions: (a) i) $Me_2S{\cdot}BH_3$, THF, 25 °C, 14 h, ii) EtOH, 6 *N* NaOH, H_2O_2, 50 °C, 1 h; (b) DAST or Deoxofluor®, DCM, 25 °C, 1.5 – 3.5 h, 95 – 98 %; (c) H_2, Pd/C, triflic acid, MeOH, 14 h, 25 °C ; (d) Et_3N, 4–benzyloxybenzoyl chloride, 2 h, 25 °C; (e) 2-chloro-1-methylpyridinium iodide, DMAP, NEt_3, DCM, 8 h, 25 °C, 75%; (f) H_2, Pd/C, THF, H_2O, AcOH, 25 °C, 10 h; (g) TFA, neat, 5 min., 25 °C, 70%.

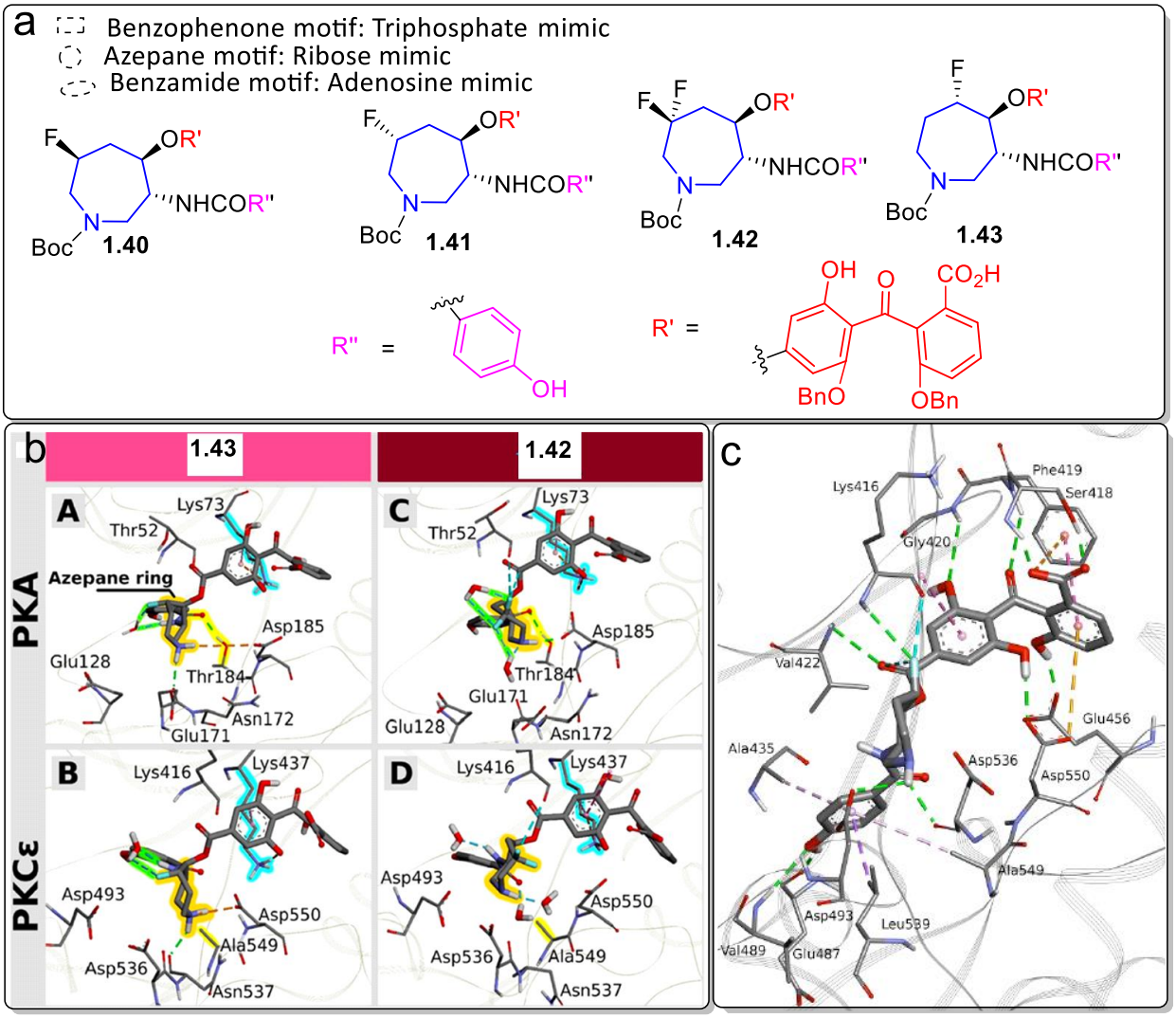

Fig. 5. Fluorinated analogs of (-)-balanol[40, 48, 49]; (a) structures of fluorinated balanoids; (b) Interactions of **1.43** and **1.42** with PKA (A and C) and PKCε (B and D), cyan and yellow colors represent invariant lysine and azepane respectively[50]; (c) Docking analysis of **1.43** in the ATP pocket of PKCε[40].

Docking studies[51] of the fluorinated balanoids with PKC isozymes and PKA showed that **1.43** in its bound form has synergistic chemical and conformational effects in PKCε (Fig. 5b). The hydrogen bonding between the positively charged nitrogen on the azepane ring and the nearby carboxylate amino acid residue was facilitated by oxygen-fluorine *gauche* effects. Furthermore, the stereoselective fluorination aided highly selective protein-ligand interactions between the benzophenone motif and the flexible glycine loop without disturbing the existing interactions. Other fluorinated balanoids (**1.40**, **1.41**, **1.42**), however,

do not show such synergistic conformational effects, and reduction of protein-ligand interactions can be attributed to the loss of fluorine gauche effects or ligand interactions.

Our molecular dynamics (MD) studies[50] on balanoid C5-F **1.43** in PKCε showed that fluorination (Fig. 5b) enhances the interaction between benzophenone and the key catalytic invariant Lys437 residue. This lysine residue is involved in the phosphoryl group transfer, aligns ATP for catalysis and stabilizes the conformation of other catalytically active kinases. In PKA, the fluorination caused a decrease in ligand **1.43** (Fig. 5b) interaction with the equivalent lysine Lys73 residue. In PKA, Thr 184 diminishes the global fluorine effects by isolating the fluorine effects to the azepane binding sites, whereas in PKCε, Ala549, facilitates the transmission of global fluorine effect to other binding sites resulting in enhanced interactions with the key invariant Lys437 residue.

Our previous docking and MD studies[50, 51] have also identified the imperative role of the D ring of benzophenone in interacting with the active sites and flexible loops of the protein. Replacement of the hydroxyl group or insertion of one or two fluorine substituents may provide new hydrogen bonding interactions with the flexible loops and potentially enhance isozyme selectivity. Based on these findings, this Masters training approaches the synthesis of fluorinated BP fragments to turn into fluorinated balanoids for biological testing in the future.

1.3 Synthetic approaches of the BP fragment of (-)-balanol

To date, around 50 studies based on total and formal syntheses have been reported for balanol. Majority of the protocols correspond to Lamp's or Nicolaou's methods involving a key Fries intramolecular rearrangement for assembling the congested BP fragment. Depending on the key bond formation reactions, a few different strategy class methods are described in (Table 2). Synthesis of congested benzophenones such as the tetra-ortho-substituted benzophenone core is often capricious.

Table 2. Summary of key approaches to the BP core synthesis of balanol.

Synthetic Route	Steps	Yield %	Key Synthetic Reactions
Lamp & Hughes[43]	13	10	Carbonylation via Li-X, homo-Fries rearrangement
Nicolaou[42]	15	20	Carbonylation via Li-X, Mitsunobu esterification, homo-Fries rearrangement, Pinnick oxidation
Vicker[48]	9	4	Acyl substitution via aryl Grignard
Barbier	8	Not reported	Acyl substitution with benzodioxol-2-one
Skrydstrup[46]	5	19	Intramolecular Heck reaction
Noncovich[52]	11	12	OBoc directed magnesiation
Tanner[47]	10	25	Aryl Li quench with DMF to the aldehyde
Anderson[53]	11	2.7	S_NAr *via* organoiron arene complex
Naito[54]	11	3.7	Baeyer-Villiger oxidation of anthraquinone

Lamp and Hughes's protocol[16]

Lamp and Hughes[16] were the first to report the total synthesis of balanol soon after its isolation (Scheme 2). The targeted BP moiety **1.3** was accessed in thirteen steps using 4-bromo-3,5-dihydroxybezoic acid and 2-bromo-3-benzyloxybenzyl alcohol with an overall yield of 10%, involving key reactions such as lithium-halogen exchange and carbon dioxide trapping, followed by an anionic homo-Fries rearrangement.

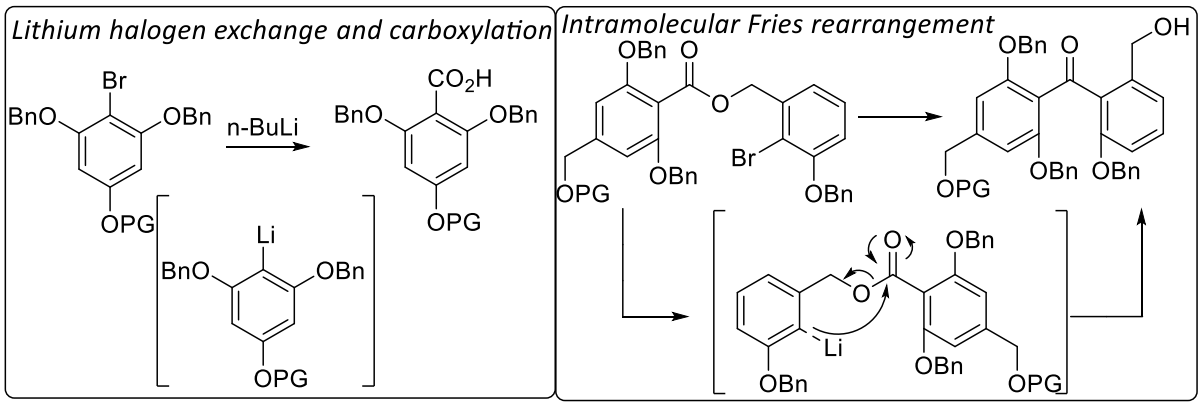

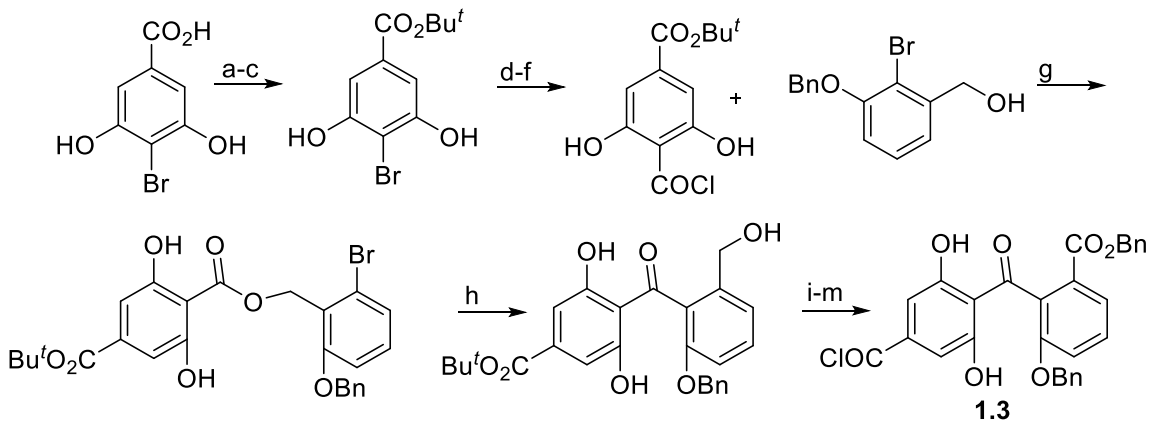

Scheme 2. Lamp and Hughes's BP synthesis, reagents and conditions. (a) BnBr, K_2CO_3; (b) NaOH; (c) CDI, *t*–BuOH, DBU; (d) *n*–BuLi, -78 °C; (e) CO_2; (f) $(COCl)_2$; (g) *t*–BuOK, THF; (h) *n*–BuLi, THF, -78 °C; (i) PDC, DMF; (j) Bu_4NMnO_4, pyr; (k) BnBr, K_2CO_3; (l) quinoline, 205 °C; (m) $(COCl)_2$, DMF.

Nicolaou's protocol[19]

Nicolaou and co-workers[19] synthesized BP **1.3** with a net yield of 20% in fifteen steps using hydroxyl benzaldehyde as the starting material (scheme 3). The methods synthesis BP using a protocol similar to Lamp with minor modifications. The key ones are Mitsunobu reaction and Pinnick oxidation. The tetrahydroazepane fragment was accessed from D-serine, involving diastereoselective allylboration and base-catalyzed, ring closure reaction as key steps. Protected benzophenone and azepane fragments were coupled by an ester linkage following the Mukaiyama protocol.

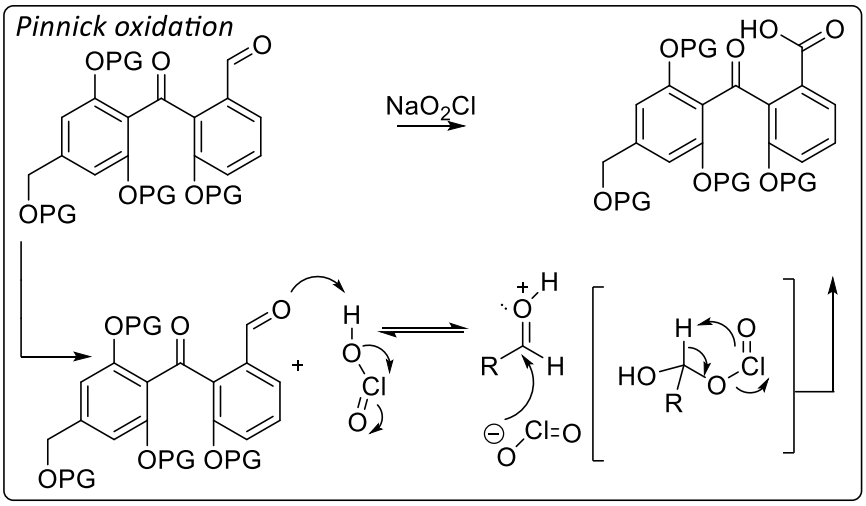

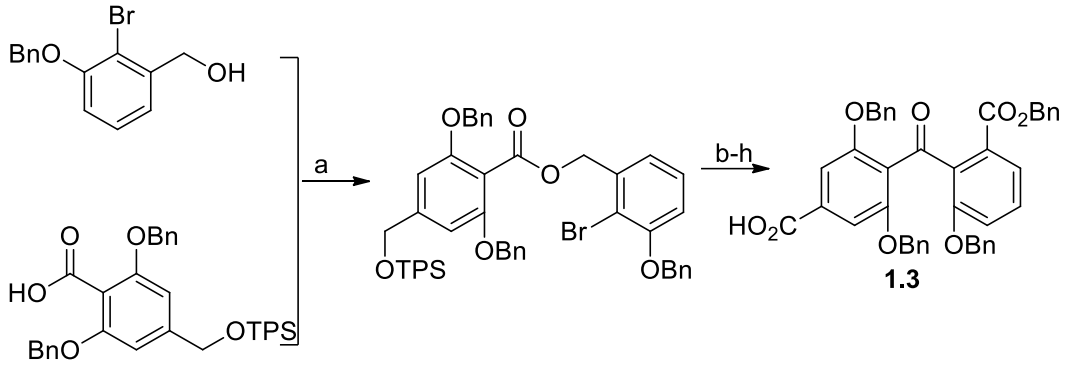

Scheme 3. Nicolaou's BP synthesis, reagents and conditions. (a) DEAD, PPh_3, THF; (b) *n*–BuLi, THF, -78 °C, aq. NH_4Cl; (c) NMO, TPAP, MeCN; (d) $NaClO_2$, NaH_2PO_4, 2–methyl–2–butene, THF, *t*–BuOH, H_2O; (e) BnBr, K_2CO_3, DMF; (f) TBAF, THF; (g) NMO, TPAP, MeCN; (h) $NaClO_2$, NaH_2PO_4, 2–methyl–2–butene, THF, *t*–BuOH, H_2O.

Barbier's protocol[55]

Barbier and colleges synthesized BP **1.4** in just eight steps using protocols correspondent to Nicolaou, Lamps and Hughes methods. BP fragment is accessed using the key Fries rearrangement reaction (Scheme 4). However, this protocol deviates from Lamp's and Nicolaou's methods mainly in accessing di-acyl fragment using benzodioxol-2-one. The advantage of this method is that the BP core synthesized is accomplished in less steps, albeit with unspecified yields, which increases the ambiguities in its practical use.

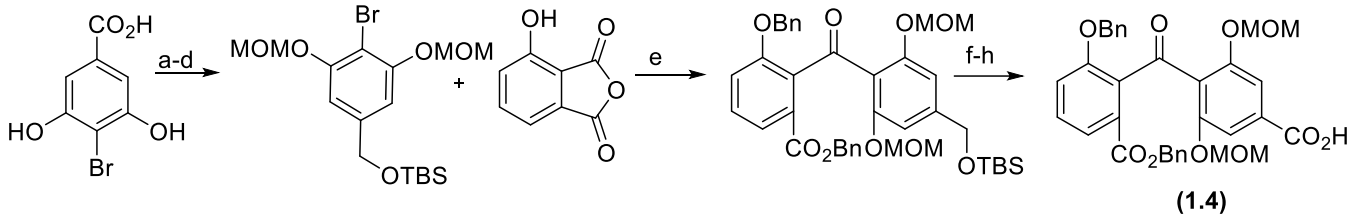

Scheme 4. Barbier's BP synthesis, reagents and conditions. (a) MeOH, HCl (g); (b) i) NaH, THF, DMF; ii) MOMCl; (c) $LiAlH_4$, THF; (d) TBDMSCl, imidazole, DMF; (e) i) *n*–BuLi, THF; ii) BnBr; (f) Bu_4NF, THF; (g) MnO_2, DCM; (h) MMPP, DMF.

Hollinshead's protocol[56]

Hollinshead (Scheme 5) and co-workers synthesized the tetra-*ortho* substituted BP core **1.5** of balanol, using 3-benzyloxy benzyl alcohol and 4-bromo–3, 5–dihydroxybenzoic acid as starting materials. Tri substituted, cyclic ketal protected aldehyde was prepared *via* lithium–

bromine exchange, followed by quenching with DMF. The tetra substituted, *ortho* MOM (Methoxymethyl) protected BP was accessed involving a homo-Fries rearrangement.

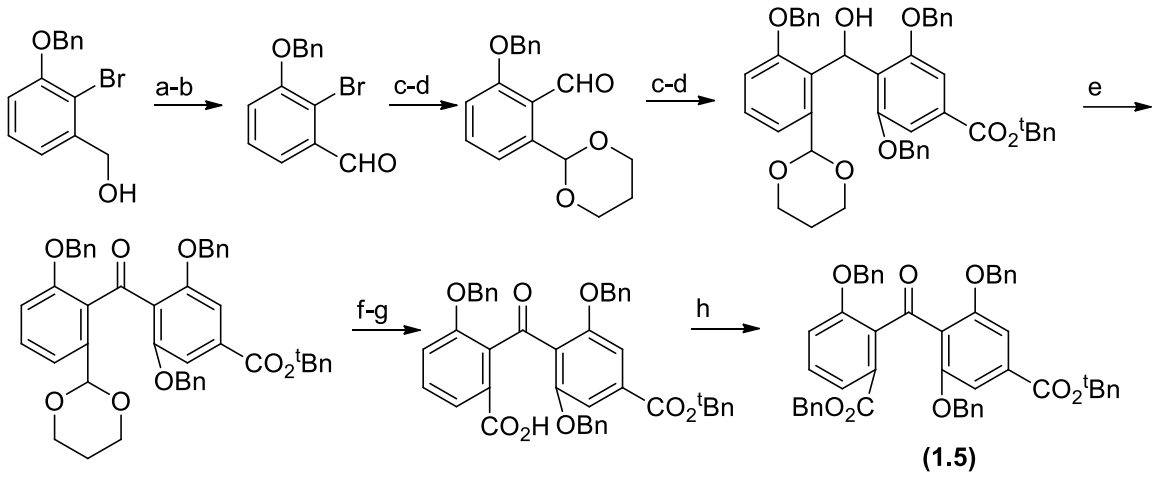

Scheme 5. Hollinshead's BP synthesis, reagents and conditions. (a) *n*–BuLi, PhME, -20 °C; (b) $BrF_2CH_2CH_2F_2Br$; (c) TEMPO, THF, NaBr, NaOCl, 0 °C; (c) $HO(CH_2)_3OH$, *p*–TSA, PhMe, reflux; (d) *n*–BuLi, THF, -78 °C, DMF; (e) *n*–BuLi, THF, -78 °C; (f) MnO_2, DCM; (e) *p*–TSA, acetone, H_2O, reflux; (f) $NaClO_2$, NH_2SO_3H, ACN, H_2O; (g) BnBr, K_2CO_3, DMF; (h) quinolone, 205 °C.

Tanner's protocol[57]

Tanner and associates[57] synthesized the BP **1.6** with modification of the Hollinshead method at low temperatures in the presence of TPAP rather than MnO_2 as an oxidizing agent (Scheme 6). The key steps in accessing the BP correspond to Lamp's anionic Fries rearrangement using *n*-BuLi and $NaClO_2$ mediated Pinnick oxidation. However, the main drawbacks of the Tanner/Hollishead methods are poor yields in the key lithium halogen exchange reaction for carboxylation and elaborate chromatographic purifications for obtaining Fries rearrangement product.

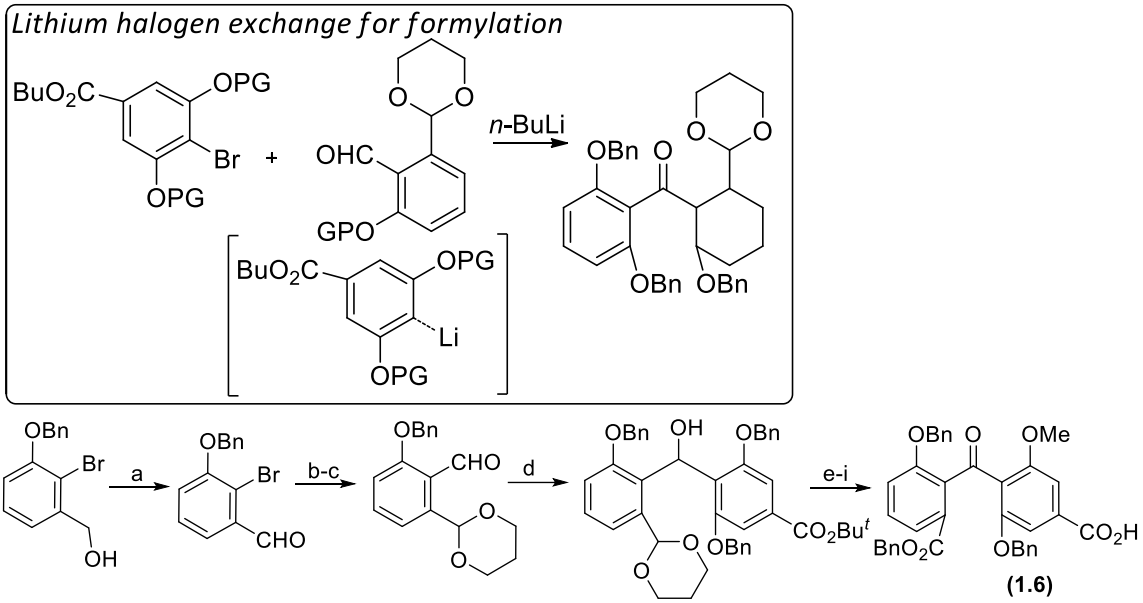

Scheme 6. Tanner's BP synthesis, reagents and conditions. (a) TEMPO, THF, NaBr, NaOCl, 0 °C; (b) $HO(CH_2)_3OH$, p–TSA, PhMe, reflux; (c) *n*–BuLi, THF, -78 °C, DMF; (d) 1.12, *n*–BuLi, THF, -110 °C; (e) TPAP, NMO, DCM; (f) *p*–TSA, acetone, H_2O, reflux; (g) $NaClO_2$, H_2NSO_3H, MeCN, H_2O; (h) BnBr, K_2CO_3, DMF; (i) quinoline, 205 °C

Noncovich's protocol[52]

Recently, Noncovich sought to access highly congested BP utilizing OBoc directed magnesiation with an overall yield of 12%. Substituted arenes were accessed through a lithium halogen exchange, coupling between aryl lithiate and aldehyde through Hollinshead-like condensation which corresponds to the Lamp and Nicolaus's protocols. This method has reported complex mixture formation in the methoxymethyl ether (MOM) deprotection step and overall the BP is furnished in a relatively low overall yield of 11%.

Skrydstrup's protocol[58]

Skrydstrup[58] sought to synthesize benzophenone by application of intramolecular Heck's coupling reaction between two aryl rings. The Heck's reaction proved feasible for furnishing a biaryl-substituted, seven-membered ring lactone with an exocyclic alkene, which upon hydrolysis and oxidative cleavage in presence of ruthenium tetraoxid, afforded the

benzophenone fragment. The key intramolecular Heck's reaction is lower yielding at an elevated temperature with 10–20% catalytic loading, compared to the Lamp/Nicolaou approach via anionic Fries rearrangement that produced the BP core in good yields.

Vicker's protocol[59]

Vicker and colleagues[59] afforded the tetra-ortho-substituted BP **1.7** in a net 4% yield in just nine steps, featuring a key acyl substitution reaction via an aryl Grignard reagent (Scheme 7). The method furnishes BP in low yields however, which limits its practical application.

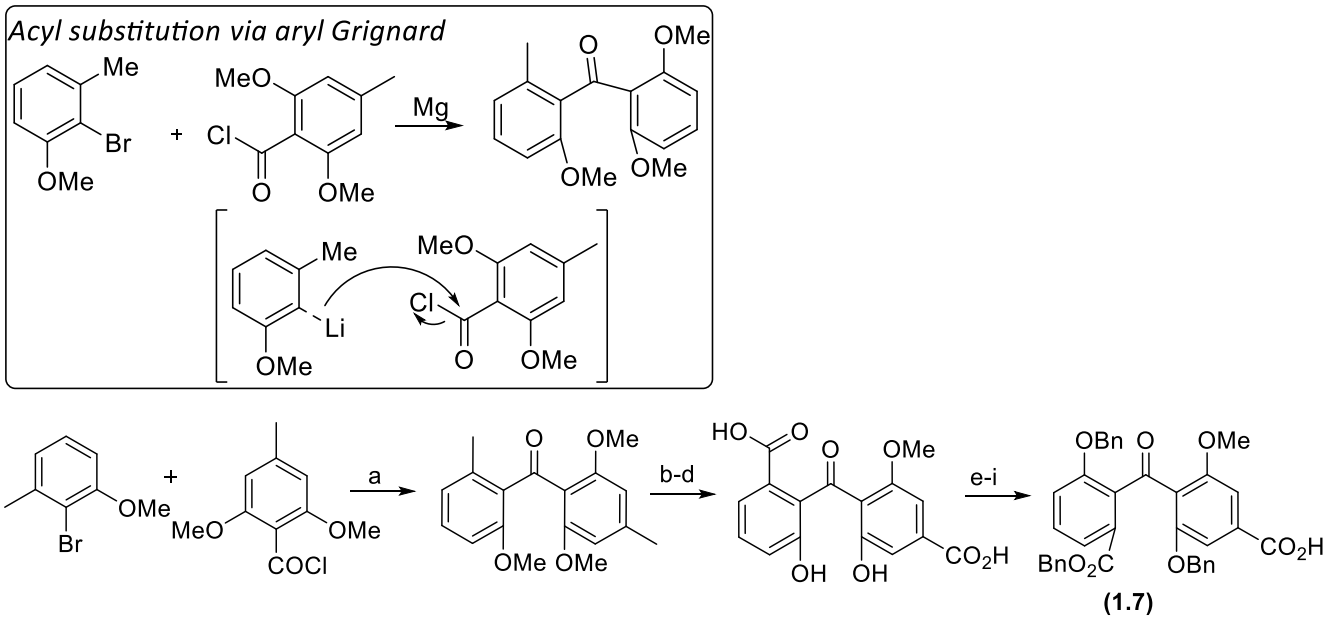

Scheme 7. Vicker's BP synthesis, reagents and conditions. (a) Mg, THF; (b) $KMnO_4$, pyridine (aq.); (c) $SOCl_2$, MeOH; (d) BBr_3, DCM; (e) $SOCl_2$, MeOH; (f) NaH, BnBr, DMF; (g) BBr_3, DCM; (h) NaH, BnBr, DMF; (h) Na_2CO_3 (aq.), EtOH

Miscellaneous BP synthesis

Anderson accessed the BP **1.8** core via an organoiron arene complex in 11 steps with an overall yield of 2.7%. (Scheme 8A). However, this method suffers limited scope due to the sluggish reaction rates and low yields.

A.

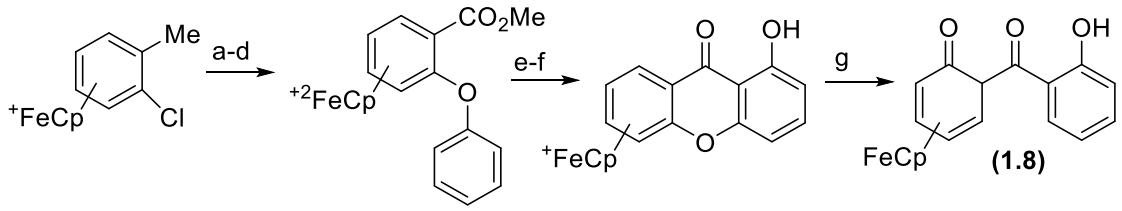

B.

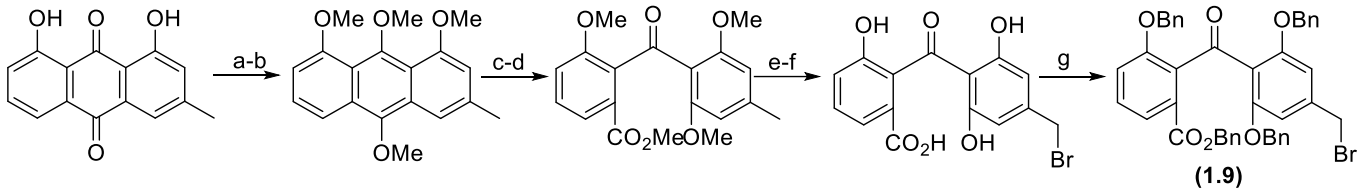

Scheme 8. Miscellaneous BP syntheses, reagents and conditions. A. Anderson's protocol; (a) aq. $KMnO_4$, $MgSO_4$, reflux; (b) $SOCl_2$, 3 h; (c) MeOH, r.t, 1 h; (d) PhONa, acetone, -70 °C, 5 h; (e) LiOH, MeOH/H_2O, r.t, 16 h; (f) PPA, 100 °C, 3 h; (g) NaOH, MeOH/H_2O, r.t, 3 h. B. Naito's protocol; (a) Me_2SO_4, K_2CO_3, $(CH_3)_2CO$, reflux; (b) i) $Na_2S_2O_4$, Bu_4NBr, THF, H_2O; ii) 6 *N* KOH, Me_2SO_4, r.t.; (c) O_2/hv, Et_2O, H_2SO_4, acetone; (d) NaH, MeI, DMF; (e) NBS, AIBN, CCl_4, reflux; (e) BBr_3, DCM, r.t.; (f) BnBr, K_2CO_3, DMF.

Naito[54] synthesised BP **1.9** via Baeyer-Villiger oxidation of anthraquinone. This synthesis was accomplished in 11 steps with an overall yield of 3.7% via a possible biomimetic Baeyer-Villiger approach of synthesis (Scheme 8B). Presumably, this method offers limited scope to scaffolds bearing acid sensitive functional groups and may lead to undesirable side reactions/deleterious effects.

In this Mres project, fluorinated BP's will be accessed using Nicolaou protocol given the scalability and versatility of this protocol. The group's previous investigations in the alternative routes such as Grignard's coupling and magnesium halogen exchange for carboxylation for assembling the BP fragment did not yield fruitful results in reproducing reported yields. The Nicolaou protocol has turned out to be a reproducible protocol in our

group. Furthermore, the key reactions such as lithium halogen exchange and intramolecular Fries rearrangement have been widely employed for the synthesis of congested benzophenones analogues to the BP fragment of balanol.

1.4 Project Outline

Following our general strategy of using fluorinated natural-product like fragments to access conformationally tuneable chemical diversity, this project will explore the benzophenone fragment of (-)-balanol.

Previous SAR and docking studies have indicated the important role of the D ring hydroxy groups in forming H bonding and tolerance to modification of D-ring. The current goal is to access mono- and difluorinated BP fragments, capable of forming hydrogen and halogen bonding, coupled to the two fragments of balanol to expand SAR for PKC isozyme selectivity. Retrosynthetically, the BP fragments would be constructed via the Nicolaou's protocol utilizing key reactions such as Li halogen exchange followed by the trapping of the resultant aryl lithiate with dry ice affording the acid for Mitsunobu esterification. Intramolecular Fries rearrangement of the mono- and difluorinated esters **2.18** and **2.36** will then furnish the corresponding benzophenones**.** Access to the mono and di fluorinated D-ring of the BP will be through commercially available 2-bromo-4-fluorobenzyl alcohol and 2-bromo-3, 4-difluorobenzoic acid, respectively (Scheme 9). Part of this project is also to investigate the effects of fluorine in the Fries rearrangement product.

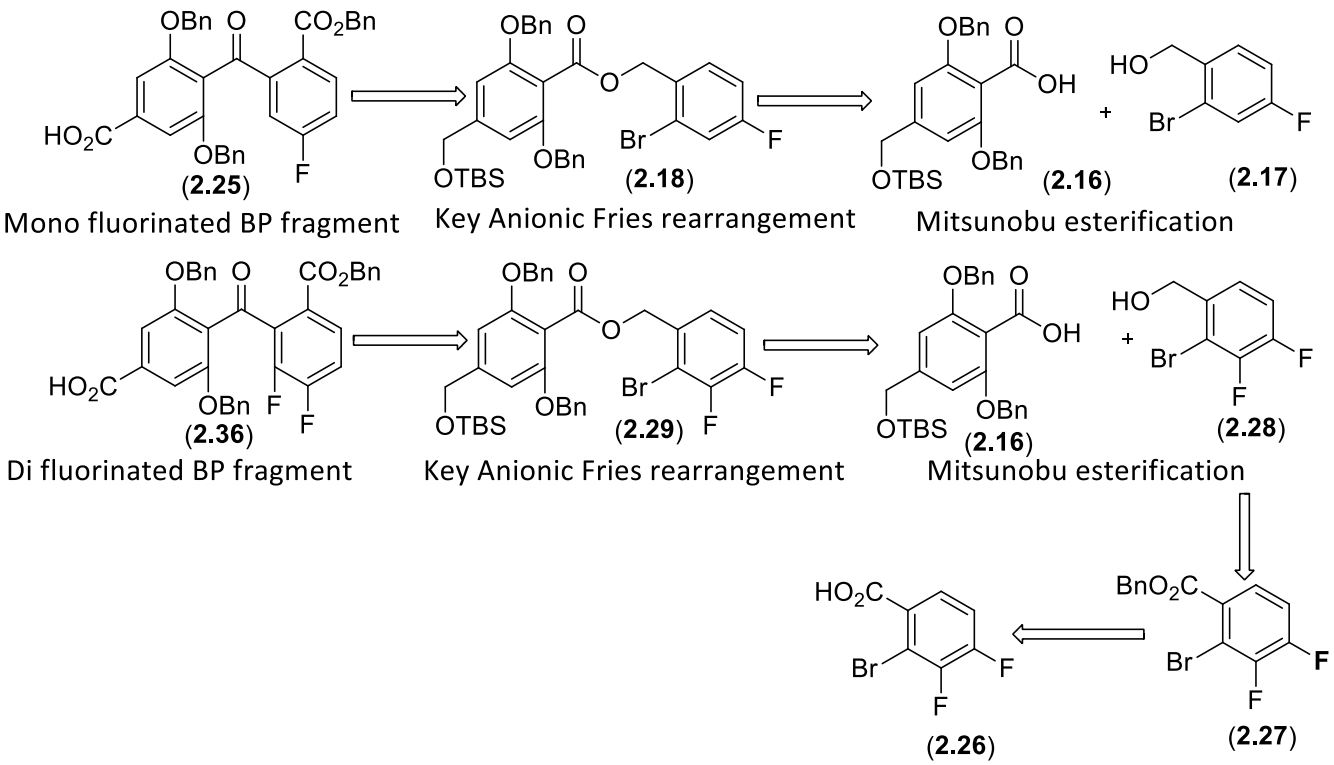

Scheme 9. Retrosynthesis of the fluorinated BP fragments.

2. Experimental

Synthetic procedures, characterization and spectral data of all compounds are discussed in the following sections. All relevant spectra for new compounds are presented in the Appendix at the end of the thesis.

2.1 General Methods

Unless stated otherwise, all reactions were conducted in flame-dried glassware under either nitrogen or argon atmosphere. DCM was distilled from calcium hydride. DMF, and THF were obtained from solvent purification system and stored over 4 Å beads. THF for Li halogen exchange reactions was either distilled from sodium-benzophenone still (a gift from UNSW) or calcium hydride. TMSCl obtained from Oakwood's was freshly sublimed. Imidazole obtained from Fluka was recrystallized from DCM and acetone. Air and moisture sensitive materials were manipulated under nitrogen or argon using vacuum lines and syringe techniques. All other commercially reagents were used without further purification. All reactions were magnetically stirred and monitored by thin-layer chromatography (TLC) using Merck silica gel 60 F254 pre-coated plates (0.25 mm). Flash column chromatography was performed using silica-gel (0.032-0.063 mm particle size) from Fisher Scientific. ^{1}H NMR spectra were obtained at 25 °C on either a Bruker DRX500K or DPX400 NMR spectrometer and are reported in ppm using the specified solvent as the internal standard, 7.26 ppm for $CDCl_3$, 5.2 ppm for CD_2Cl_2, 3.2 ppm and 4.7 ppm for methanol-d_4, 2.05 ppm $(CD_3)_2$ CO. ^{13}C NMR spectra were obtained using the same instruments and reported in ppm, using the specified solvent as the internal standard (77.37 ppm for $CDCl_3$, 53.9 ppm for CD_2Cl_2, 48.2 ppm for methanol-d_4).LRMS (ESI) was conducted using an Agilent LCMS 1260 Infinity. IR spectra (thin film) were recorded on FTIR Nicolet iS10.

2.2 Synthetic procedures and characterization of intermediates

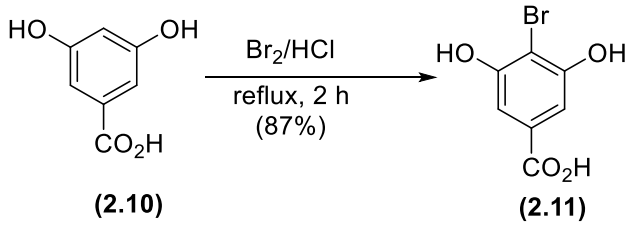

(2.10) **(2.11)**

4-bromo-3, 5-dihydroxybenzoic acid (**2.11**): Bromine (3.1 g, 19.5 mmol) was added dropwise to a suspension of 3, 5-dihydroxy benzoic acid **2.10** (3 g, 19.5 mmol) in 20% hydrochloric acid (33 mL) under nitrogen. The reaction was allowed to reflux for 2 h (TLC) until completion. The reaction mixture was cooled down to room temperature before extraction with diethyl ether (4 x 4 mL). The combined organic layer was washed with sodium thiosulphate (6 mL), brine (4 mL), water (2 mL) and dried over Na_2SO_4. The volatiles were removed under reduced pressure to afford **2.11** (3.9 g, 87%) as a white solid with ^{1}HNMR and ^{13}C matching to those reported previously[19]. ^{1}H NMR (400 MHz, d_6-acetone) δ 7.2; ^{13}C NMR (100MHz, *d*-acetone) δ 166.2, 155.3, 130.6, 120.7, 116.2, 108.1, and 103.5.

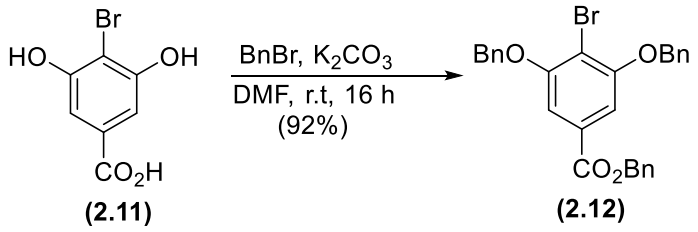

Benzyl 3,5-bis(benzyloxy)-4-bromobenzoate (**2.12**): To a solution of 4-bromo, 3, 5-dihydroxybenzoic acid **2.11** (0.69 g, 15 mmol), and K_2CO_3 (2.1 g, 15 mmol) in DMF (6 mL), benzyl bromide (1.7 g, 2.8 mmol) was added dropwise for 10 min. The reaction was allowed to stir for 16 h, at ambient temperature under nitrogen. The reaction was quenched by addition of water (35 mL), and the precipitate formed was filtrated, rinsed with water (10 mL), and diethyl ether (2 x 2 mL). The solid residue was then recrystallized from ethyl acetate to obtain the desired ester **2.12** (1.38 g, 92%) as white crystals with the ^{1}H NMR and ^{13}C NMR spectra matching to those reported previously[19]. ^{1}HNMR (400 MHz, $CDCl_3$) δ 7.29-7.43 (m, 17 H), 5.34 (s, 2H), 5.22 (s, 4H); ^{13}C NMR (100MHz, $CDCl_3$) δ 156.4, 141.5, 136.6, 128.6, 127.9, 127.0, 104.9, 101.5, 70.9, 65.1.

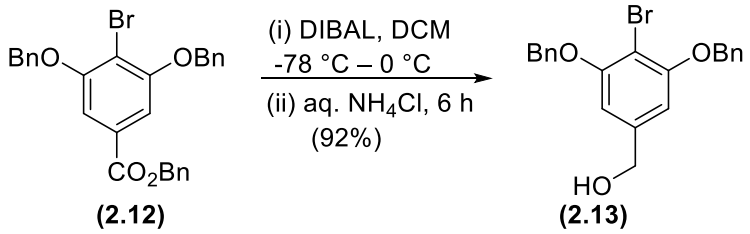

(3,5-bis(benzyloxy)-4-bromophenyl)methanol (**2.13**): Diisobutylaluminium hydride (15.5 mL, 1M in DCM) was added over 10 min to **2.12** in dichloromethane (30 mL) at -78 °C under nitrogen. The reaction mixture was stirred at 0 °C for 2 h before quenching with aq. NH_4Cl (0.62 mL) and dilution with DCM (20 mL). The reaction mixture was further stirred for 4 h, at ambient temperature. The aqueous layer was extracted with DCM (2 x 10 mL), washed with brine (5 mL), water (3 mL) and dried over $MgSO_4$. The volatiles were removed under reduced pressure and the crude product was recrystallized from EtOAC: hexane to afford the desired alcohol **2.13** (1.7 g, 92%) as white crystals with ^{1}H NMR and ^{13}C matching to those reported previously[19]. ^{1}H NMR (400 MHz, $CDCl_3$) δ 7.26-7.51 (m, 10H), 6.62 (s, 2H), 5.21 (s, 4H), 4.62 (s, 2H); ^{13}C NMR (100 MHz, $CDCl_3$) δ 156.4, 141.5, 136.6, 128.6, 127.9, 127.0, 104.9, 101.5, 70.9, 65.1.

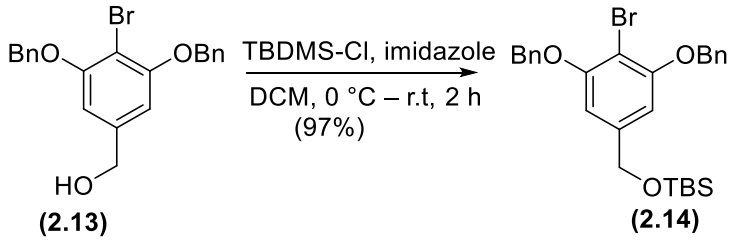

((3,5-bis(benzyloxy)-4-bromobenzyl)oxy)(tert-butyl) dimethylsilane (**2.14**): Freshly sublimed tert-butyldimethylsilyl chloride (TBDMS-Cl), (0.91 g, 6 mmol) was added to a solution of alcohol **2.13** (1.6 g, 4 mmol) and imidazole (0.41g, 6 mmol) in dry DCM (52 mL) at 0 °C under nitrogen. The reaction mixture was allowed to stir for 2 h at room temperature before quenching with water (30 mL). The aqueous layer was extracted with EtOAC (30 mL), washed with brine (5 mL), water (2 mL) and dried over $MgSO_4$. The volatiles were removed under reduced pressure. The crude reaction mixture was subjected to flash chromatography (10% EtOAC: hexanes) to afford **2.14** (2 g, 97%) as white crystals with ^{1}H and ^{13}C matching to those reported previously[19]. ^{1}H NMR (400 MHz, $CDCl_3$) δ 7.26-7.49 (m, 10H), 6.62 (s, 2H), 5.23 (s, 4H), 4.62 (s, 2H), 0.93 (s, 9H), 0.05 (s, 6H); ^{13}C NMR (100MHz. $CDCl_3$) δ 156.2, 142.3, 136.7, 128.6, 127.8, 126.9, 104.2, 100.5, 70.8, 64.6, 25.9, 18.4, and 5.3.

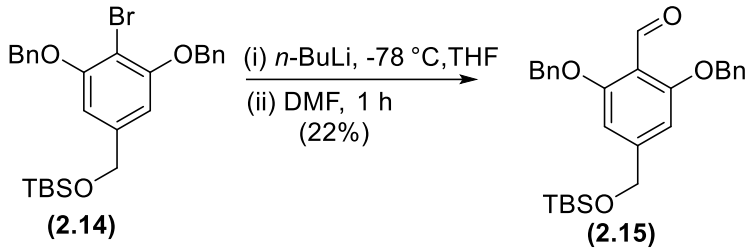

2,6-bis(benzyloxy)-4-(((tert-butyldimethylsilyl)oxy)methyl)benzaldehyde (**2.15**): *n*-BuLi (0.1 mL, 2 M in cyclohexane) was added dropwise, over 4 min to a solution of silyl ether **2.14** (470 mg, 0.92 mmol) in THF (1.5 mL) from SPS at -78 °C under argon and stirred for 20 min. The reaction was quenched with dry DMF (5 equiv. 350 µl) and allowed to stir for 40 min at -60 °C. The volatiles were removed under reduced pressure followed by the addition of aqueous NH_4Cl (1 mL) and DCM (5 mL). The aqueous layer was extracted with DCM (2 x 5 mL). The combined organic layer was washed with brine (1 mL), dried over MgSO4, filtered and concentrated under reduced pressure. The crude reaction mixture was purified by flash chromatography (10% EtOAC: hexanes) to furnish **2.15** (85 mg, 22%) as a white solid. IR v_{max} cm^{-1} 1682, 1611, 1440, 1101; ^{1}H NMR (400 MHz, $CDCl_3$) δ 10.54 (s, 1H, CHO), 7.39-7.18 (m, 10H), 6.54 (s, 2H), 5.12 (s, 4H), 4.60 (s, 2H), 0.86 (s, 9H), -0.001 (s, 6H); ^{13}C NMR (100MHz. $CDCl_3$) δ 188.8, 161.3, 150.5, 136.4, 128.6, 127.9, 127.5, 126.9, 113.8, 102.6, 70.5, 64.6, 25.8, 18.3, -5.3; LRMS (ESI) *m/z* (relative intensity) 463.1 (100% M + H^+).

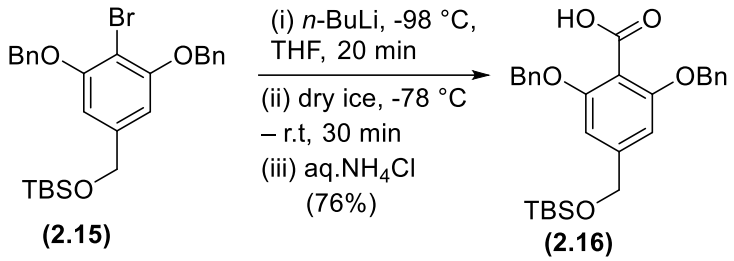

2,6-bis(benzyloxy)-4-(((tert-butyldimethylsilyl)oxy)methyl)benzoic acid (**2.16**): *n*-BuLi (1.9 mL, 2.5 M in cyclohexane) was added drop wise over 10 min to a solution of silyl ether **2.15** (2 g, 4.05 mmol) in THF (38 mL) freshly distilled from benzophenone-sodium still at -98 °C under argon and stirred for 20 min. The reaction was quenched with excess of freshly crushed dry ice and allowed to stir for 40 min at -60 °C. The volatiles were removed under reduced pressure followed by the addition of aqueous NH_4Cl (5 mL). The aqueous layer was extracted with DCM (5 x 5 mL) and the combined organic layer was washed with

brine (5 mL), dried over $MgSO_4$, filtered and concentrated under reduced pressure. The crude reaction mixture was subjected to flash chromatography (2–5% MeOH:DCM) to obtain **2.16** as white crystals (1.14 g, 76%) with ^{1}H and ^{13}C spectra matching to those reported previously[19]. ^{1}H NMR (400 MHz, $CDCl_3$) δ 7.37-7.28 (m, 4H), 7.28-7.24 (m, 4H), 7.21-7.18 (m, 2H), 6.55 (s, 2H), 5.10 (s, 4H), 4.60 (s, 2H), 0.87 (s, 9H), 0.001 (s, 6H); ^{13}C NMR (100MHz. $CDCl_3$) δ 169.9, 157.2, 146.2, 128.4, 128.3, 127.9, 127.8, 127.8, 127.5, 127.4, 127.2, 127.1, 126.9, 125.9, 11.2, 103.4, 77.1, 76.7, 70.6, 64.6, 25.9, 18.4, 5.3.

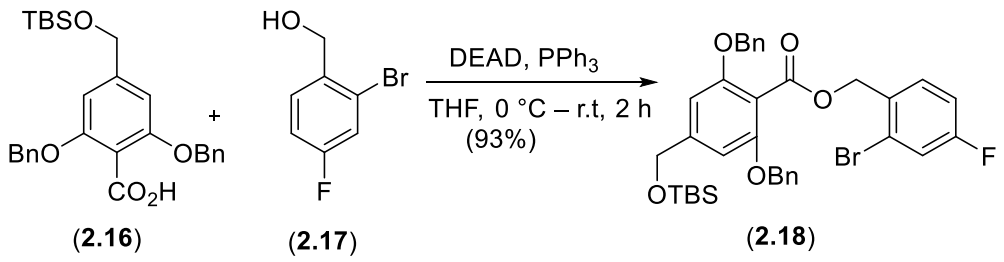

2-bromo-4-fluorobenzyl 2,6-bis(benzyloxy)-4-(((tert butyldimethylsilyl)oxy)methyl)benzoate (**2.18**): To a mixture of benzyl alcohol **2.17** (386 mg, 1.88 mmol), acid **2.16**, (900 mg, 1.88 mmol), triphenylphosphine (542 mg, 1.1 equiv.) in THF (9.2 mL), diethyl azodicarboxylate (0.26 mL, 1.1 equiv.) was added dropwise at 0 °C under argon. The reaction mixture was allowed to stir for 2 h before the volatiles were removed under reduced pressure. The crude reaction mixture was subjected to flash chromatography (15% EtOAC: hexane) to afford **2.18** as white crystals (1.2 g, 93%). IR v_{max} cm^{-1} 1737, 1486, 1257, 1096, 850; ^{1}H NMR (400 MHz, CD_2Cl_2) δ 7.31-7.18 (m, 12 H), 6.65-6.6.1 (m, 1H), 6.60 (s, 2H), 5.26 (s, 2H), 5.03 (s, 2H), 4.60 (s, 2H), 0.85 (s, 9H), -0.002 (s, 6H); ^{13}C NMR (100MHz. CD_2Cl_2) δ 165.7, 163.1 (d, J_{CF} =248.3 Hz), 156.4, 145.8, 145.8, 136.7, 131.5 (d, J_{CF} = 3.6 Hz), 130.9 (d, J_{CF} = 8.6Hz), 128.5, 127.9, 127.2, 123.0 (d, J_{CF} = 10.0Hz), 119.8 (d, J_{CF} =24.5 Hz), 114.5 (d, J_{CF} =20.7 Hz), 112.1, 102.9, 70.4, 65.6, 64.5, 25.6, 18.2, -5.6; LRMS (ESI) *m/z* (relative intensity) 665.1 (27% M +H$^+$).

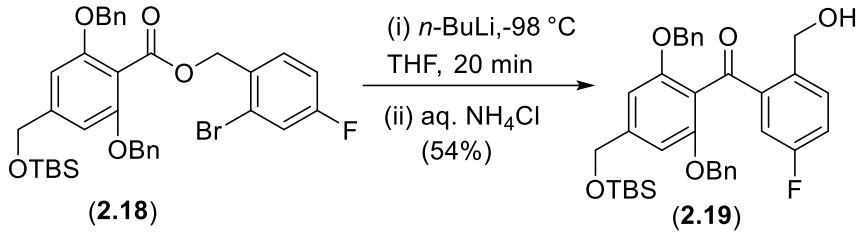

(2,6-bis(benzyloxy)-4-(((tert-butyldimethylsilyl)oxy)methyl)phenyl)(5-fluoro-2-(hydroxymethyl)phenyl)methanone (**2.19**): *n*-BuLi (0.6 mL, 2.5M) was added over 5 min to a solution of ester **2.18** (820 mg, 1.23 mmol) in THF (27 mL) distilled from benzophenone-sodium at -98 °C under argon. The reaction was allowed to stir for 20 min at the same temperature. The reaction mixture was then quenched with aqueous NH_4Cl (5 mL) after the removal of volatiles under reduced pressure. The aqueous layer was extracted with DCM (5 x 3 mL) and the combined organic layer was washed with brine (2 mL), water (3 mL) and dried over Na_2SO_4. The volatiles were removed under reduced pressure and the crude reaction mixture was subjected to flash chromatography (10% EtOAC: hexanes) to afford **2.19** (386 mg, 54%) as white crystals. IR v_{max} cm^{-1} 3026, 1607, 1581, 1455, 1291, 1133, 933; ^{1}H NMR (400 MHz, CD_3OD) δ 7.69-7.65 (m, 1H), 7.26-7.13 (m, 7H), 7.05-6.99 (m, 5H) 6.68 (s, 2H), 5.41 (s, 1H), 4.97 (s, 4H), 4.68 (s, 2H), 0.85 (s, 9H), -0.001 (s, 6H); ^{13}C NMR (100MHz. CD_3OD) δ 196.8, 162.5 (d, J_{CF} = 243.6 Hz), 156.5, 146.1, 138.9 (d, J_{CF} = 4.0Hz), 138.2 (d, J_{CF} =6.0 Hz), 136.6, 129.2 (d, J_{CF} = 7.4 Hz), 128.1, 127.5 126.7, 118.8 (d, J_{CF} = 21.0 Hz), 117.8 (d, J_{CF} = 23.0 Hz), 103.2, 69.9, 64.4, 61.5, 48.7, 48.2, 48.1, 47.8, 47.6, 47.4, 47.2, 46.9, 25.1, 17.8, 6.5; LRMS (ESI) *m/z* (relative intensity) 609.3 (23% M +Na^+).

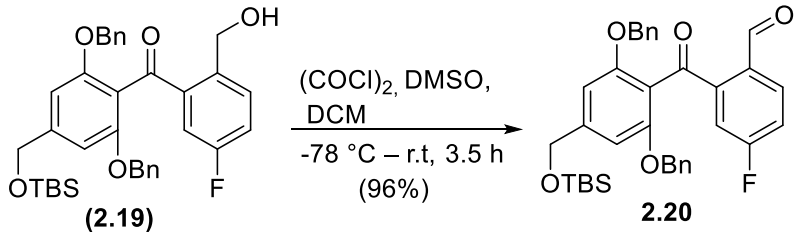

2-(2,6-bis(benzyloxy)-4-(((tert-butyldimethylsilyl)oxy)methyl)benzoyl)-4-fluorobenzaldehyde (**2.20**): DMSO (2.7 mL, 38.7 mmol) was added dropwise to a cold solution of oxalyl chloride (5 equiv., 2M in DCM) in DCM (3.5 mL) at -78 °C under argon. The mixture was stirred for 30 min before a solution of alcohol **2.19** (378 mg, 0.64 mmol) in DCM

(3.5 mL) was added dropwise over 6 min. The reaction was stirred for 1 h before being quenched with triethyl amine (8.1 mL, 58 mmol). After an additional 2 h stirring at room temperature, the volatiles were removed under reduced pressure. The residue was re-suspended in DCM, and stirred for an hour after the addition of 30% oxone solution (5 mL). The aqueous layer was extracted with DCM (2 x 5 mL), washed with sodium bicarbonate (5 mL), brine (2 mL), water (1 mL), dried over Na_2SO_4 and concentrated under reduced pressure. The solid residue was recrystallized from EtOAC: hexanes to afford **2.20** (362 mg, 96%) as pale yellow crystals. IR v_{max} cm^{-1} 1698, 1662, 1432, 1264, 1123, 853; ^{1}H NMR (400 MHz, CD_2Cl_2) δ 9.95 (1H), 7.75-7.74 (m, 1H), 7.14-6.99 (m, 13H), 6.58 (s, 2H), 4.89 (s, 4H), 4.62 (s, 2H), 0.84 (s, 9H), -0001 (s, 6H); ^{13}C NMR (100MHz. CD_2Cl_2) δ 193.9, 190.2, 166.1 (d, J_{CF} = 254 Hz), 157.3, 147.3, 145.5 (d, J_{CF} = 7.3 Hz), 136.2, 132.7 (d, J_{CF} = 3.4 Hz), 130.5 (d, J_{CF} = 8.9 Hz), 128.4, 127.9, 127.2, 118.6 (d, J_{CF} = 21.7 Hz), 116.5 (d, J_{CF} = 6.8 Hz), 116.3, 102.9 , 70.5, 64.5, 25.6, 18.2, -5.6; LRMS (ESI) *m/z* (relative intensity) 585.2 (100% M + H^+).

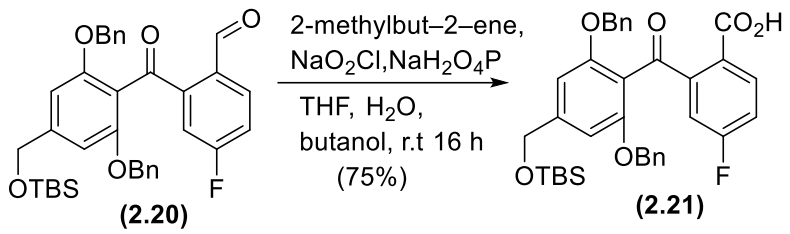

2-(2,6-bis(benzyloxy)-4-(((tert-butyldimethylsilyl)oxy)methyl)benzoyl)-4-fluorobenzoic acid (**2.21**): 2-methylbut-2-ene (330 mg, 4.7 mmol) was added to a stirring solution of aldehyde (344 mg, 0.59 mmol) **2.20** in THF (1 mL), butanol (0.9 mL) at room temperature followed by a solution of sodium chlorite (160 mg, 1.76 mmol) and sodium dihydrogen phosphate (212 mg, 1.76 mmol) in water (0.3 mL). The reaction was stirred at room temperature for 16 h. The volatiles were removed under reduced pressure and the crude reaction mixture was extracted with EtOAC (10 mL), washed with aq. NH_4Cl (5 mL), brine (3 mL), aq. sodium thiosulphate (5 mL) and water (2 mL), dried over Na_2SO_4. The crude reaction mixture was purified by flash chromatography (2 – 3% MeOH :DCM) to afford **2.21** (255 mg, 75%) as white crystals. ^{1}H NMR (400 MHz, CD_2Cl_2) δ 7.66-7.63 (m, 1H), 7.24-6.99 (m, 12H), 6.57 (s, 2H), 4.86 (s, 4H), 4.62 (s, 2H), 0.85 (s, 9H), 0.00 (s, 6H); ^{13}C NMR (100MHz.

CD_2Cl_2) δ 192.9, 170.3, 165.4 (d, J_{CF} = 260 Hz), 158.2, 147.7, 144.7, 136.3, 135.1, 132.6 (d, J_{CF} = 30 Hz), 128. 6, 128.5, 128.3, 128.2, 127.8, 127.2, 126.5, 117.4 (d, J_{CF} = 21.4 Hz), 116.4 (d, J_{CF} = 23.4 Hz), 115.9, 102.91, 71.6, 70.5, 25.7, 18.2, -5.6.

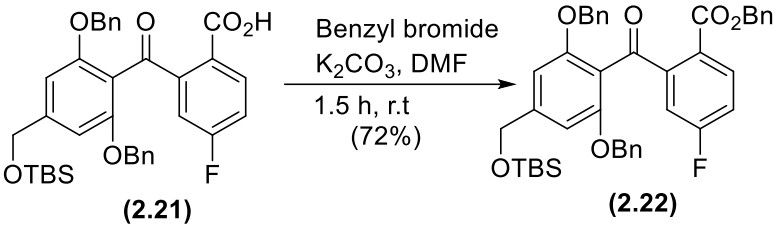

Benzyl 2-(2,6-bis(benzyloxy)-4-(((tert-butyldimethylsilyl)oxy)methyl)benzoyl)-4-fluorobenzoate (**2.22**): To a stirring mixture of acid **2.21** (255 mg, 0.42 mmol), K_2CO_3 (129 mg, 2.2 equiv.) in DMF (2.7 mL), benzyl bromide (109 mg, 1.5 equiv.) was added dropwise over 2 min under argon. The reaction was stirred for 1.5 h. Reaction was quenched with water (3 mL) and extracted with EtOAC (3 x 3 mL). The combined organic layer was washed with sodium thiosulphate (5 mL), brine (1 mL) and water (1 mL) before drying over Na_2SO_4. The volatiles were removed under reduced pressure and the crude reaction mixture was subjected to flash chromatography (10% EtOAC: hexanes) to afford **2.22** (210 mg, 72%) as colorless oil. IR v_{max} cm^{-1} 1722, 1605, 1578, 1454, 1269, 1113, 839; ^{1}H NMR (400 MHz, CD_2Cl_2) δ 7.46-7.43 (m, 2H), 7.12-6.99 (m, 16H), 6.54 (s, 2H), 4.98 (s, 2H), 4.83 (s, 4H), 4.61 (s, 2H), 0.84 (s, 9H), -0.001 (s, 6H); ^{13}C NMR (100MHz. CD_2Cl_2) δ 191.9, 167.4 (d, J_{CF} = 257 Hz), 162.3, 158.1, 147.3, 143.4 (d, J_{CF} = 6.8 Hz), 136.4, 135.8, 131.2 (d, J_{CF} = 8Hz), 128.3, 128.2, 128.0, 127.9, 127.7, 127.1, 117.5 (d, J_{CF} = 22Hz), 116.3, 116.0 (d, J_{CF} = 7.4 Hz), 102.9, 70.4, 67.1, 64.5, 25.6, 18.2, -5.6.

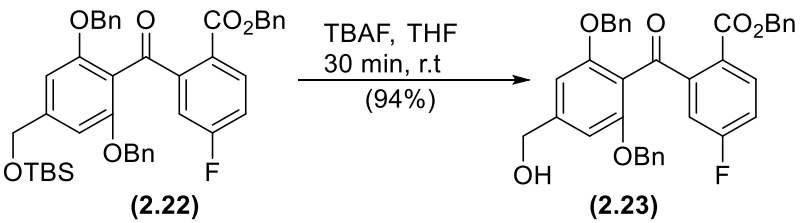

Benzyl 2-(2,6-bis(benzyloxy)-4-(hydroxymethyl)benzoyl)-4-fluorobenzoate (**2.23**): To a stirring solution of ester **2.22** (197 mg, 285 µM) in THF (3 mL), tetra-n-butylammonium

fluoride (1.2 equiv. 1M in THF) was added dropwise under argon. Upon the addition of TBAF, the color of the reaction mixture turned dark green. The reaction was allowed to stir for 30 min. The THF was removed under reduced pressure and the crude reaction mixture was subjected to flash chromatography (20 – 40% EtOAC: hexanes) to afford **2.23** (154 mg, 94%) as a white solid. IR v_{max} cm^{-1}, 3064, 1721, 1604, 1575, 1478, 1266, 1156, 1109, 733, 695; ^{1}H NMR (400 MHz, CD_2Cl_2) δ 7.48-7.02 (m, 18H), 6.61 (s, 2H), 5.02 (s, 2H), 4.87 (s, 4H), 4.06 (s, 2H); ^{13}C NMR (100MHz. CD_2Cl_2) δ 191.8, 167.4, 164.8 (d, J_{CF} = 250 Hz), 158.3, 146.8, 143.3, 136.3, 135.8, 131.2 (d, J_{CF} = 9 Hz), 128.3, 128.2, 128.0,127.9, 127.7, 127.1, 117.6 (d, J_{CF} = 22Hz), 116.3 (d, J_{CF} = 23 Hz), 103.6, 70.5, 67.1, 64.7; LRMS (ESI) *m/z* (relative intensity) 577.2 (100% M + H^+).

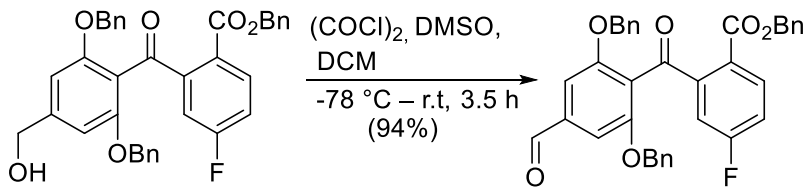

(2.23) **(2.24)**

Benzyl 2-(2, 6-bis (benzyloxy)-4-formylbenzoyl)-4-fluorobenzoate (**2.24**)**:** DMSO (0.47 mL, 6.7 mmol) was added dropwise to a cold solution of oxalyl chloride (5 equiv., 2M in DCM) in DCM (1 mL) at -78 °C under argon. The mixture was stirred for 30 min before a solution of alcohol **2.23** (64 mg, 0.11 mmol) in DCM (1 mL) was added dropwise over 2 min. The reaction was stirred for 1 h before being quenched with triethyl amine (1.4 mL, 10 mmol). After an additional 2 h stirring at ambient temperature, the volatiles were removed under nitrogen blow down. The residue was re-suspended in DCM, washed with water (2 mL), sodium bicarbonate (5 mL), brine (5 mL), water (2 mL), and dried over $MgSO_4$. The volatiles were again removed under nitrogen blow down to afford **2.24** (60 mg, 94%) as pale yellow solid. IR v_{max} cm^{-1} 1723, 1601, 1577, 1431, 1267, 1106, 734, 695; ^{1}H NMR (400 MHz, CD_2Cl_2) δ 9.85 (s, 1H), 7.54 (q, 1H), 7.16-7.07 (m, 19H), 5.02 (s, 2H), 4.95 (s, 4H); ^{13}C NMR (100MHz. CD_2Cl_2) δ 191.2, 191.1, 167.3, 164.8 (d, J_{CF} = 250.7 Hz), 158.2, 141.6 (d, J_{CF} = 6.4 Hz), 139.3, 135.7, 131.2 (d, J_{CF} = 8.2 Hz), 128.4, 128.3, 128.1, 128.0, 127.9, 127.2, 122.5, 118.4 (d, J_{CF} = 21.7 Hz), 116.7(d, J_{CF} = 23.2 Hz), 106.6, 70.8, 67.3; LRMS (ESI) *m/z* (relative intensity) 597.0 (100% M + Na^+).

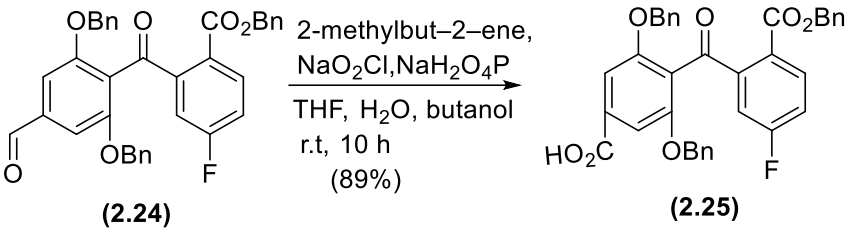

3, 5-bis (benzyloxy)-4-(2-((benzyloxy)carbonyl)-5-fluorobenzoyl)benzoic acid (**2.25**)**:** 2-butyl, 2-ene (45 mg, 0.64 mmol) was added to a stirring solution of aldehyde **2.24** (45 mg, 80 µmol) in THF (0.3 mL), BuOH (0.1 mL) at room temperature. A solution of sodium chlorite (22 mg, 0.24 mmol) and sodium dihydrogen phosphate (29 mg, 0.24 mmol) in water (0.1 mL) was added to the stirring reaction mixture. The reaction was stirred for 10 h at room temperature. The volatiles were removed under reduced pressure and the residue was re-suspended in DCM (2 x 3 mL), washed with brine (3 mL), water (3 mL) and dried over $MgSO_4$. The volatiles were again removed under reduced pressure and the residue was recrystallized from EtOAC: hexanes to afford **2.25** (41 mg, 89%) as a white solid. IR v_{max} cm^{-1} 3303, 1718, 1686, 1423, 1265, 1115, 868; ^{1}H NMR (400 MHz, CD_2Cl_2) δ 7.54-7.51 (m, 1H), 7.32 (s, 2H), 7.19-7.04 (m, 17H), 5.04 (s, 2H), 4.95 (s, 4H); ^{13}C NMR (100MHz. CD_2Cl_2) δ 191.3, 169.0, 167.3, 164.7 (d, J_{CF} = 250.6 Hz), 157.6, 141.7 (d, J_{CF} = 6.7 Hz), 135.8, 132.5, 135.7, 131.2 (d, J_{CF} = 8.2 Hz), 128.6, 128.3, 128.1, 127.9, 127.2, 122.1, 118.4 (d, J_{CF} = 21.6 Hz), 116.7 (d, J_{CF} = 23.2 Hz), 107.3, 70.7, 67.3; LRMS (ESI) *m/z* (relative intensity) 591.0 (38% M + H^+).

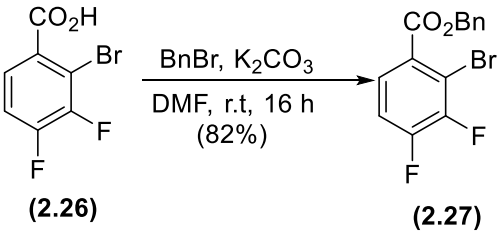

Benzyl 2-bromo-3,4-difluorobenzoate (**2.27**)**:** To a solution of 2-bromo, 3, 4-dihydroxy benzoic acid (3g, 12.7 mmol) **2.26** and K_2CO_3 (1.75 g, 12.7 mmol) in DMF (25.6 mL), benzyl bromide (2.17 g, 12.7 mmol) was added dropwise and the reaction mixture was allowed to stir for 16 h, at ambient temperature under argon. The reaction mixture was quenched by

adding water (5 mL) and extracted with EtOAC (9 mL), dried over $MgSO_4$. The volatiles were removed under reduced pressure and the crude product was purified by flash column chromatography (10% EtOAC: hexanes) to afford the desired ester **2.27** as yellow oil (3.4 g, 82%). ^{1}H NMR (400 MHz, $CDCl_3$) δ 7.71-7.67 (m, 1H), 7.47-7.37 (m, 5H), 7.21-7.16 (m, 1H), 5.38 (s, 2H); ^{13}C NMR (100MHz, $CDCl_3$) δ 164.2, 154.1, 153.9, 151.4 (d, J_{CF} = 15 Hz), 149.7 (d, J_{CF} = 14 Hz), 147.3 (d, J_{CF} = 14 Hz), 135.2, 115.9 (d, J_{CF} = 18 Hz), 112.1, 111.9, 67.7.

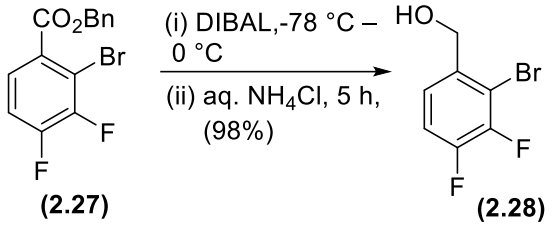

(2-bromo-3,4-difluorophenyl)methanol (**2.28**): To a solution of difluorinated ester **2.27** (2.67 g, 8.58 mmol) in DCM (41 mL), DIBAL (20.6 mL, 1M in DCM), was added drop wise at -78 °C under nitrogen. The reaction mixture was stirred at 0 °C for 1.5 h. The mixture was quenched with aq. NH_4Cl (0.82 mL) and stirred for 3.5 h before filtering through celite pad. The organic layer was washed with brine (2 mL), water (1 mL), and dried over $MgSO_4$. The volatiles were removed under reduced pressure and the crude reaction mixture was recrystallized from (EtOAC: hexanes) to afford alcohol **2.28** as white needle like crystals (1.85 g, 98%). IR v_{max} cm^{-1} 3265, 1494, 1442, 1283, 1063, 948, 851; ^{1}H NMR (400 MHz, CD_2Cl_2) δ 7.33-7.22 (m, 2H), 4.7 (d, 2H, J_{HF} = 6.1 Hz); ^{13}C NMR (100MHz. $CDCl_3$) δ 149.12 (d, J_{CF} = 15 Hz), 136.84, 123.3 (m), 116.1 (d, J_{CF} = 17 Hz), 110.5 (d, J_{CF} = 17.7 Hz), 64.2 (d, J_{CF} = 3 Hz); LRMS (ESI) *m/z* (relative intensity) 261.2 (70% M + K$^+$).

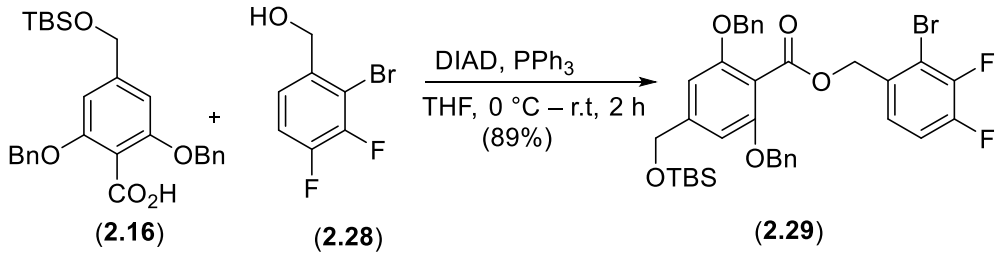

2-bromo-3,4-difluorobenzyl 2,6-bis(benzyloxy)-4-(((tert-butyldimethylsilyl)oxy)methyl)benzoate (**2.29**)**:** To a mixture of benzyl alcohol **2.28** (560 mg, 2.5 mmol), acid **2.16**, (1.2 g, 2.5 mmol), triphenylphosphine (720 mg, 1.1 equiv.) in THF (12 mL), diisopropyl azodicarboxylate (0.46mL, 1.1 equiv.) was added dropwise at 0 °C under argon. The reaction was allowed to stir for 2 h before the volatiles were removed under reduced pressure. The crude reaction mixture was subjected to flash chromatography (15% EtOAC: hexane) to afford **2.29** as white crystals (1.5 g, 89%). IR v_{max} cm^{-1} 1738, 1496, 1250, 1071, 850, 833; ^{1}H NMR (400 MHz, CD_2Cl_2) δ 7.28-7.25 (m, 9H), 7.09-7.05 (m, 1H), 6.70-6.63 (m, 1H), 6.57 (s, 2H), 5.25 (s, 2H), 5.02 (s, 4H), 4.60 (s, 2H), 0.85 (s, 9H), 0.00 (s, 6H); ^{13}C NMR (100MHz. CD_2Cl_2) δ 165.5, 156.4, 151.3 (d, J_{CF} = 13.8 Hz), 148 (qt), 146.5 (d, J_{CF} = 15 Hz), 146.0, 136.6, 132.7 (d, J_{CF} = 3 Hz), 128.5, 127.9, 127.3, 124.6 (qt), 115.8 (d, J_{CF} = 17.3 Hz),111.8, 111.1(d, J_{CF} = 99 Hz),102.9, 70.5, 65.2 (d, J_{CF} = 2 Hz), 64.5, 25.6, 18.2, -5.6; LRMS (ESI) *m/z* (relative intensity) 705.5 (36% M + Na^+).

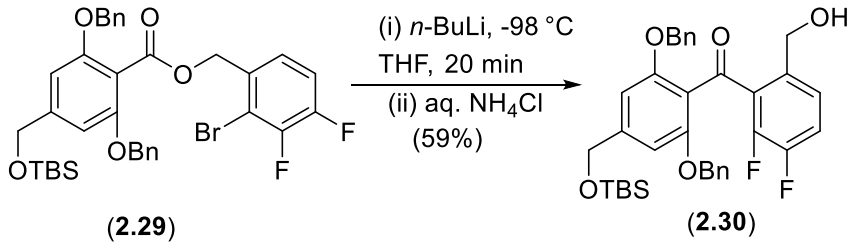

(2,6-bis(benzyloxy)-4-(((tert-butyldimethylsilyl)oxy)methyl)phenyl)(2,3-difluoro-6-(hydroxymethyl)phenyl)methanone (2.30): *n*-BuLi (0.68 mL, 2.5M) was added over 8 min to a solution of ester **2.29** (975 mg, 1.43 mmol) in THF (12 mL) distilled from benzophenone – sodium at -98 °C under argon. The reaction was allowed to stir for 20 min at the same temperature before quenching with aqueous NH_4Cl (6 mL). Following the removal of volatiles under reduced pressure, the crude reaction mixture was extracted with DCM (5 x 3 mL) and the combined organic layer was dried over Na_2SO_4. The crude reaction mixture was subjected to flash chromatography (15 – 20% EtOAC: hexanes) to afford **2.30** (504 mg, 59%) as white crystals. IR v_{max} cm^{-1} 3508, 1651, 1578, 1459, 1142, 835; ^{1}H NMR (400 MHz, CD_2Cl_2) δ 7.19-6.86 (m, 12H), 6.56 (s, 2H), 4.86 (s, 4H), 4.62 (s, 2H), 4.08 (d, J = 6.8 Hz), 0.84 (s, 9H), 0.00 (s, 6H); ^{13}C NMR (100MHz. CD_2Cl_2) δ 193.3, 157.3, 150.6 (d, J_{CF} = 80 Hz), 147.3, 138.2 (d,

J_{CF} = 4 Hz), 136.2 , 131.3 (d, J_{CF} = 9 Hz), 128.4, 128.0, 127.8, 127.5, 125.2 (d, J_{CF} = 4 Hz), 118.8 (d, J_{CF} = 16 Hz), 102.6, 70.5, 64.5, 63.0, 25.6, 18.2, -5.6; LRMS (ESI) *m/z* (relative intensity) 587.2 (100% M + H^+).

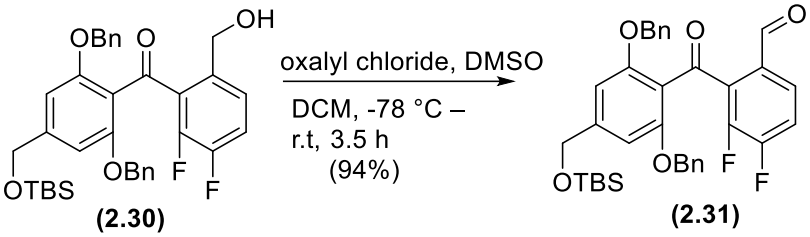

2-(2,6-bis(benzyloxy)-4-(((tert-butyldimethylsilyl)oxy)methyl)benzoyl)-3,4-difluorobenzaldehyde (**2.31**)**:** DMSO (2.9 mL, 41.4 mmol) was added dropwise to a cold solution of oxalyl chloride (5 equiv., 2M in DCM) in DCM (5 mL) at -78 °C under argon. The mixture was stirred for 30 min before a solution of alcohol **2.30** (417 mg, 690 µmol) in DCM (5 mL) was added dropwise over 5 min. The reaction was allowed to stir for 1 h before quenching with triethyl amine (3.85 mL, 27.6 mmol). After an additional 2 h stirring at ambient temperature, the volatiles were removed under nitrogen blow down. The residue was re-suspended in DCM, washed with water (2 mL), sodium bicarbonate (5 mL), brine (5 mL) water, and dried over $MgSO_4$, concentrated under reduced pressure. The crude reaction mixture was purified by flash chromatography (20% EtOAC: hexanes) to furnish **2.31** as pale yellow solid (582 mg, 96%). IR v_{max} cm^{-1} 1696, 1654, 1576, 1454, 1300, 1106, 857, 836; ^1H NMR (400 MHz, CD_2Cl_2) δ 9.64 (s, 1H), 7.34-7.03 (m, 12H), 6.57 (s, 2H), 4.88 (s, 4H), 4.62 (s, 2H), 0.84 (s, 9H), 0.00 (s, 6H); ^{13}C NMR (100MHz. CD_2Cl_2) δ 188.9, 188.6, 158.1, 154.5 (d, J_{CF} = 13 Hz), 151.9 (d, J_{CF} = 9 Hz), 151.9 (d, J_{CF} = 13 Hz), 149.1, 148.5, 135.9, 135.4 (d, J_{CF} = 12 Hz), 131.8 (d, J_{CF} = 3 Hz), 128.4, 128.1, 127.5, 124.7(m), 118.2 (d, J_{CF} = 18 Hz), 117.3, 102.6, 70.7, 64.5, 25.6, 18.2, -5.6; LRMS (ESI) *m/z* (relative intensity) 603.2 (100% M + H^+).

3. Results and Discussion

As described in the introduction section, this training thesis work is focused on the synthesis of mono- and difluorinated benzophenone fragments that will contribute to the synthesis of novel fluorinated balanoids for biological testing. Previous SAR and docking results have identified the imperative role of the D ring of benzophenone in interacting with the active sites and flexible loops of the protein. Replacement of the hydroxyl group or insertion of one or two fluorine substituents may provide new hydrogen bonding interactions with the flexible loops and potentially enhance isozyme selectivity. This work approaches the synthesis of the targeted fluorinated BP fragments **2.25** and **2.36** (Fig.6) from 2-bromo-4-fluorobenzyl alcohol **2.17** and 2-bromo-3,4-difluorobenzyl alcohol **2.28** intermediates as shown below in Scheme 10 and 11, respectively.

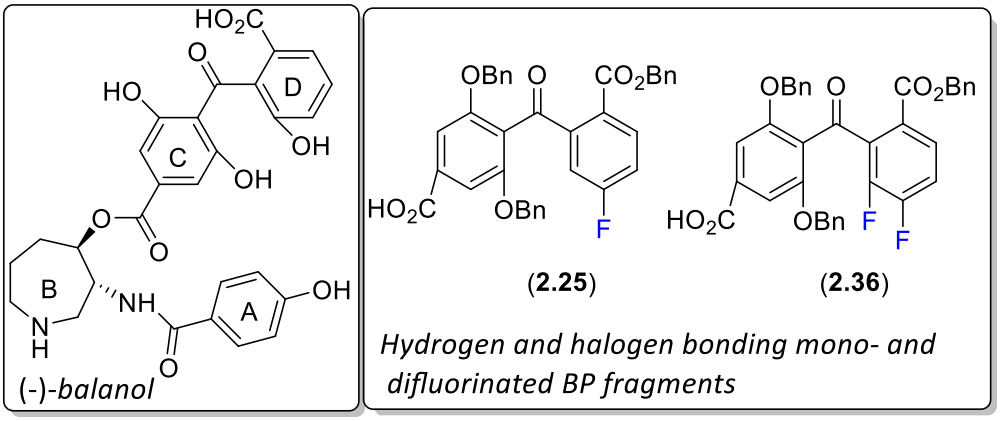

Fig. 6. Structures of (-)-balanol and the targeted mono- and difluorinated benzophenone fragments

<u>3.1 Synthesis of (-)-balanol mono and difluorinated esters **2.8** and **3.9**</u>

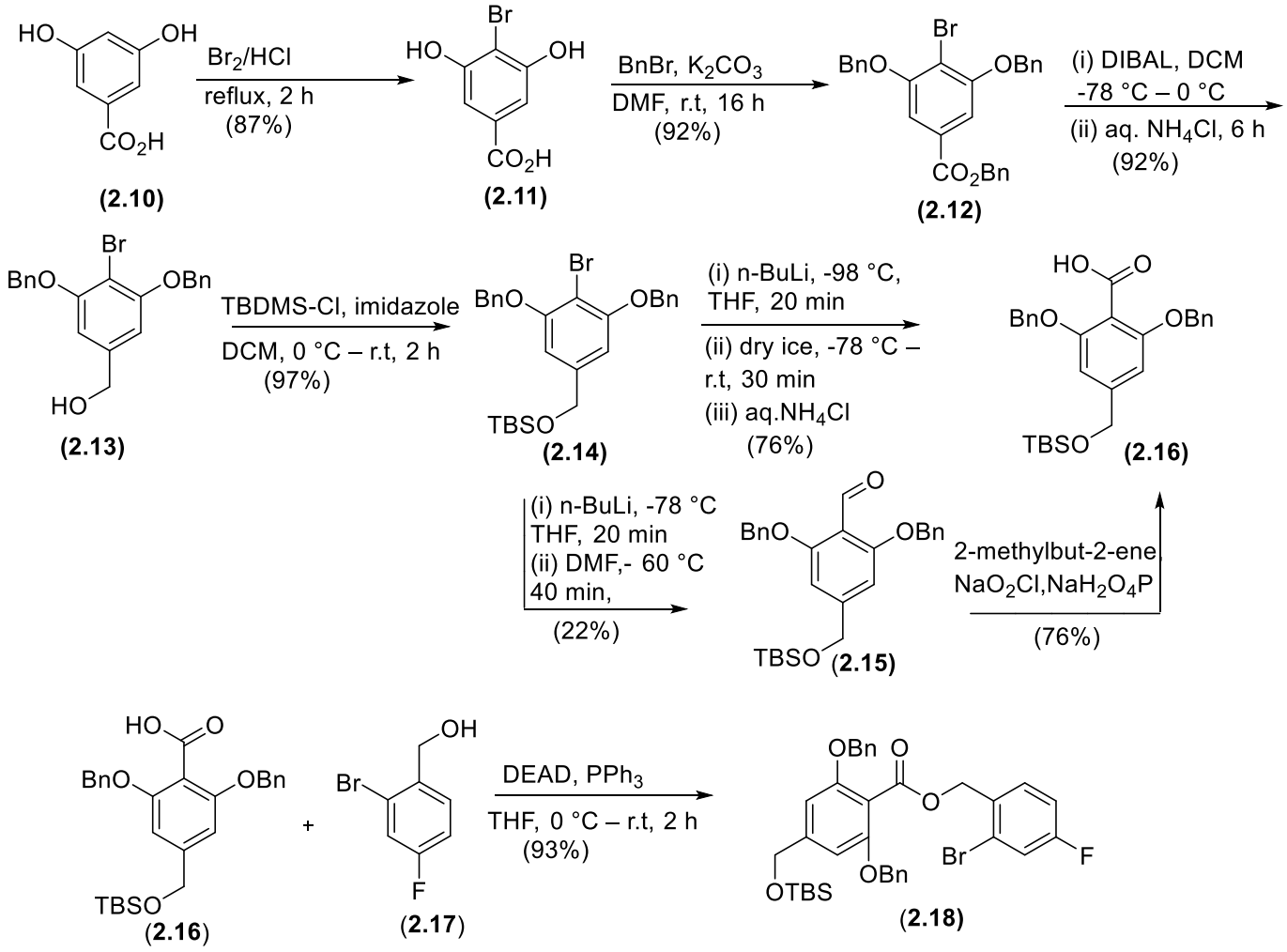

Scheme 10. Synthesis of mono fluorinated ester **2.18** via Nicolaus's protocol

The mono fluorinated ester **2.18** was accessed in 6 steps (Scheme 10) with an overall yield of 50.5% following Nicolaus's protocol. The key steps involved are Li halogen exchange for carbon dioxide trapping and Mitsunobu esterification. The coupling of fragment **2.16** was accomplished in five steps starting from commercially available 3, 5-di hydroxy benzoic acid. The first step is the electrophilic bromination of **2.10** using liquid bromine in acidic medium to furnish **2.11** in 87% yield. The resultant aryl bromide was tribenzylated using benzyl bromide to afford **2.12** in 92% yield, which was subsequently reduced by DIBAL-H to afford the benzyl alcohol **2.13** in 90% yield. In the next step, the alcohol was silyl protected to access **2.14** in 95% yield. The silyl protected alcohol underwent lithium halogen exchange with *n*-BuLi for trapping carbon dioxide from dry ice to afford the desired acid **2.16** in 76% yield. The coupling of the acid **2.16** and commercially available mono fluorinated benzyl

alcohol **2.17** was accomplished utilizing Mitsunobu esterification to furnish the key intermediate **2.18** in 93% as shown in scheme 10.

The reaction sequence (Scheme 10) was generally high yielding, with the exception of the carboxylation step to provide **2.16**. Despite the great synthetic application of metal halogen exchange, the mechanism of the reaction remains somewhat of an enigma, predominately due to the capricious nature of organic lithium when treated with organic halides. Multiple mechanisms have been proposed[60-63] involving a radical mediated model, as well as nucleophilic and four-center transition states. Competing side-reactions, such as reduction of organic halide, β-elimination, α-metallation, Wurtz type coupling reactions have also been identified. Apart from the aforementioned problems, mechanistic investigation is obscured by the fact that metal halogens exist as aggregates for which the degree of association is affected by factors such as solvent, temperature and concentration. Lithium organics are well known electron deficient species in the context that there are more interatomic interactions than the availability of valance electron pairs for bonding. The tetra coordinate nature of lithium in majority of structures and the presence of electron donating solvents such as THF coordinate strongly to lithium.

For accessing congested systems such as **2.16** reaction conditions were therefore optimized by changing the temperature of lithium halogen exchange in THF (Table 3). Freshly distilled THF from sodium and benzophenone gave the best yield at 76% (Table 3, entry 6). THF obtained from a solvent purification system (SPS) distilled over CaH_2 led to lithium halogen exchange but failed to lead to carbon dioxide trapping, presumably due to radical impurities that may interfere (Table 3, entry 1). Control reactions performed using 1-bromo-3-fluoro benzene in dry THF, freshly distilled from CaH_2 and stored over 3Å molecular sieves gave only low yields (Table 3, entry 4). Chromatographic (TLC) and spectroscopic analysis (NMR) of the reaction mixture suggested the formation of the de-brominated reduced product along with complex side products.

Alternatives to the metal halogen exchange route for carboxylation were also investigated. A control reaction with 1-bromo-3-fluoro benzene for LDA proton abstraction in THF (distilled from CaH_2), followed by carbon dioxide trapping, provided the carboxylated product in only 25% isolated yield. Next, synthesis of compound **2.16** *via* Li halogen exchange for formylation followed by Pinnick oxidation was attempted. However, similar to

the carboxylation reaction, majority of the aryl halide was reduced with 22% of isolated yield of aldehyde **2.15**. This route was not efficient for accessing acid **2.16**. Due to the limited time frame of this training thesis, the condition (Table 3, entry 6) was used to continue the synthesis

Table 3. Summarized results of Li halogen exchange by *n*-BuLi and LDA proton abstraction for formylation/carboxylation using THF from different sources.

Entry	Substrate	THF source	Temp	Result
1[a]	**2.14**	SPS, distilled over CaH_2	-98 °C	Failed carboxylation
2[a]	**2.14**	SPS, stored over 3Å beads	-98 °C	10% isolated yield
3[a]	**2.14**	SPS, distilled over CaH_2	-78 °C	Failed carboxylation
4[b]	**1-bromo-3-fluoro benzene**	SPS, distilled over CaH_2, stored over 3Å beads	-78 °C	25% isolated yield
5[c]	**2.14**	SPS, stored over 3Å beads	-78 °C	22% isolated yield
6[a]	**2.14**	sodium-benzophenone still	-98 °C	76% isolated yield

a indicates Li halogen exchange for carbon dioxide trapping; *b* LDA proton abstraction for carbon dioxide trapping; and *c* Li halogen exchange for formylation.

Similarly, the difluorinated ester **2.29** was synthesized in 9 steps with an overall yield of 39% *via* Nicolaus's protocol (Scheme 11). Difluorinated benzyl alcohol **2.28** was accessed in two steps: (a) benzylation of the commercially available 2-bromo-3, 4-difluoro benzoic acid **2.26** using K_2CO_3 and DMF to provide the difluoro ester **2.27** in 82% yield; and (b) DIBAL reduction of **2.27** to afford the desired benzyl alcohol **2.28** in 98% yield. The Mitsunobu

coupling between acid **2.16** and difluoronated benzyl alcohol **2.28** in THF afforded **2.29** in 89% yield (Scheme 11).

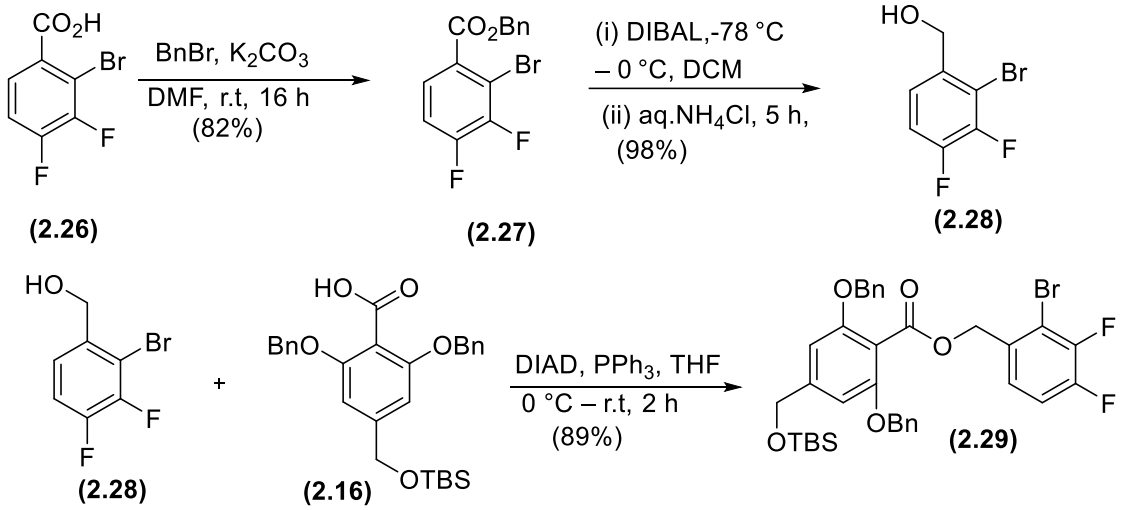

Scheme 11. Synthesis of difluorinated Mitsunobu ester **2.29** *via* Nicolaus's protocol.

3.2 Anionic Fries rearrangement of the mono fluorinated ester and difluorinated ester

The mono- and difluorinated benzophenones were accessed from their corresponding esters **2.18** and **2.29** using *n*-BuLi in freshly distilled THF from sodium-benzophenone in an un-optimized yield of 54% and 59% respectively (Scheme 12). Mechanistically, mono- and difluorinated esters **2.18** and **2.29** on treatment with *n*-BuLi form an aryl lithiate that rapidly undergoes intramolecular Fries rearrangement (Scheme 12).

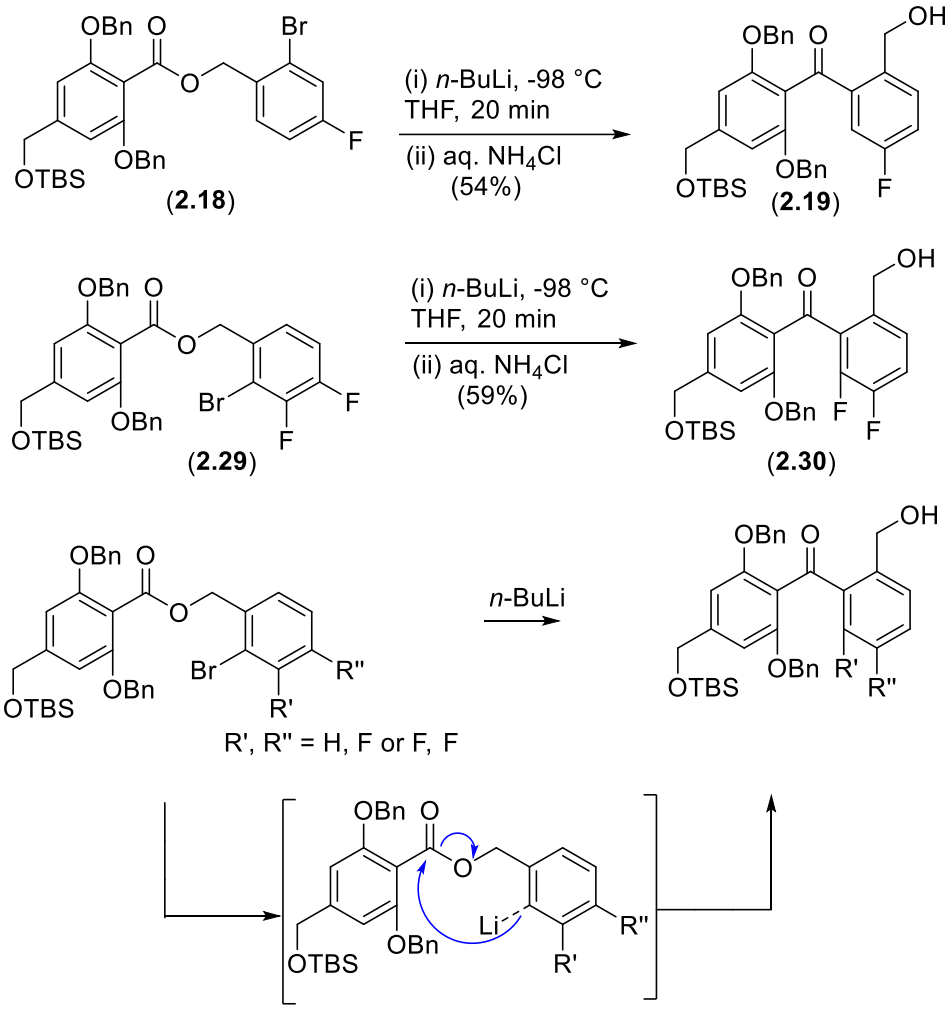

Scheme 12. Intramolecular Fries rearrangement reactions of **2.18** and **2.29** *via* Nicolaus's protocol.

Chromatographic (TLC) and spectroscopic analysis (NMR) of the reaction mixture suggest the formation of de-brominated reduced product **3.10**. The predominating factors for the formation of the de-brominated product **3.10** are likely solvent, temperature and the rate of *n*-BuLi addition. The proton is potentially brought upon by THF α-proton abstraction (scheme 13). Due to the time constraint, the conditions were not optimized at this stage. Future optimization efforts will involve the rate of addition of *n*-BuLi and concentration of

the reactants, along with temperature variations.

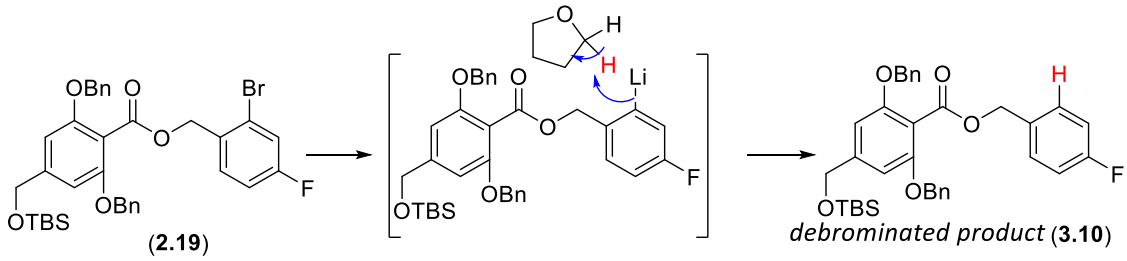

Scheme 13. Plausible mechanism of the formation of de-brominated product in key Fries rearrangement reaction.

3.3 Chemo selective oxidation reactions of the mono- and difluorinated benzophenones

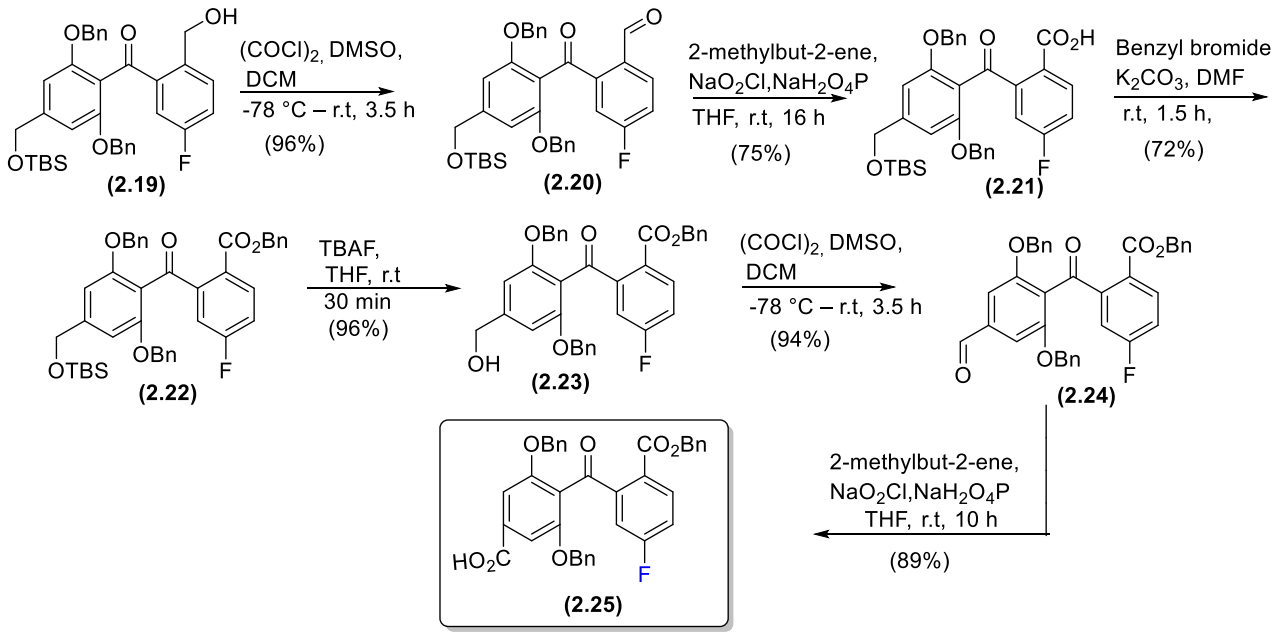

Scheme 14. Synthesis of mono fluorinated BP fragment **2.25** *via* a modified Nicolaou's protocol[19].

The oxidation of alcohol **2.19** was sought to be accessed using NMO/TPAP according to the Nicolaou's protocol (Scheme 14). Chromatographic (TLC) and spectroscopic data showed complete conversion of the starting material **2.19** into aldehyde **2.20**, however the isolated yield was 20%. To understand the cause(s) of low isolated yield, a control reaction using NMO/TPAP oxidation of *p*-nitro benzaldehyde was performed in parallel to the actual material **2.19** under similar conditions and scale. An isolated yield of 62% was obtained from the control reaction and 19% of **2.20** from the oxidation of **2.19**. Literature data[64, 65]

suggests that TPAP oxidation can fail due to steric congestion or chelation with ruthenium salts. This suggested that chelation may have contributed to low isolated yields.

In order to secure aldehyde **2.20** under mild and scalable oxidation conditions, an alternative oxidation was trialed using the Swern oxidation conditions reported by Thompson *et al*[66] for the synthesis of sesquiterpene isovelleral. This Swern oxidation conditions were developed to avoid the rearrangement of an acid sensitive cyclopropane methanol motif (Scheme 15b).

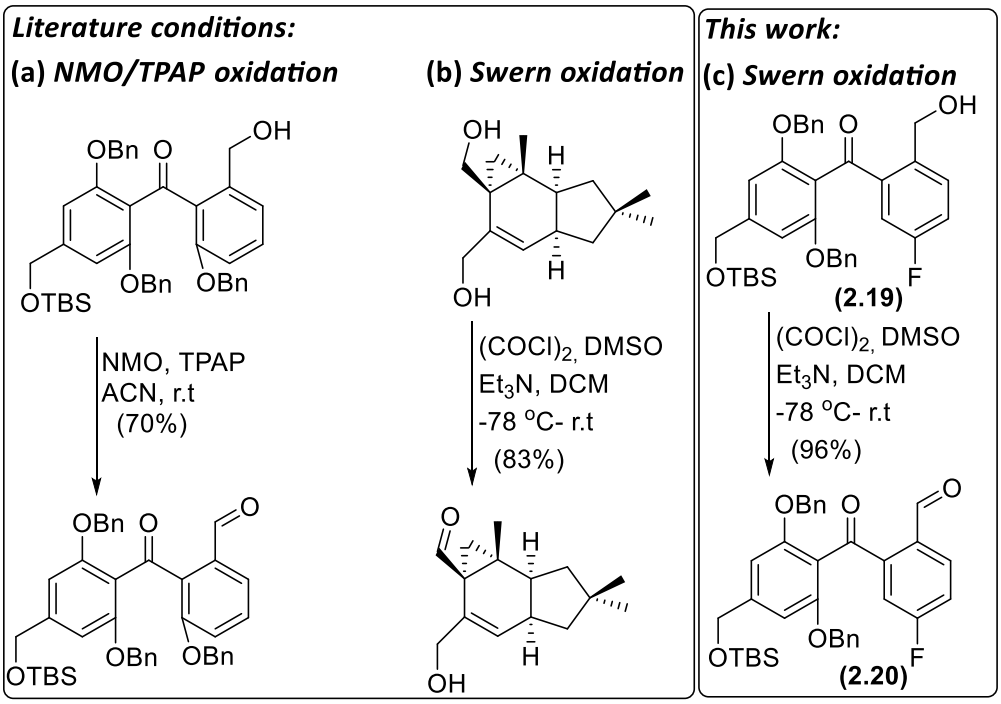

Scheme 15. Chemo selective oxidation of **2.19** using activated DMSO.

Oxidation of alcohol **2.19** under Swern conditions proceeded with complete conversion of alcohol **2.19** into aldehyde **2.20** in 96% yield, appreciably, higher than that reported in the literature under both NMO/TPAP (Scheme 15a) and Swern conditions[19, 66] (Scheme 15b). Moreover, the product did not need any further purification. NaO_2Cl mediated Pinnick oxidation of **2.20** afforded **2.21** in 75% yield, and **2.21** was subsequently protected as a benzyl ether to secure **2.22** in 72% yield. Subsequent, TBAF desilylation provided the primary alcohol **2.23** in 96% yield. The alcohol was oxidized to acid by sequential Swern and Pinnick methods to afford **2.25** in 85% over two steps.

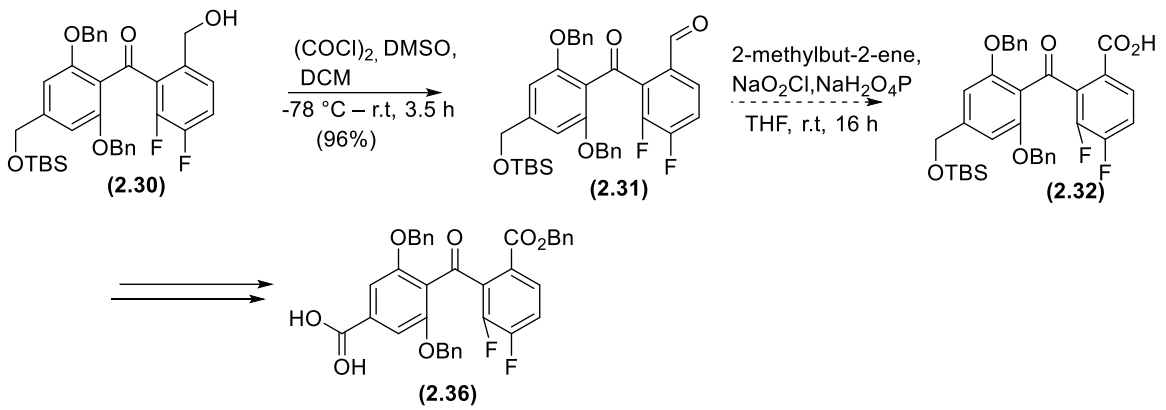

Scheme 16. Synthesis of difluorinated benzophenone *via* a modified Nicolaus's protocol

Following the Fries rearrangement, difluorinated acid **2.36** (Scheme 16) was aimed to be synthesized in a similar fashion as that for **2.25**. Beginning with a Swern oxidation, difluorinated alcohol **2.30** furnished aldehyde **2.31** in an excellent yield of 94%, which is consistent to the case for the monofluorinated **2.20**. However, the Pinnick oxidation conditions failed to yield acid **2.31**. This was disappointing but can be rationalized by the presence of the two fluorine groups rendering the carbonyl highly electron deficient. Considering the wide application of Pinnick oxidation in natural product chemistry[67-69] and the mild conditions it utilizes, further optimization was attempted by replacing disodium hydrogen phosphate with sulfamic acid to access the desired acid **2.31**. However, these conditions were intolerant to the TBS protecting group and resulted in its removal. Another mild oxidation protocol[70] using oxone in DMF was also attempted. Again, this method proved capricious and led to the loss of the TBS group. Further oxidation attempts[71, 72] utilizing Pd/C with $NaBH_4$/ KOH and $AgNO_3$ in aqueous sodium hydroxide also resulted in no conversion and recovered starting material.

Methods to achieve efficient transformation of aldehydes to carboxylic acids under mild conditions are scare. Silver (I)-catalyzed aerobic oxidation of aldehydes in water under mild temperature conditions and low catalyst loading has been recently reported as a proficient method to oxidize more than 50 different kinds of aldehydes including the ones with electron deficient carbonyls to their corresponding acids in high to quantitative yields[73].

Mechanistically, after the introduction of aqueous NaOH, the –Cl group of silver catalyst NHC-Ag (I)-Cl is substituted with a hydroxyl to form the proposed Ag (I)-OH complex. The catalyst then coordinates with the aldehyde and exchanges its hydroxyl group with the

proton of the aldehyde involving either a nucleophilic attack of the hydroxy followed by β-hydride elimination or through the formation of a four-centered transition state where exchange of the –OH and –H takes place simultaneously. The catalyst then releases the acid as the product and silver (I)-hydride species (scheme 17). However, this Ag (I) catalyzed oxidation protocol[73] applied to our difluorinated aldehyde led to no conversion.

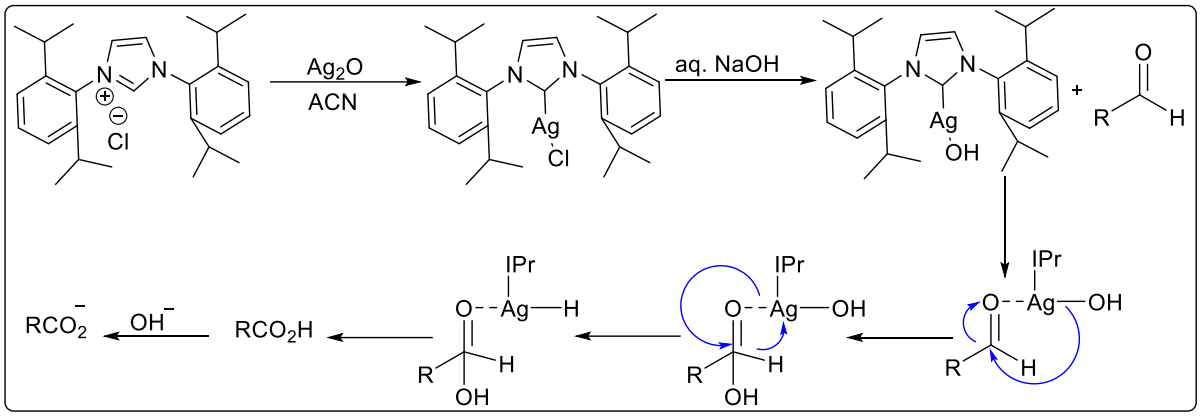

Scheme 17. Plausible mechanism of Ag (I) catalyzed oxidation of aldehydes to carboxylic acids.

As an alternative, primary alcohol **2.30** (scheme 18) was deprotected with TBAF in 91% yield. The alcohol **2.30** was subsequently oxidized to acid **3.13** under Swern and Pinnick conditions with a combined yield of 83% over two steps. Due to the limited time frame of this training thesis, the efforts for accessing **2.36** will continue later. An alternative route to secure the desired acid **2.36** would be to install a more stable protective group such as tert-butylchlorodiphenylsilane or methyl ether to enable Pinnick oxidation with sulfamic acid (Scheme 19)

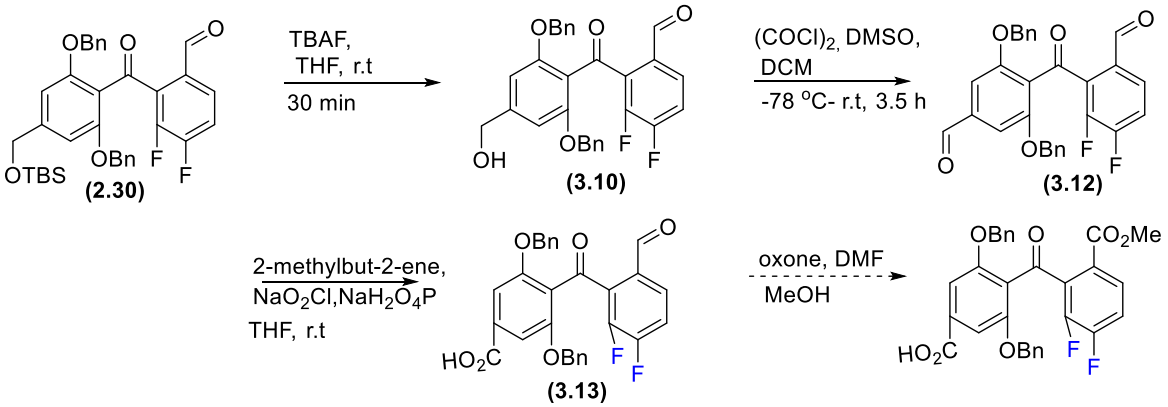

Scheme 18. Alternate route for the synthesis of ester **2.36**

4. Conclusion and Future Directions

This work focused on the synthesis of new mono and difluorinated benzophenone **2.25** and **2.36** fragments. Monofluorinated BP was accessed in 13 steps with an overall yield of 11.35% utilizing key reactions such as Li halogen exchange, anionic Fries rearrangement and chemo selective oxidation. Our results demonstrate that the Fries rearrangement is feasible for accessing mono- and difluorinated scaffolds. Access to the difluorinated benzophenone compound **2.36** is currently at the penultimate step due to the unsuccessful Pinnick oxidation. In future access to the difluorinated benzophenone **2.36** will continue to be investigated by other oxidant that may require the modification the protecting group on the benzyl alcohol on ring A. These new fluorinated benzophenone fragments are expected to be coupled with the other two fragments of balanol to furnish fluorinated balanoids for biological testing.

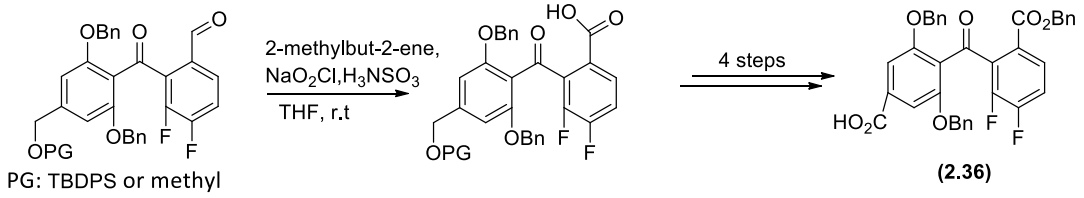

Scheme 19. Proposed route for the synthesis of **2.36** by modification of protecting group

5. References

1. Romines, K. R.; Freeman, G. A.; Schaller, L. T.; Cowan, J. R.; Gonzales, S. S.; Tidwell, J. H.; Andrews, C. W.; Stammers, D. K.; Hazen, R. J.; Ferris, R. G.; Short, S. A.; Chan, J. H.; Boone, L. R. Structure−Activity Relationship Studies of Novel Benzophenones Leading to the Discovery of a Potent, Next Generation HIV Nonnucleoside Reverse Transcriptase Inhibitor. *Journal of Medicinal Chemistry* **2006,** 49, 727-739.
2. Wyatt, P. G.; Bethell, R. C.; Cammack, N.; Charon, D.; Dodic, N.; Dumaitre, B.; Evans, D. N.; Green, D. V. S.; Hopewell, P. L. Benzophenone Derivatives: A Novel Series of Potent and Selective Inhibitors of Human Immunodeficiency Virus Type 1 Reverse Transcriptase. *Journal of Medicinal Chemistry* **1995,** 38, 1657-1665.
3. Husain, S. S.; Nirthanan, S.; Ruesch, D.; Solt, K.; Cheng, Q.; Li, G.-D.; Arevalo, E.; Olsen, R. W.; Raines, D. E.; Forman, S. A.; Cohen, J. B.; Miller, K. W. Synthesis of Trifluoromethylaryl Diazirine and Benzophenone Derivatives of Etomidate that Are Potent General Anesthetics and Effective Photolabels for Probing Sites on Ligand-Gated Ion Channels. *Journal of Medicinal Chemistry* **2006,** 49, 4818-4825.
4. Belluti, F.; De Simone, A.; Tarozzi, A.; Bartolini, M.; Djemil, A.; Bisi, A.; Gobbi, S.; Montanari, S.; Cavalli, A.; Andrisano, V.; Bottegoni, G.; Rampa, A. Fluorinated benzophenone derivatives: Balanced multipotent agents for Alzheimer's disease. *European Journal of Medicinal Chemistry* **2014,** 78, 157-166.
5. Vooturi, S. K.; Cheung, C. M.; Rybak, M. J.; Firestine, S. M. Design, Synthesis, and Structure−Activity Relationships of Benzophenone-Based Tetraamides as Novel Antibacterial Agents. *Journal of Medicinal Chemistry* **2009,** 52, 5020-5031.
6. Hayashi, Y.; Takeno, H.; Chinen, T.; Muguruma, K.; Okuyama, K.; Taguchi, A.; Takayama, K.; Yakushiji, F.; Miura, M.; Usui, T.; Hayashi, Y. Development of a New Benzophenone–Diketopiperazine-Type Potent Antimicrotubule Agent Possessing a 2-Pyridine Structure. *ACS Medicinal Chemistry Letters* **2014,** 5, 1094-1098.
7. Jabeen, I.; Pleban, K.; Rinner, U.; Chiba, P.; Ecker, G. F. Structure-activity relationships, ligand efficiency, and lipophilic efficiency profiles of benzophenone-type inhibitors of the multidrug transporter P-glycoprotein. *J Med Chem* **2012,** 55, 3261-73.
8. Roux, D.; Hadi, H. A.; Thoret, S.; Guénard, D.; Thoison, O.; Païs, M.; Sévenet, T. Structure−Activity Relationship of Polyisoprenyl Benzophenones from Garcinia pyrifera on the Tubulin/Microtubule System. *Journal of Natural Products* **2000,** 63, 1070-1076.
9. Kumar, S.; Chattopadhyay, S. K.; Darokar, M. P.; Garg, A.; Khanuja, S. P. S. Cytotoxic Activities of Xanthochymol and Isoxanthochymol Substantiated by LC-MS/MS. *Planta Med* **2007,** 73, 1452-1456.
10. Williams, R. B.; Hoch, J.; Glass, T. E.; Evans, R.; Miller, J. S.; Wisse, J. H.; Kingston, D. G. I. A Novel Cytotoxic Guttiferone Analogue from Garcinia macrophylla from the Suriname Rainforest. *Planta Med* **2003,** 69, 864-866.
11. Datta, S.; Li, J.; Mahdi, F.; Jekabsons, M. B.; Nagle, D. G.; Zhou, Y.-D. Glycolysis Inhibitor Screening Identifies the Bis-geranylacylphloroglucinol Protonophore Moronone from Moronobea coccinea. *Journal of Natural Products* **2012,** 75, 2216-2222.
12. Pardo-Andreu, G. L.; Nuñez-Figueredo, Y.; Tudella, V. G.; Cuesta-Rubio, O.; Rodrigues, F. P.; Pestana, C. R.; Uyemura, S. A.; Leopoldino, A. M.; Alberici, L. C.; Curti, C. The anti-cancer agent nemorosone is a new potent protonophoric mitochondrial uncoupler. *Mitochondrion* **2011,** 11, 255-263.
13. Kulanthaivel, P.; Hallock, Y. F.; Boros, C.; Hamilton, S. M.; Janzen, W. P.; Ballas, L. M.; Loomis, C. R.; Jiang, J. B.; Katz, B. Balanol: a novel and potent inhibitor of protein kinase C from the fungus Verticillium balanoides. *Journal of the American Chemical Society* **1993,** 115, 6452-6453.
14. Fields, A. P.; Murray, N. R. Protein kinase C isozymes as therapeutic targets for treatment of human cancers. *Advances in enzyme regulation* **2008,** 48, 166-178.
15. Narayana, N.; Diller, T. C.; Koide, K.; Bunnage, M. E.; Nicolaou, K. C.; Brunton, L. L.; Xuong, N.-H.; Ten Eyck, L. F.; Taylor, S. S. Crystal Structure of the Potent Natural Product Inhibitor Balanol in Complex with the Catalytic Subunit of cAMP-Dependent Protein Kinase. *Biochemistry* **1999,** 38, 2367-2376.
16. Lampe, J. W.; Biggers, C. K.; Defauw, J. M.; Foglesong, R. J.; Hall, S. E.; Heerding, J. M.; Hollinshead, S. P.; Hu, H.; Hughes, P. F.; Jagdmann, G. E.; Johnson, M. G.; Lai, Y.-S.; Lowden, C. T.; Lynch, M. P.; Mendoza, J. S.; Murphy, M. M.; Wilson, J. W.; Ballas, L. M.; Carter, K.; Darges, J. W.; Davis, J. E.; Hubbard, F. R.; Stamper, M. L. Synthesis and Protein Kinase Inhibitory Activity of Balanol Analogues with Modified Benzophenone Subunits. *Journal of Medicinal Chemistry* **2002,** 45, 2624-2643.
17. Fürstner, A.; Thiel, O. R. Formal Total Synthesis of (−)-Balanol: Concise Approach to the Hexahydroazepine Segment Based on RCM. *The Journal of Organic Chemistry* **2000,** 65, 1738-1742.

18. Nicolaou, K. C.; Bunnage, M. E.; Koide, K. Total Synthesis of Balanol. *Journal of the American Chemical Society* **1994,** 116, 8402-8403.
19. Nicolaou, K. C.; Koide, K.; Bunnage, M. E. Total Synthesis of Balanol and Designed Analogues. *Chemistry – A European Journal* **1995,** 1, 454-466.
20. Koide, K.; Bunnage, M. E.; Gomez Paloma, L.; Kanter, J. R.; Taylor, S. S.; Brunton, L. L.; Nicolaou, K. C. Molecular design and biological activity of potent and selective protein kinase inhibitors related to balanol. *Chemistry & Biology* **1995,** 2, 601-608.
21. Heerding, J. M.; Lampe, J. W.; Darges, J. W.; Stamper, M. L. Protein kinase C inhibitory activities of balanol analogs bearing carboxylic acid replacements. *Bioorganic & Medicinal Chemistry Letters* **1995,** 5, 1839-1842.
22. Lai, Y.-S.; Menaldino, D. S.; Nichols, J. B.; Jagdmann, G. E., Jr.; Mylott, F.; Gillespie, J.; Hall, S. E. Ring size effect in the PKC inhibitory activities of perhydroazepine analogs of balanol. *Bioorg. Med. Chem. Lett.* **1995,** 5, 2151-4.
23. Lai, Y.-S.; Mendoza, J. S.; Hubbard, F.; Kalter, K. Synthesis and PKC inhibitory activities of balanol analogs with a cyclopentane substructure. *Bioorg. Med. Chem. Lett.* **1995,** 5, 2155-60.
24. Lai, Y.-S.; Stamper, M. Heteroatom effect in the PKC inhibitory activities of perhydroazepine analogs of balanol. *Bioorg. Med. Chem. Lett.* **1995,** 5, 2147-50.
25. Jagdmann, G. E., Jr.; Defauw, J. M.; Lai, Y.-S.; Crane, H. M.; Hall, S. E.; Buben, J. A.; Hu, H.; Gosnell, P. A. Novel PKC inhibitory analogs of balanol with replacement of the ester functionality. *Bioorg. Med. Chem. Lett.* **1995,** 5, 2015-20.
26. Defauw, J. M.; Murphy, M. M.; Jagdmann, G. E.; Hu, H.; Lampe, J. W.; Hollinshead, S. P.; Mitchell, T. J.; Crane, H. M.; Heerding, J. M.; Mendoza, J. S.; Davis, J. E.; Darges, J. W.; Hubbard, F. R.; Hall, S. E. Synthesis and Protein Kinase C Inhibitory Activities of Acyclic Balanol Analogs That Are Highly Selective for Protein Kinase C over Protein Kinase A. *Journal of Medicinal Chemistry* **1996,** 39, 5215-5227.
27. Hu, H.; Hollinshead, S. P.; Hall, S. E.; Kalter, K.; Ballas, L. M. Synthesis and protein kinase C inhibitory activities of indane analogs of balanol. *Bioorg. Med. Chem. Lett.* **1996,** 6, 973-978.
28. Jagdmann, G. E.; Defauw, J. M.; Lampe, J. W.; Darges, J. W.; Kalter, K. Potent and selective PKC inhibitory 5-membered ring analogs of balanol with replacement of the carboxamide moiety. *Bioorganic & Medicinal Chemistry Letters* **1996,** 6, 1759-1764.
29. Fried, J.; Sabo, E. F. 9α-FLUORO DERIVATIVES OF CORTISONE AND HYDROCORTISONE. *Journal of the American Chemical Society* **1954,** 76, 1455-1456.
30. McGrath, N. A.; Brichacek, M.; Njardarson, J. T. A Graphical Journey of Innovative Organic Architectures That Have Improved Our Lives. *Journal of Chemical Education* **2010,** 87, 1348-1349.
31. Zhou, Y.; Wang, J.; Gu, Z.; Wang, S.; Zhu, W.; Aceña, J. L.; Soloshonok, V. A.; Izawa, K.; Liu, H. Next Generation of Fluorine-Containing Pharmaceuticals, Compounds Currently in Phase II–III Clinical Trials of Major Pharmaceutical Companies: New Structural Trends and Therapeutic Areas. *Chemical Reviews* **2016,** 116, 422-518.
32. Gillis, E. P.; Eastman, K. J.; Hill, M. D.; Donnelly, D. J.; Meanwell, N. A. Applications of Fluorine in Medicinal Chemistry. *Journal of Medicinal Chemistry* **2015,** 58, 8315-8359.
33. Piel, M.; Vernaleken, I.; Rösch, F. Positron Emission Tomography in CNS Drug Discovery and Drug Monitoring. *Journal of Medicinal Chemistry* **2014,** 57, 9232-9258.
34. Bégué, J. P.; Bonnet-Delpon, D. Chapter 13 - Biological Impacts of Fluorination: Pharmaceuticals Based on Natural Products. In *Fluorine and Health*, Tressaud, A., Ed. Elsevier: Amsterdam, 2008; pp 553-622.
35. O'Hagan, D.; B. Harper, D. Fluorine-containing natural products. *Journal of Fluorine Chemistry* **1999,** 100, 127-133.
36. Aldemir, H.; Kohlhepp, S. V.; Gulder, T.; Gulder, T. A. M. Structure of a Putative Fluorinated Natural Product from Streptomyces sp. TC1. *Journal of Natural Products* **2014,** 77, 2331-2334.
37. Thomas, C. J. Fluorinated natural products with clinical significance. *Curr Top Med Chem* **2006,** 6, 1529-43.
38. Chan, K. K.; O'Hagan, D. The rare fluorinated natural products and biotechnological prospects for fluorine enzymology. *Methods Enzymol* **2012,** 516, 219-35.
39. Kingston, D. G. I. Tubulin-interactive natural products as anticancer agents. *Journal of natural products* **2009,** 72, 507-515.
40. Patel, A. R.; Hardianto, A.; Ranganathan, S.; Liu, F. Divergent response of homologous ATP sites to stereospecific ligand fluorination for selectivity enhancement. *Organic & biomolecular chemistry* **2017,** 15, 1570-1574.

41. Yamamoto, I.; Jordan, M. J. T.; Gavande, N.; Doddareddy, M. R.; Chebib, M.; Hunter, L. The enantiomers of syn-2,3-difluoro-4-aminobutyric acid elicit opposite responses at the GABAC receptor. *Chemical Communications* **2012,** 48, 829-831.
42. Wilcken, R.; Zimmermann, M. O.; Lange, A.; Joerger, A. C.; Boeckler, F. M. Principles and Applications of Halogen Bonding in Medicinal Chemistry and Chemical Biology. *Journal of Medicinal Chemistry* **2013,** 56, 1363-1388.
43. Metrangolo, P.; Murray, J. S.; Pilati, T.; Politzer, P.; Resnati, G.; Terraneo, G. Fluorine-Centered Halogen Bonding: A Factor in Recognition Phenomena and Reactivity. *Crystal Growth & Design* **2011,** 11, 4238-4246.
44. Olsen, J. A.; Banner, D. W.; Seiler, P.; Wagner, B.; Tschopp, T.; Obst-Sander, U.; Kansy, M.; Muller, K.; Diederich, F. Fluorine interactions at the thrombin active site: protein backbone fragments H-C(alpha)-C=O comprise a favorable C-F environment and interactions of C-F with electrophiles. *Chembiochem* **2004,** 5, 666-75.
45. Barton, D. H. R. The Principles of Conformational Analysis. *Science* **1970,** 169, 539-544.
46. Patel, A. R.; Ball, G.; Hunter, L.; Liu, F. Conformational regulation of substituted azepanes through selective monofluorination. *Organic & biomolecular chemistry* **2013,** 11, 3781-3785.
47. Patel, A. R.; Hardianto, A.; Ranganathan, S.; Liu, F. Divergent response of homologous ATP sites to stereospecific ligand fluorination for selectivity enhancement. *Org Biomol Chem* **2017,** 15, 1570-1574.
48. Patel, A. R.; Liu, F. Diastereospecific fluorination of substituted azepanes. *Tetrahedron* **2013,** 69, 744-752.
49. Patel, A. R.; Hunter, L.; Bhadbhade, M. M.; Liu, F. Conformational Regulation of Substituted Azepanes through Mono-, Di-, and Trifluorination. *European Journal of Organic Chemistry* **2014,** 2014, 2584-2593.
50. Hardianto, A.; Liu, F.; Ranganathan, S. Molecular Dynamics Pinpoint the Global Fluorine Effect in Balanoid Binding to PKCε and PKA. *Journal of Chemical Information and Modeling* **2018,** 58, 511-519.
51. Hardianto, A.; Yusuf, M.; Liu, F.; Ranganathan, S. Exploration of charge states of balanol analogues acting as ATP-competitive inhibitors in kinases. *BMC Bioinformatics* **2017,** 18, 572.
52. Noncovich, A.; Ung, J.; Patron, A. Total synthesis of the novel benzophenone NP-011694. *Tetrahedron Letters* **2015,** 56, 4836-4839.
53. Denieul, M.-P.; Skrydstrup, T. Application of an intramolecular Heck reaction for the construction of the balanol aryl core structure. *Tetrahedron Letters* **1999,** 40, 4901-4904.
54. Miyabe, H.; Torieda, M.; Inoue, K.; Tajiri, K.; Kiguchi, T.; Naito, T. Total Synthesis of (−)-Balanol. *The Journal of Organic Chemistry* **1998,** 63, 4397-4407.
55. Barbier, P.; Stadlwieser, J. Total Synthesis of Enantiomerically Pure (−)-Balanol. *CHIMIA International Journal for Chemistry* **1996,** 50, 530-532.
56. Hollinshead, S. P.; Nichols, J. B.; Wilson, J. W. Two Practical Syntheses of Sterically Congested Benzophenones. *The Journal of Organic Chemistry* **1994,** 59, 6703-6709.
57. Tanner, D.; Tedenborg, L.; Almario, A.; Pettersson, I.; Csöregh, I.; Kelly, N. M.; Andersson, P. G.; Högberg, T. Total synthesis of balanol, part 2. Completion of the synthesis and investigation of the structure and reactivity of two key heterocyclic intermediates. *Tetrahedron* **1997,** 53, 4857-4868.
58. Denieul, M.-P.; Laursen, B.; Hazell, R.; Skrydstrup, T. Synthesis of the Benzophenone Fragment of Balanol via an Intramolecular Cyclization Event. *The Journal of Organic Chemistry* **2000,** 65, 6052-6060.
59. Adams, C. P.; Fairway, S. M.; Hardy, C. J.; Hibbs, D. E.; Hursthouse, M. B.; Morley, A. D.; Sharp, B. W.; Vicker, N.; Warner, I. Total synthesis of balanol: a potent protein kinase C inhibitor of fungal origin. *Journal of the Chemical Society, Perkin Transactions 1* **1995**, 2355-2362.
60. Wakefield, B. J. *The chemistry of organolithium compounds [by] B. J. Wakefield*. Pergamon Press: Oxford, New York, 1974.
61. Sunthankar, S. V.; Gilman, H. HALOGEN-METAL INTERCONVERSION AND METALATION IN THE NAPHTHALENE SERIES. *The Journal of Organic Chemistry* **1951,** 16, 8-16.
62. Winkler, H. J. S.; Bollinger, R.; Winkler, H. Photolytic alkylation of aromatic hydrocarbons using alkyllithium compounds. *The Journal of Organic Chemistry* **1967,** 32, 1695-1699.
63. Bryce-Smith, D. 318. Organometallic compounds of the alkali metals. Part VI. Evidence for the formation of free alkyl radicals during certain Wurtz reactions. Homolytic reactions between alkyl-lithium compounds and alkyl halides. *Journal of the Chemical Society (Resumed)* **1956**, 1603-1610.
64. Tokoroyama, T.; Kotsuji, Y.; Matsuyama, H.; Shimura, T.; Yokotani, K.; Fukuyama, Y. Synthetic studies on terpenoid compounds. Part 27. Total synthesis of calodendrolide. *Journal of the Chemical Society, Perkin Transactions 1* **1990**, 1745-1752.

65. Ley, S. V.; Norman, J.; Griffith, W. P.; Marsden, S. P. Tetrapropylammonium Perruthenate, Pr4N+RuO4-, TPAP: A Catalytic Oxidant for Organic Synthesis. *Synthesis* **1994,** 1994, 639-666.
66. Thompson, S. K.; Heathcock, C. H. Total synthesis of some marasmane and lactarane sesquiterpenes. *The Journal of Organic Chemistry* **1992,** 57, 5979-5989.
67. Ishihara, J.; Hagihara, K.; Chiba, H.; Ito, K.; Yanagisawa, Y.; Totani, K.; Tadano, K.-i. Synthetic studies of viridenomycin. Construction of the cyclopentene carboxylic acid part. *Tetrahedron Letters* **2000,** 41, 1771-1774.
68. Kuramochi, K.; Nagata, S.; Itaya, H.; Takao, K.-i.; Kobayashi, S. Convergent total synthesis of epolactaene: application of bridgehead oxiranyl anion strategy. *Tetrahedron Letters* **1999,** 40, 7371-7374.
69. Dehoux, C.; Fontaine, E.; Escudier, J.-M.; Baltas, M.; Gorrichon, L. Total Synthesis of a Thymidine 2-Deoxypolyoxin C Analogue. *The Journal of Organic Chemistry* **1998,** 63, 2601-2608.
70. Travis, B. R.; Sivakumar, M.; Hollist, G. O.; Borhan, B. Facile Oxidation of Aldehydes to Acids and Esters with Oxone. *Organic Letters* **2003,** 5, 1031-1034.
71. Lim, M.; Yoon, C. M.; An, G.; Rhee, H. Environmentally benign oxidation reaction of aldehydes to their corresponding carboxylic acids using Pd/C with NaBH4 and KOH. *Tetrahedron Letters* **2007,** 48, 3835-3839.
72. McMurry, J. E.; Dushin, R. G. Total synthesis of (.+-.)-isolobophytolide and (.+-.)-crassin by titanium-induced carbonyl coupling. *Journal of the American Chemical Society* **1990,** 112, 6942-6949.
73. Liu, M.; Wang, H.; Zeng, H.; Li, C.-J. Silver(I) as a widely applicable, homogeneous catalyst for aerobic oxidation of aldehydes toward carboxylic acids in water—“silver mirror”: From stoichiometric to catalytic. *Science Advances* **2015,** 1, e1500020.

Appendix

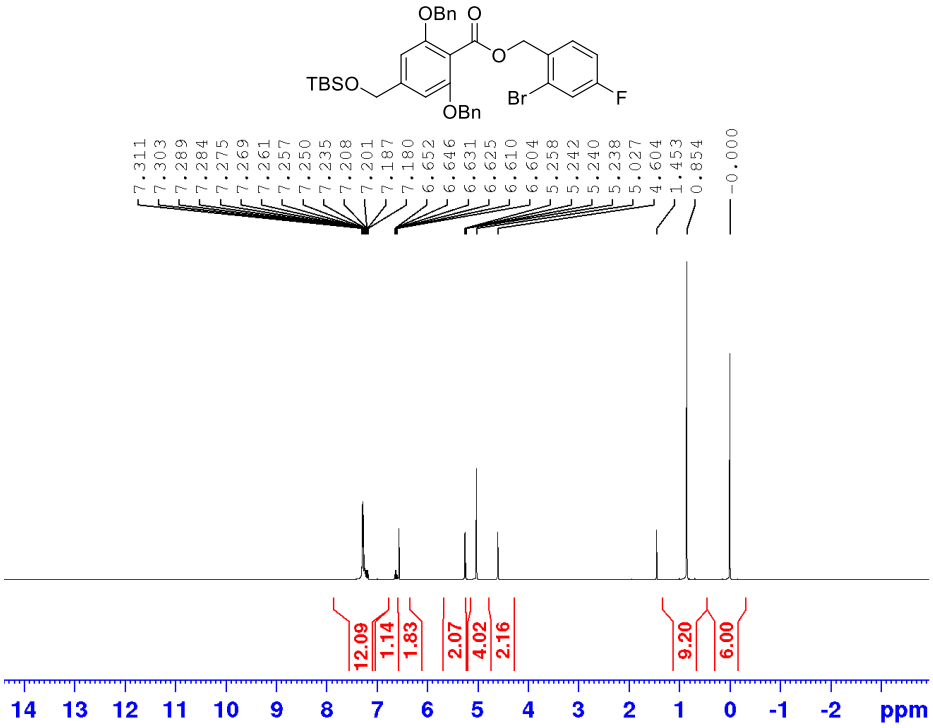
OBn O
O
TBSO
OBn
Br
F
7.311
7.303
7.289
7.284
7.275
7.269
7.261
7.257
7.250
7.235
7.208
7.201
7.187
7.180
6.652
6.646
6.631
6.625
6.610
6.604
5.258
5.242
5.240
5.238
5.027
4.604
1.453
0.854
-0.000
12.09
1.14
1.83
2.07
4.02
2.16
9.20
6.00
14 13 12 11 10 9 8 7 6 5 4 3 2 1 0 -1 -2 ppm

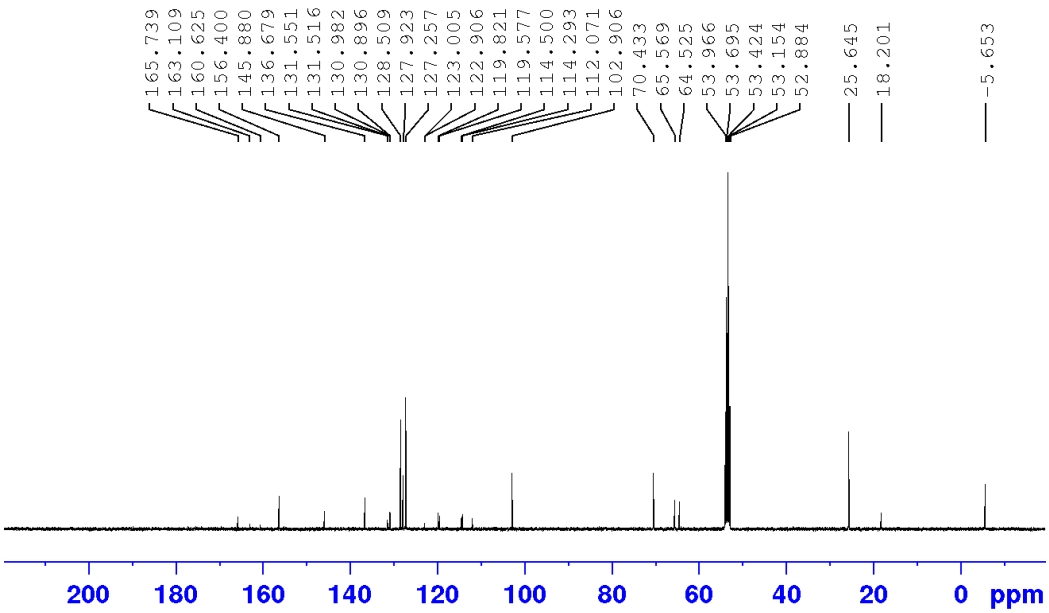
165.739
163.109
160.625
156.400
145.880
136.679
131.551
131.516
130.982
130.896
128.509
127.923
127.257
123.005
122.906
119.821
119.577
114.500
114.293
112.071
102.906
70.433
65.569
64.525
53.966
53.695
53.424
53.154
52.884
25.645
18.201
-5.653
200 180 160 140 120 100 80 60 40 20 0 ppm

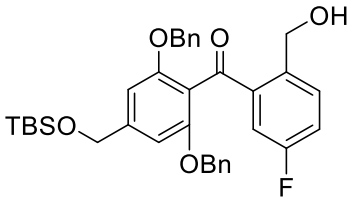
OH
OBn
O
TBSO
OBn
F

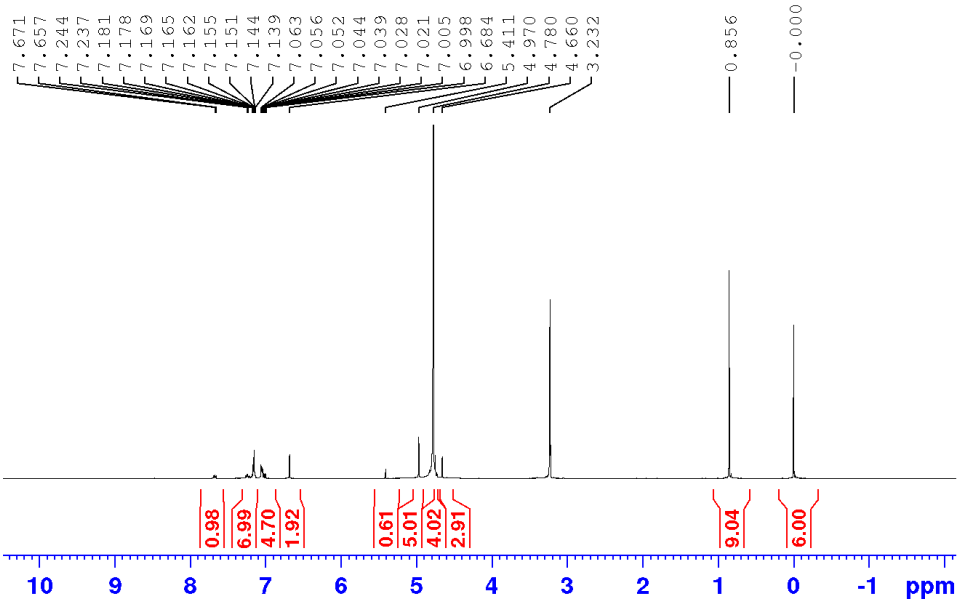
7.671
7.657
7.244
7.237
7.181
7.178
7.169
7.165
7.162
7.155
7.151
7.144
7.139
7.063
7.056
7.052
7.044
7.039
7.028
7.021
7.005
6.998
6.684
5.411
4.970
4.780
4.660
3.232
0.856
-0.000
0.98
6.99
4.70
1.92
0.61
5.01
4.02
2.91
9.04
6.00
10
9
8
7
6
5
4
3
2
1
0
-1
ppm

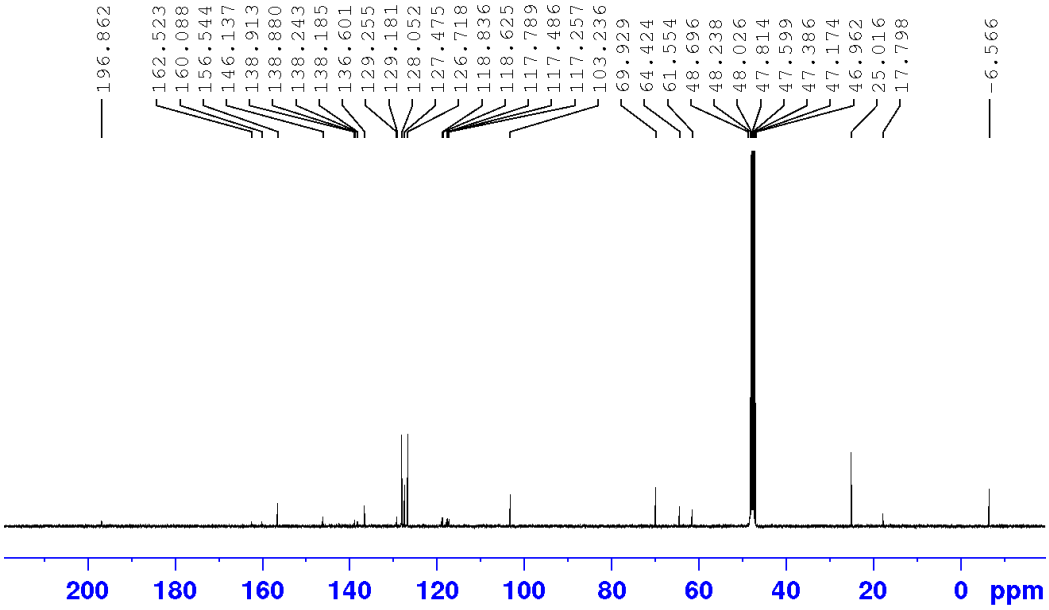
196.862
162.523
160.088
156.544
146.137
138.913
138.880
138.243
138.185
136.601
129.255
129.181
128.052
127.475
126.718
118.836
118.625
117.789
117.486
117.257
103.236
69.929
64.424
61.554
48.696
48.238
48.026
47.814
47.599
47.386
47.174
46.962
25.016
17.798
-6.566
200
180
160
140
120
100
80
60
40
20
0
ppm

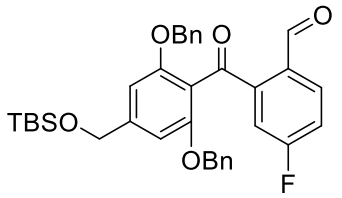
OBn
O
O
TBSO
OBn
F

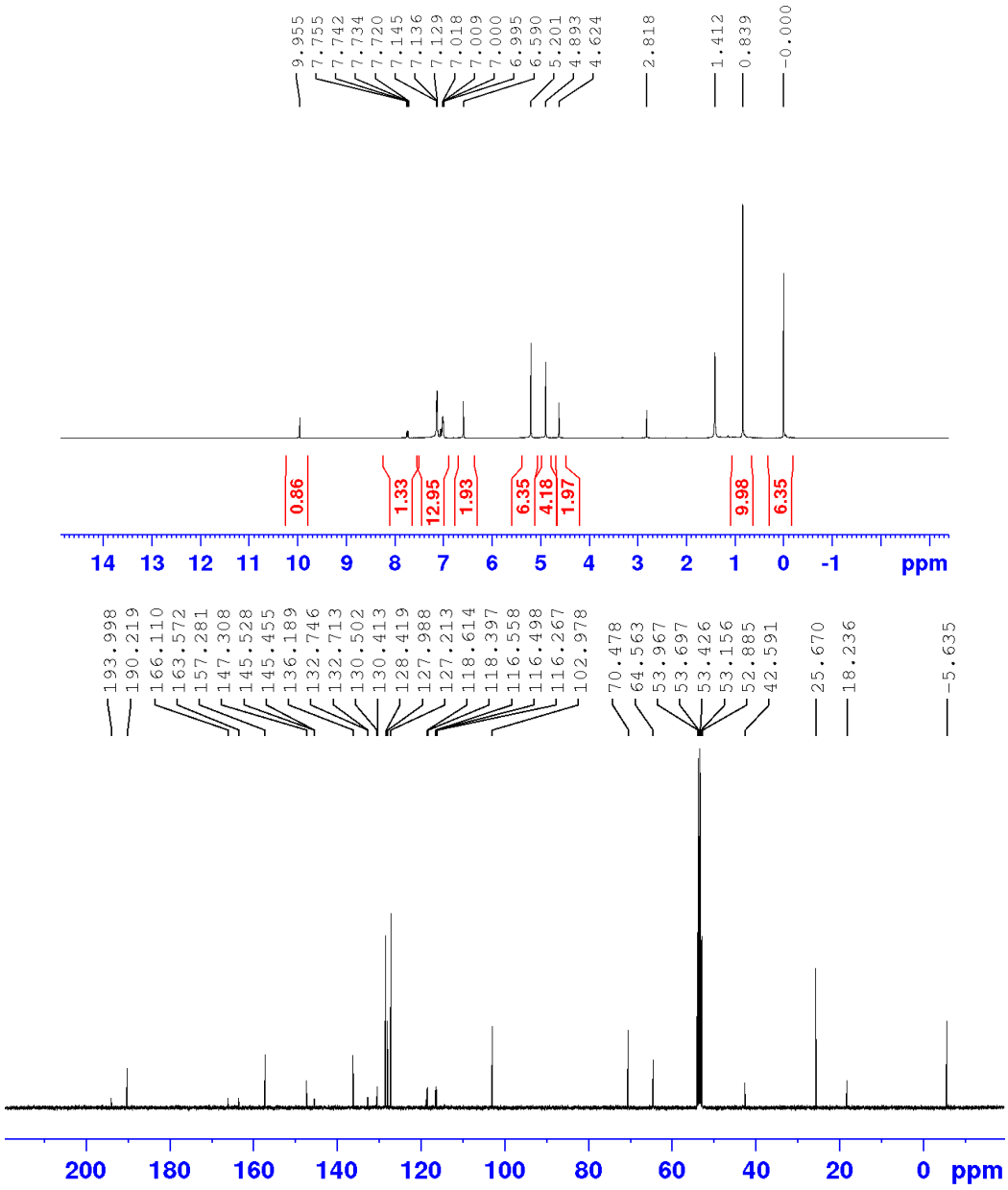
9.955
7.755
7.742
7.734
7.720
7.145
7.136
7.129
7.018
7.009
7.000
6.995
6.590
5.201
4.893
4.624
2.818
1.412
0.839
-0.000
0.86
1.33
12.95
1.93
6.35
4.18
1.97
9.98
6.35
14 13 12 11 10 9 8 7 6 5 4 3 2 1 0 -1 ppm
193.998
190.219
166.110
163.572
157.281
147.308
145.528
145.455
136.189
132.746
132.713
130.502
130.413
128.419
127.988
127.213
118.614
118.397
116.558
116.498
116.267
102.978
70.478
64.563
53.967
53.697
53.426
53.156
52.885
42.591
25.670
18.236
-5.635
200 180 160 140 120 100 80 60 40 20 0 ppm

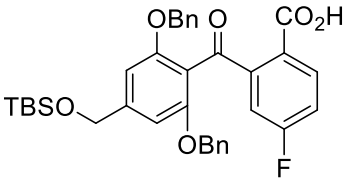
OBn
O
CO_2H
TBSO
OBn
F

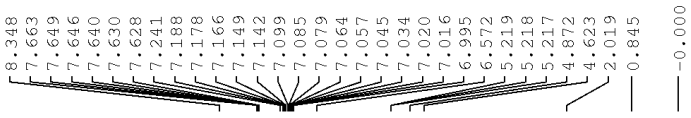
8.348
7.663
7.649
7.646
7.640
7.630
7.628
7.241
7.188
7.178
7.166
7.149
7.142
7.099
7.085
7.079
7.064
7.057
7.045
7.034
7.020
7.016
6.995
6.572
5.219
5.218
5.217
4.872
4.623
2.019
0.845
-0.000

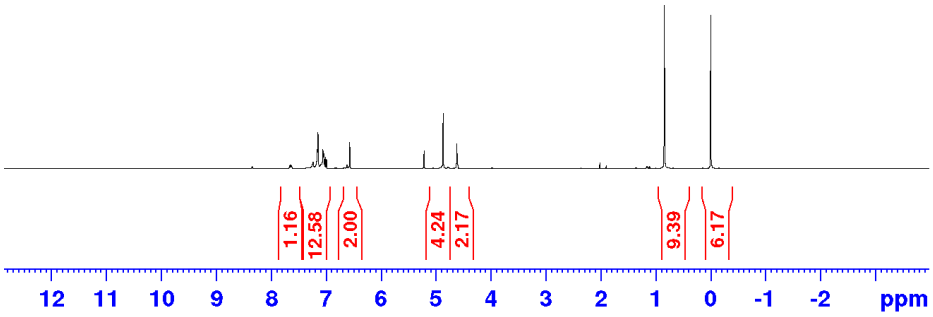
1.16
12.58
2.00
4.24
2.17
9.39
6.17
12 11 10 9 8 7 6 5 4 3 2 1 0 -1 -2 ppm

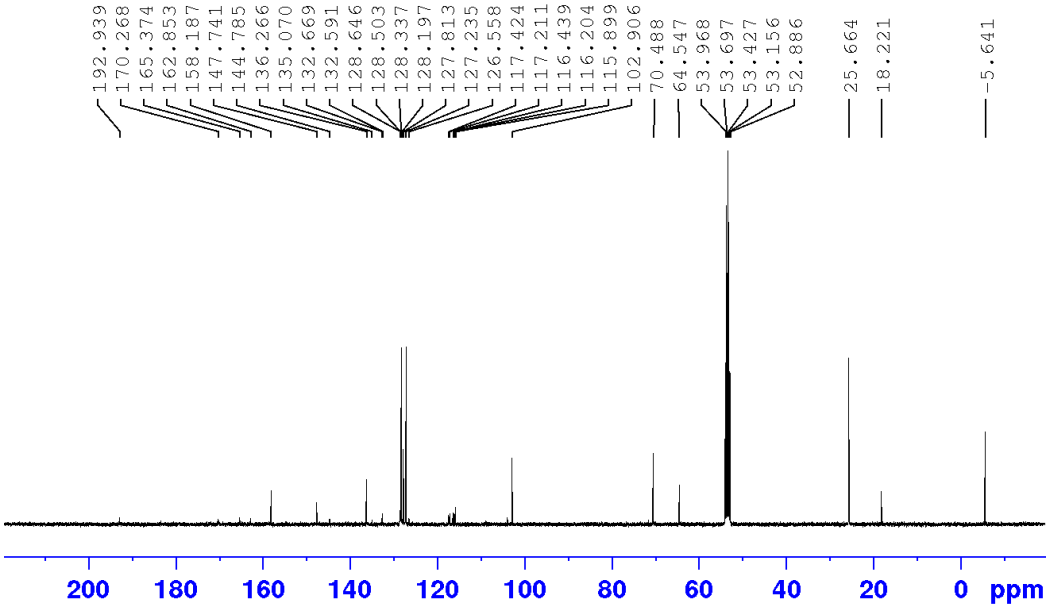
192.939
170.268
165.374
162.853
158.187
147.741
144.785
136.266
135.070
132.669
132.591
128.646
128.503
128.337
128.197
127.813
127.235
126.558
117.424
117.211
116.439
116.204
115.899
102.906
70.488
64.547
53.968
53.697
53.427
53.156
52.886
25.664
18.221
-5.641
200 180 160 140 120 100 80 60 40 20 0 ppm

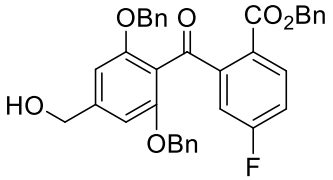
OBn
O
CO_2Bn
HO
OBn
F

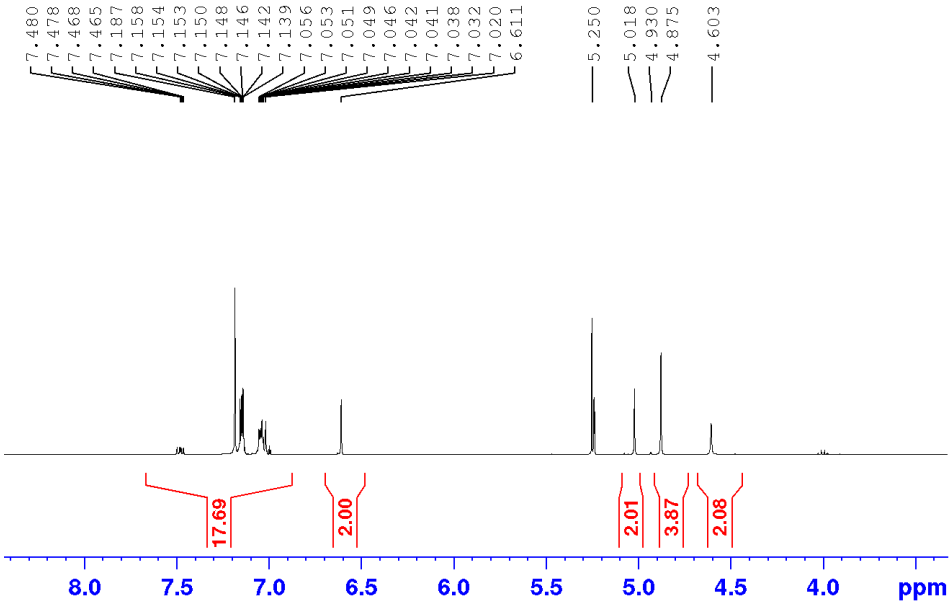
7.480
7.478
7.468
7.465
7.187
7.158
7.154
7.153
7.150
7.148
7.146
7.142
7.139
7.056
7.053
7.051
7.049
7.046
7.042
7.041
7.038
7.032
7.020
6.611
5.250
5.018
4.930
4.875
4.603
17.69
2.00
2.01
3.87
2.08
8.0
7.5
7.0
6.5
6.0
5.5
5.0
4.5
4.0
ppm

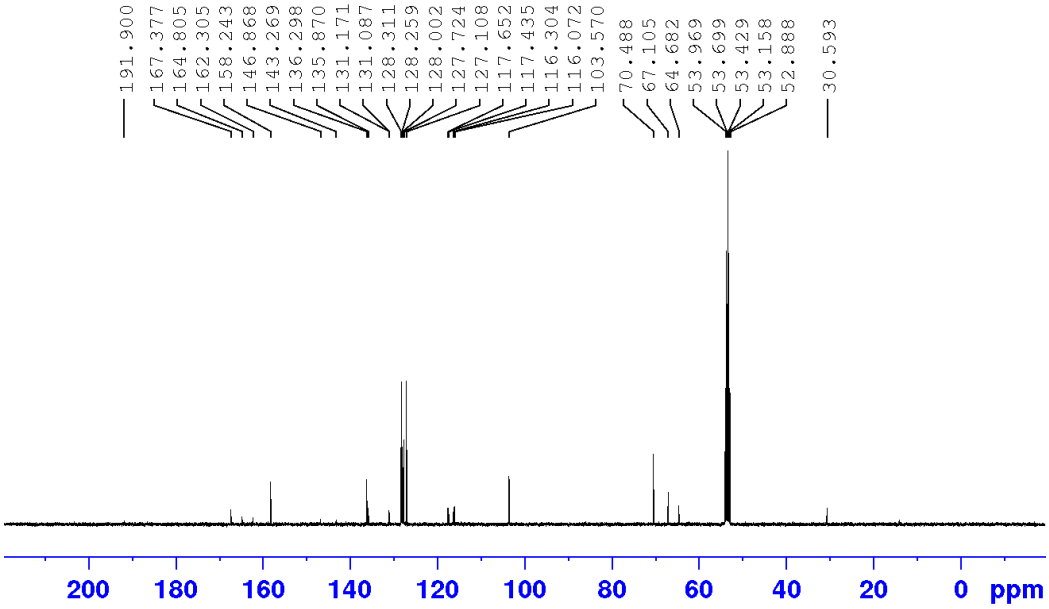
191.900
167.377
164.805
162.305
158.243
146.868
143.269
136.298
135.870
131.171
131.087
128.311
128.259
128.002
127.724
127.108
117.652
117.435
116.304
116.072
103.570
70.488
67.105
64.682
53.969
53.699
53.429
53.158
52.888
30.593
200
180
160
140
120
100
80
60
40
20
0
ppm

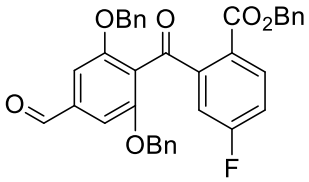
OBn
O
CO2Bn
O
OBn
F

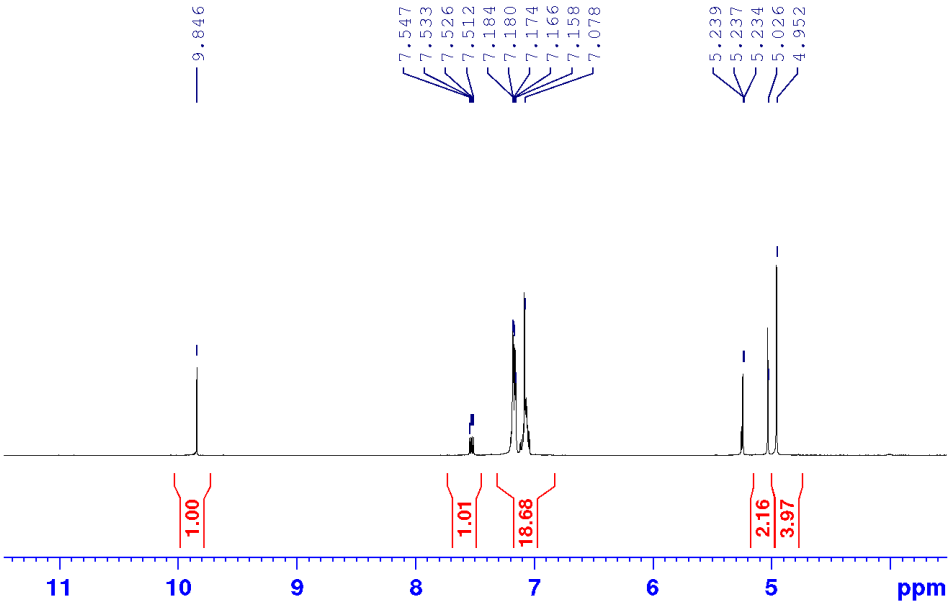
9.846
7.547
7.533
7.526
7.512
7.184
7.180
7.174
7.166
7.158
7.078
5.239
5.237
5.234
5.026
4.952
1.00
1.01
18.68
2.16
3.97
11
10
9
8
7
6
5
ppm

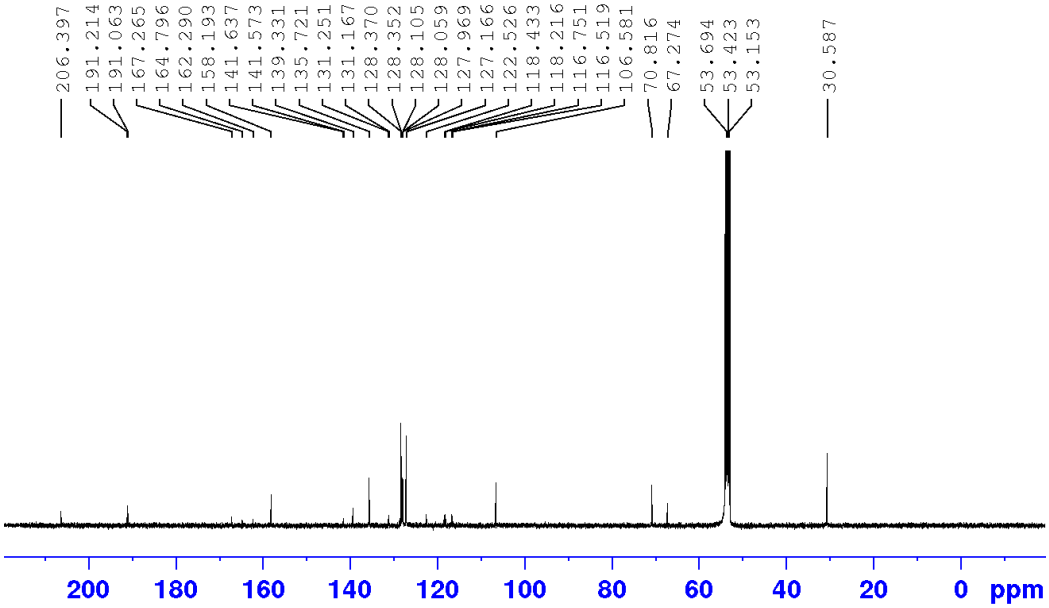
206.397
191.214
191.063
167.265
164.796
162.290
158.193
141.637
141.573
139.331
135.721
131.251
131.167
128.370
128.352
128.105
128.059
127.969
127.166
122.526
118.433
118.216
116.751
116.519
106.581
70.816
67.274
53.694
53.423
53.153
30.587
200
180
160
140
120
100
80
60
40
20
0
ppm

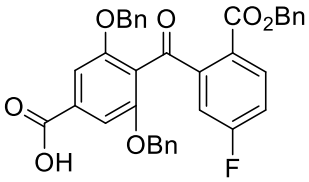
OBn
O
CO2Bn
O
OH
OBn
F

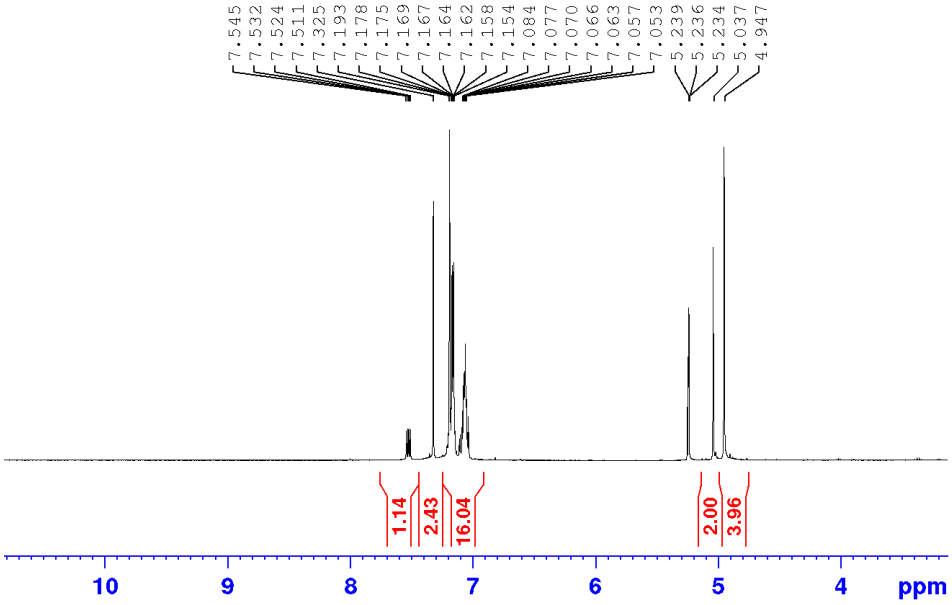
7.545
7.532
7.524
7.511
7.325
7.193
7.178
7.175
7.169
7.167
7.164
7.162
7.158
7.154
7.084
7.077
7.070
7.066
7.063
7.057
7.053
5.239
5.236
5.234
5.037
4.947
1.14
2.43
16.04
2.00
3.96
10
9
8
7
6
5
4
ppm

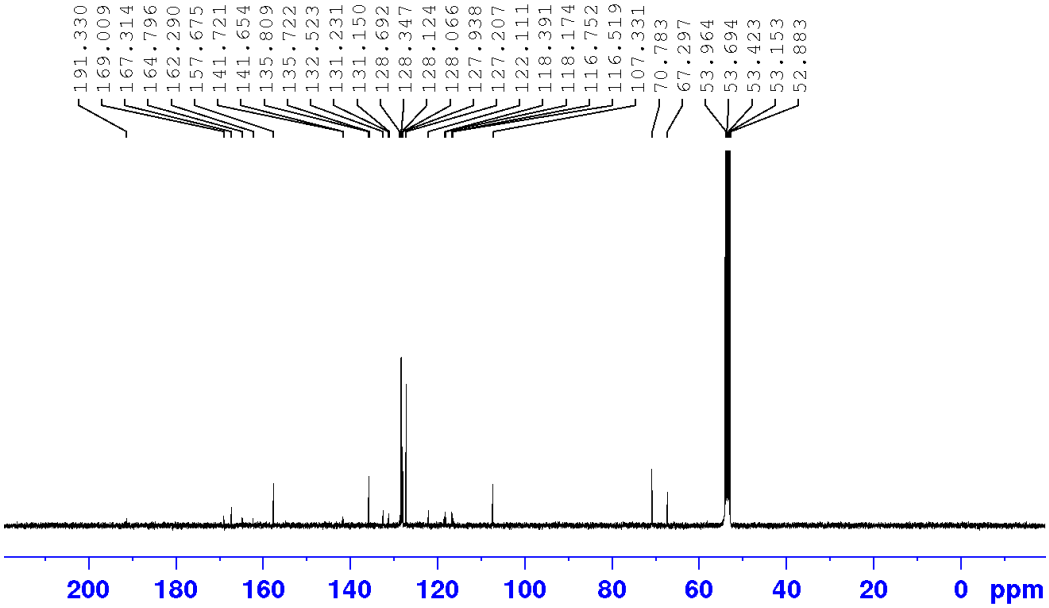
191.330
169.009
167.314
164.796
162.290
157.675
141.721
141.654
135.809
135.722
132.523
131.231
131.150
128.692
128.347
128.124
128.066
127.938
127.207
122.111
118.391
118.174
116.752
116.519
107.331
70.783
67.297
53.964
53.694
53.423
53.153
52.883
200
180
160
140
120
100
80
60
40
20
0
ppm

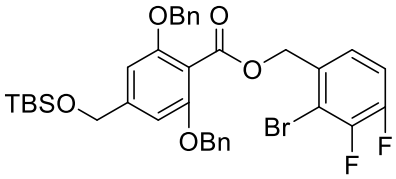
OBn
O
O
TBSO
OBn
Br
F
F

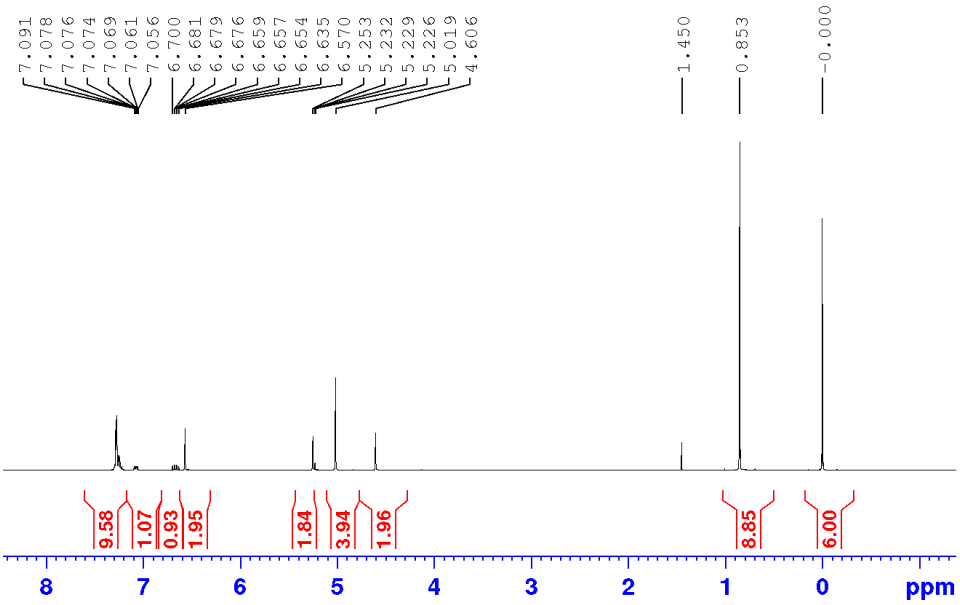
7.091
7.078
7.076
7.074
7.069
7.061
7.056
6.700
6.681
6.679
6.676
6.659
6.657
6.654
6.635
6.570
5.253
5.232
5.229
5.226
5.019
4.606
1.450
0.853
-0.000
9.58
1.07
0.93
1.95
1.84
3.94
1.96
8.85
6.00
8
7
6
5
4
3
2
1
0
ppm

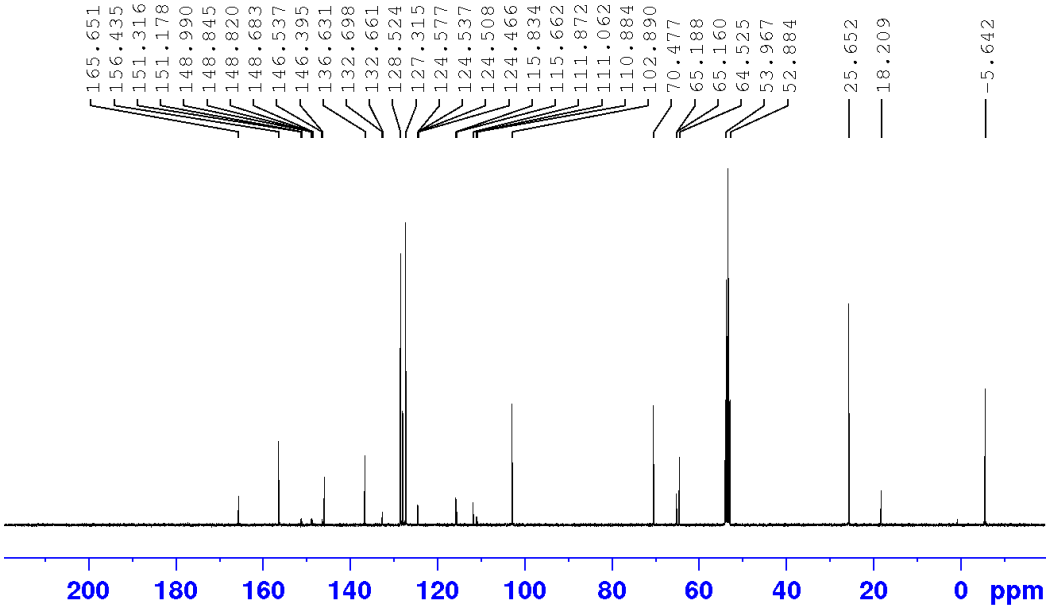
165.651
156.435
151.316
151.178
148.990
148.845
148.820
148.683
146.537
146.395
136.631
132.698
132.661
128.524
127.315
124.577
124.537
124.508
124.466
115.834
115.662
111.872
111.062
110.884
102.890
70.477
65.188
65.160
64.525
53.967
52.884
25.652
18.209
-5.642
200
180
160
140
120
100
80
60
40
20
0
ppm

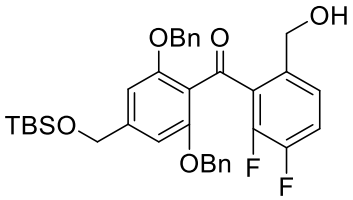
OH
OBn O
TBSO
OBn F
F

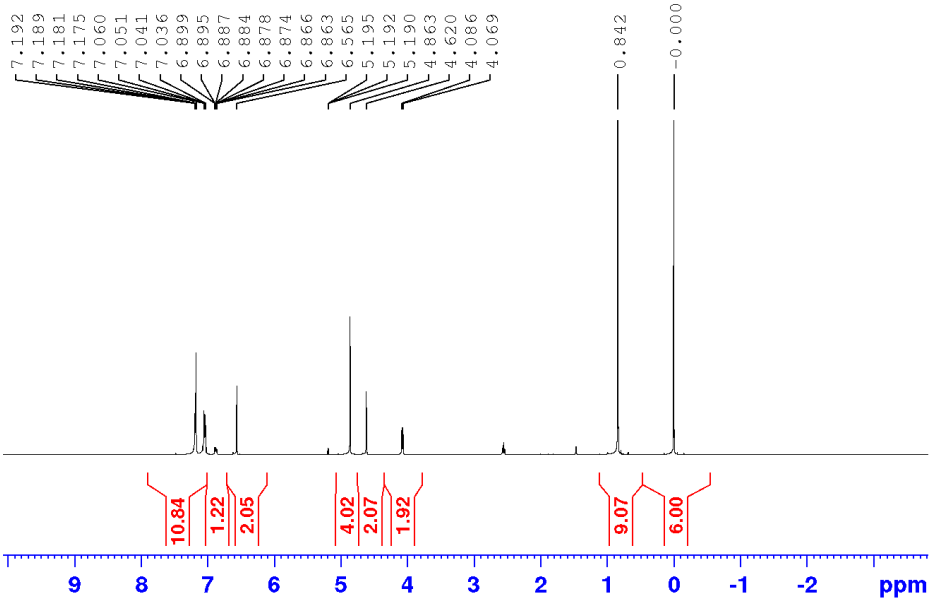
7.192
7.189
7.181
7.175
7.060
7.051
7.041
7.036
6.899
6.895
6.887
6.884
6.878
6.874
6.866
6.863
6.565
5.195
5.192
5.190
4.863
4.620
4.086
4.069
0.842
-0.000
10.84
1.22
2.05
4.02
2.07
1.92
9.07
6.00
9 8 7 6 5 4 3 2 1 0 -1 -2 ppm

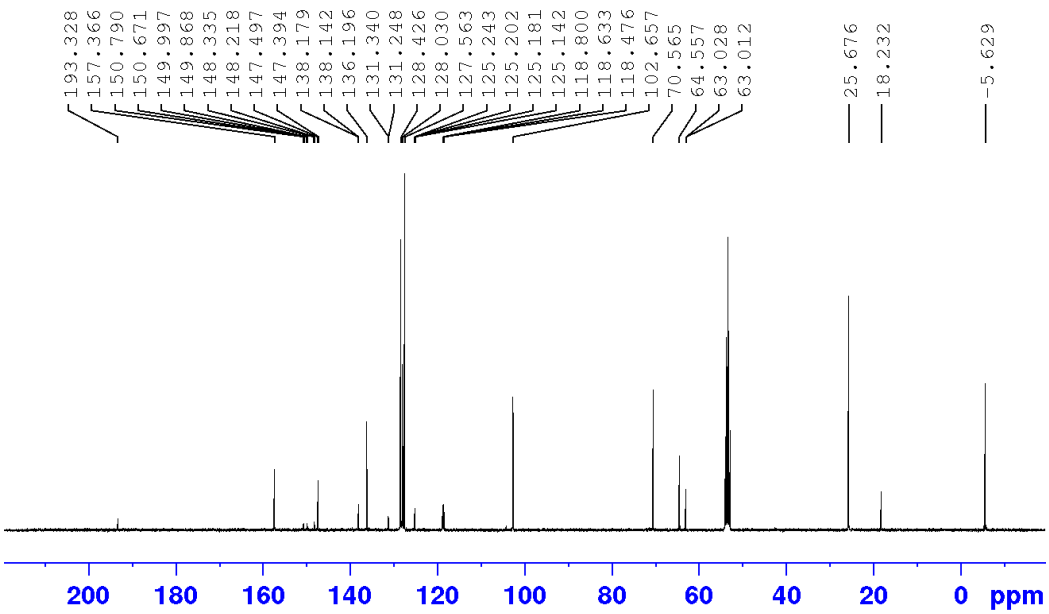
193.328
157.366
150.790
150.671
149.997
149.868
148.335
148.218
147.497
147.394
138.179
138.142
136.196
131.340
131.248
128.426
128.030
127.563
125.243
125.202
125.181
125.142
118.800
118.633
118.476
102.657
70.565
64.557
63.028
63.012
25.676
18.232
-5.629
200 180 160 140 120 100 80 60 40 20 0 ppm

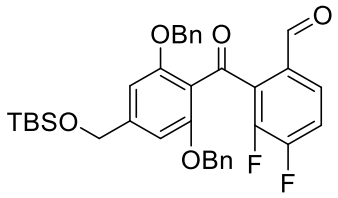
OBn
O
O
TBSO
OBn
F
F

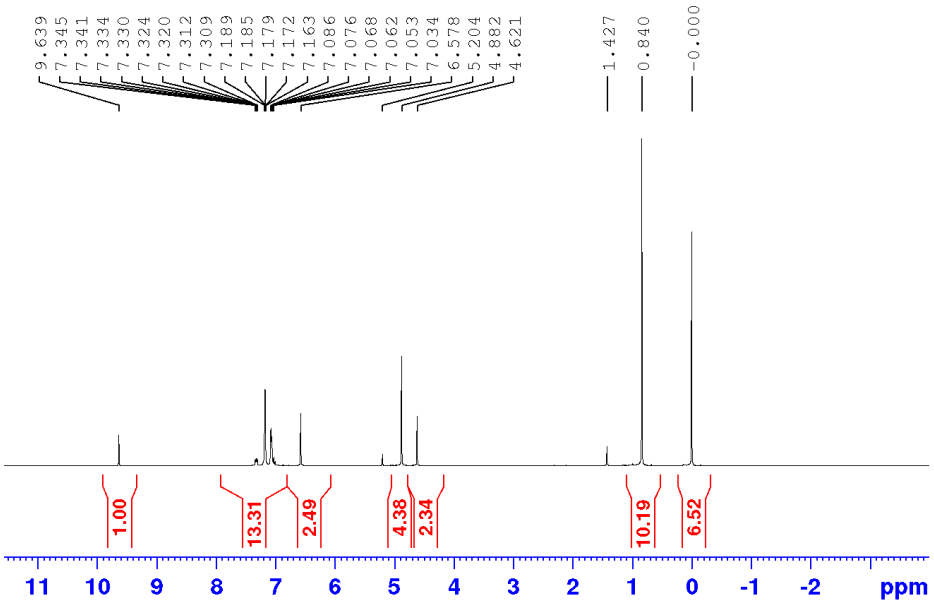
9.639
7.345
7.341
7.334
7.330
7.324
7.320
7.312
7.309
7.189
7.185
7.179
7.172
7.163
7.086
7.076
7.068
7.062
7.053
7.034
6.578
5.204
4.882
4.621
1.427
0.840
-0.000
1.00
13.31
2.49
4.38
2.34
10.19
6.52
11 10 9 8 7 6 5 4 3 2 1 0 -1 -2 ppm

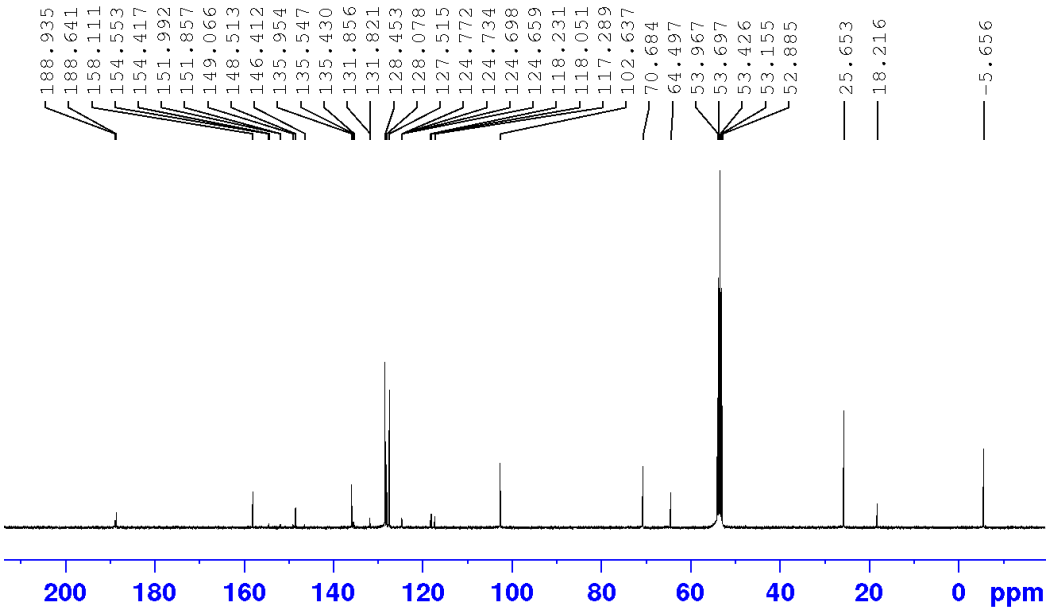
188.935
188.641
158.111
154.553
154.417
151.992
151.857
149.066
148.513
146.412
135.954
135.547
135.430
131.856
131.821
128.453
128.078
127.515
124.772
124.734
124.698
124.659
118.231
118.051
117.289
102.637
70.684
64.497
53.967
53.697
53.426
53.155
52.885
25.653
18.216
-5.656
200 180 160 140 120 100 80 60 40 20 0 ppm